UNIVERSITY OF PARDUBICE
Department of physical chemistry
&
J. HEYROVSKÝ INSTITUTE OF PHYSICAL CHEMISTRY OF ACADEMY OF SCIENCES OF THE CZECH REPUBLIC

Selective oxidation of paraffins over metallo-zeolites

DISSERTATION

Author: Ing. Kateřina Novoveská
Supervisors: Ing. Blanka Wichterlová, DrSc.
Doc. Ing. Roman Bulánek, Ph.D.

2006

UNIVERZITA PARDUBICE
Katedra fyzikální chemie
&
ÚSTAV FYZIKÁLNÍ CHEMIE J. HEYROVSKÉHO
AKADEMIE VĚD ČESKÉ REPUBLIKY

Selektivní oxidace parafinů na metallo-zeolitech

DISERTACE

Autor: Ing. Kateřina Novoveská
Vedoucí práce: Ing. Blanka Wichterlová, DrSc.
Doc. Ing. Roman Bulánek, Ph.D.

2006

Prohlašuji:

Tuto práci jsem vypracovala samostatně. Veškeré literární prameny a informace, které jsem v práci využila, jsou uvedeny v seznamu použité literatury.

I declare that I worked out this dissertation myself and the aid of other persons is clearly stated. All data, used from literature in this dissertation, are cited.

Byla jsem seznámena s tím, že se na moji práci vztahují práva a povinnosti vyplývající ze zákona č. 121/2000 Sb., autorský zákon, zejména se skutečností, že Univerzita Pardubice má právo na uzavření licenční smlouvy o užití této práce jako školního díla podle § 60 odst. 1 autorského zákona, a s tím, že pokud dojde k užití této práce mnou nebo bude poskytnuta licence o užití jinému subjektu, je Univerzita Pardubice oprávněna ode mne požadovat přiměřený příspěvek na úhradu nákladů, které na vytvoření díla vynaložila, a to podle okolností až do jejich skutečné výše.

Souhlasím s prezenčním zpřístupněním své práce v Univerzitní knihovně Univerzity Pardubice.

V Pardubicích dne 28.4.2006

Kateřina Novoveská

The studies for this dissertation were carried out at the Department of Physical Chemistry, Faculty of Chemical Technology, University of Pardubice and the Department of Solid State Chemistry and Catalysis of the Heyrovský Institute of Physical Chemistry, Academy of Science of the Czech Republic in 2001 –2006 years.

I would like to thank to my supervisors Ing. Blanka Wichterlová DrSc. and Doc. Ing. Roman Bulánek Ph.D. for advisory opinions, worth advises and for great patience with me. Also it is important to thank to people in Department of Physical Chemistry, Faculty of Chemical Technology of University of Pardubice and Department of Solid State Chemistry and Catalysis of Academy of Sciences of the Czech Republic, namely Ing. Pavel Čičmanec Ph.D., Ing. Jiří Dědeček CSc and Ing. Zdeněk Sobalík CSc. for kind help with solution of problems concerning dissertation.

Foremost I would like to thanks to my parents for their love, advices and opportunity to study. At least, not at last, I would like to thanks to my partner who gave me his love, power, aid and encouragement.

Chemie bez katalýzy je jako meč bez kontroly,
světlo bez jasu, zvon bez zvuku.
Alvin Mittasch

ÚDAJE PRO KNIHOVNICKOU DATABÁZI

Název práce	Selective oxidation of paraffins over metallo-zeolites Selektivní oxidace parafinů na metallo-zeolitech
Autor práce	Ing. Kateřina Novoveská
Obor	Fyzikální chemie
Rok obhajoby	2006
Vedoucí práce	Ing. Blanka Wichterlová, DrSc. Doc. Ing. Roman Bulánek, Ph.D.
Anotace	Selektivní oxidace propanu a etanu byly studovány na zeolitech modifikovaných kovy (Co, Cu, Fe) v přítomnosti molekulárního kyslíku, oxidu dusného a amoniaku. Z experimentálních technik byly použity FTIR a UV-Vis v ex-situ a in-situ uspořádání, XRD, teplotně programované redukce. Byl zjištěn vliv struktury, jednotlivých typů částic a velký vliv přítomnosti amoniaku. Oxid dusný zvyšuje aktivitu katalyzátorů v oxidativní dehydrogenaci. Selective oxidation of propane and ethane has been studied over zeolites modified by transition metals (Co, Cu, Fe) in the presence of molecular oxygen, nitrous oxide and ammonia. There were used FTIR and UV-Vis in ex-situ and in-situ conditions, XRD, temperature programmed reduction. The effect of zeolite structure, type of species and ammonia was found out. Nitrous oxide increases the activity of the Co and Fe catalyst in oxidative dehydrogenation.
Klíčová slova	**keywords:** selective oxidation, oxidative dehydrogenation, ammoxidation, propane, ethane, zeolites, Co-zeolites, Fe-zeolites, ammonia, nitrous oxide **klíčová slova:** selektivní oxidace, oxidativní dehydrogenace, amoxidace, propan, etan, zeolity, Co-zeolity, Fe-zeolity, amoniak, oxid dusný

UNIVERSITY OF PARDUBICE
Department of Physical Chemistry

&

J. HEYROVSKÝ INSTITUTE OF PHYSICAL CHEMISTRY
Academy of sciences of the Czech Republic

Selective oxidation of paraffins over metallo-zeolites

ANOTATION OF DISSERTATION

Author: Ing. Kateřina Novoveská
Supervisors: Ing. Blanka Wichterlová, DrSc.
Doc. Ing. Roman Bulánek, Ph.D.

2006

Summary

In recent years metallo-zeolites have been shown to exhibit unusual catalytic behaviour in redox reactions as ammoxidation of ethane to acetonitrile, selective catalytic reduction of NO_x to nitrogen and benzene oxidation to phenol by nitrous oxide.

The study has been aimed at analysis of the structure and reactivity of Co- and Fe-zeolites and exploitation of this knowledge for understanding of the oxidation processes and catalyst design for selective oxidation and ammoxidation of low chain paraffins by molecular oxygen and nitrous oxide to olefins, aldehydes and nitriles. The main questions have concerned the effect of the nature and type of Cu, Co and Fe ion species and topology of the zeolite matrix (FER, MOR, MFI and *BEA) on the catalyst activity with respect to the above reactions.

Besides reaction kinetic measurements of hydrocarbon transformations with molecular oxygen, nitrous oxide and ammonia over metallo-zeolites, the ex-situ and in-situ (at true reaction conditions) UV-Vis and FTIR spectroscopy on Co-zeolites have been employed to obtain information on the state and behaviour of potential active sites and reaction intermediates. Zeolite catalysts were characterized by means of temperature-programmed reduction by hydrogen, the crystallinity was checked by X-ray diffraction and electron spin resonance was used to identify presence and coordination of Fe ions in Co(Fe)-zeolites.

It has been found that single Co ions coordinated to the framework in zeolites, in contrast to Co-oxo and Co oxide-like species supporting complete paraffin oxidation, are responsible for selective oxidation of ethane and propane to olefins. Substantially higher activity of Co ions in *BEA and MFI zeolites, in comparison with those in MOR and FER structures, is attributed to a high level of accessibility of the most populated β-type Co ions coordinated to the framework in open channels of *BEA zeolite and at intersection of the straight and sinusoidal channels of MFI structure to reaction intermediates. Thus strong shape selectivity effect is demonstrated.

At the ammoxidation reaction strong adsorption of ammonia on Co ion species increases substantially the rate of paraffin oxidation as well as the selectivity to and yields of olefins and nitriles. We speculate that the surprising increase of paraffin conversion and high conversion of ammonia to nitrogen might be due to coordination of ammonia and oxygen to the Co ions, oxidation of ammonia to NO_x increasing the rate of paraffin oxidation and leading to molecular nitrogen, with simultaneous ammination of the formed olefin to alkylamine and its oxidation to nitrile.

In oxidation of paraffins by nitrous oxide over Fe zeolites, the Fe sites are suggested to decompose nitrous oxide to molecular nitrogen and atomic oxygen, and enable its insertion to a hydrocarbon molecule. However, only a minor part of Fe ion species in Fe-zeolites is extremely active in hydrocarbon oxidation with N_2O. It has been revealed that the oxidation of propane over Fe-zeolites follows the reaction pathway leading mainly to propene, propanol and propanal in the following steps:

$$N_2O \rightarrow N_2 + O$$

$$propane + O \rightarrow propanol - H_2O \rightarrow propene + O \rightarrow propanal \rightarrow CO_x$$

It has been shown that propane oxidation over bifunctional Co(Fe)-zeolites, using a mixture of molecular oxygen and nitrous oxide compared to molecular oxygen, gives much higher propane conversion and yield of propene. The Co ions catalyse oxidative dehydrogenation of paraffins to olefins by molecular oxygen and over Fe ions atomic oxygen from nitrous oxide decomposition is transferred to propane molecule to yield propanol, propene and propanal. These results suggest that nitrous oxide (a harmful by-product, e.g., in adipic acid plants) added to streams of molecular oxygen could be exploited for enhancement of transformation of paraffins to olefins.

keywords: selective oxidation, oxidative dehydrogenation, ammoxidation, propane, ethane, zeolites, Co-zeolites, Fe-zeolites, ammonia, nitrous oxide

Introduction

Nowadays, oxygenates (e.g. maleic anhydride, acrylic acid, furan) and nitriles (acrylonitrile, acetonitrile) are produced from unsaturated hydrocarbons. As the unsaturated hydrocarbons belong to costly raw materials, there is an urgent need for their replacement by cheaper source or new industrial processes to leading to requested chemicals. Selective oxidation of light paraffins represents a challenge for catalysis. The advantage in the use of alkanes is their low cost (propane is 5-6 times cheaper compared to propene). Alkanes are also less toxic or noxious reactants compared to alkenes and aromatics. Their direct selective oxidation could be used for replacement of energy-intensive processes like dehydrogenation or steam-cracking of paraffins. Light alkanes are obtained as by-products in petroleum processing and as components of natural gas. So far only less than 10 % of natural gas is consumed in chemistry and the rest is consumed in energy production.

The main reason of interest focused on metallo-zeolites as heterogeneous catalysts stems from their unusual redox and acidic properties. Zeolites are highly uniformed crystalline aluminosilicates with inner channel structure of defined size of pores and architecture. A suitable choice of zeolite structure can restrict some reactants to take part in the catalytic reaction or product to be formed. The variation in composition causes changes in the concentration and properties of counter ions, i.e. metal ion species and protonic sites. The metal cations can be atomically dispersed, and by their coordination to the framework offer open coordination sphere to highly accessible to reactants. Moreover, the negative charge of the framework significantly affects their redox properties. This in combination with acidic sites gives unique catalytic behaviour of metallo-zeolites, not attainable for supported metal oxides or mixed oxides.

In recent years metallo-zeolites have been shown to exhibit exceptional catalytic behaviour in redox reactions as ammoxidation of ethane to acetonitrile, selective reduction of NO_x to nitrogen (SCR-NO_x) and benzene oxidation to phenol by N_2O.

Aim

The study has been aimed at analysis of the structure and reactivity of Co-, Fe- and Co(Fe)-zeolites and exploitation of this knowledge for understanding of the oxidation processes and catalyst design for selective oxidation and ammoxidation of low chain paraffins by molecular oxygen and nitrous oxide to olefins, aldehydes and nitriles. The main questions have concerned the effect of the character (Cu, Co and Fe) and type of metal ion species (Co) and topology of zeolite matrix (FER, MOR, MFI and *BEA) on the catalyst activity with respect to paraffin oxidation with molecular oxygen, nitrous oxide and with ammonia participation.

Experimental

Cu, Co and Fe ion species in various zeolite structures (MFI, *BEA, MOR and FER) have been prepared and compared with respect to their activity in selective (ammo)oxidation of paraffins by molecular oxygen. Catalysts were characterized by means of temperature-programmed reduction by hydrogen, the crystallinity of zeolites was checked before and after catalytic reaction by using the X-ray diffraction and electron spin resonance was used to detect presence of Fe ions in Co-zeolites. Besides reaction kinetics measurements at 450°C, the ex-situ and in-situ (at true reaction conditions with identical composition of reaction mixture and high temperature 450°C) UV-Vis and FTIR spectroscopies have been employed

to obtain information on the state and behaviour of potential active sites (metal ion species and protons) and surface reaction intermediates.

Results and Discussion

Comparison of metallo-zeolites in oxidation and ammoxidation of propane

Parent H-, and Cu-, Co- and Fe-zeolites were investigated in oxidative dehydrogenation and ammoxidation of propane. Parent H-zeolites exhibited only low conversion of propane to carbon oxides in oxidation and ammoxidation reactions. This activity was ascribed to trace concentration of Fe species. But at higher concentration of Fe the propane conversion and yields of propene were low. Cu-zeolites of the structures investigated exhibited low selectivity to propene, and some selectivity to ethane; propene formed oligomerized and cracked to ethene. The turn-over-frequency (TOF) values in paraffin conversion indicate that relatively most active Cu sites are located in MFI structure, while those in FER and *BEA exhibit lower activity. Like with H-zeolites ammonia addition with Cu-zeolites caused a significant decrease in propane and oxygen conversion and a dramatic increase in selectivity to propene and acetonitrile. The turn-over-frequency (TOF) values of paraffin conversion indicate that the most active Cu sites are located in *BEA structure, while those in FER are much less active.

Zeolites with exchanged cobalt ions were most active and selective to olefins or acetonitrile in both ethane and propane reactions among metallo-zeolites.

Oxidative dehydrogenation and ammoxidation of paraffins over Co zeolites by molecular oxygen. Effect of zeolite topology

Oxidation of ethane and propane over Co-zeolites led to corresponding olefins, CO and CO_2. A small part of propane cracked to ethene (ca 5 %), but no cracking products were observed with ethane. Dramatic differences in the activity in oxidative dehydrogenation and ammoxidation of both paraffins were observed for various zeolite structural types (*BEA > MFI >>> MOR > FER), as already reported for ethane ammoxidation [1]. We suggest the the high differences found in the activity of Co-zeolites of various topologies can be accounted for the location of Co ions in zeolite channels of different size. Three coordinations-positions of Co ions (denoted as α, β and γ sites) in pentasil ring zeolites of MFI, *BEA, MOR and FER topologies have been suggested in our laboratory (see Scheme 1, Ref. 1). The UV-Vis spectra of Co(II) ions in the investigated samples indicated that the β sites (cations

coordinated to six-membered ring in positions given in Scheme 1) were the most populated by Co ions (around 75 %) in all the zeolite structures. In *BEA and MFI structures they are located in very open channels and at the ring exposed at the intersection of the straight and sinusoidal channel, resp.. On contrary, the Co-β sites in MOR and FER structures are located in the narrow inter-connected channels and in the 8-member ring channels, respectively. All types of the Co ions (α, β and γ) in all the zeolites structures (*BEA, MFI, FER, MOR) have been found accessible to reactants (paraffin, oxygen, ammonia) as shown by Vis spectra of Co(II) ions. The more pronounced differences among the activities of Co-zeolites of various structures in ammoxidation vs. oxidative dehydrogenation support our suggestion that the low accessibility of the Co-β ions in ferrierite and mordenite for reaction intermediate complex plays predominant role for their activity [1,2].

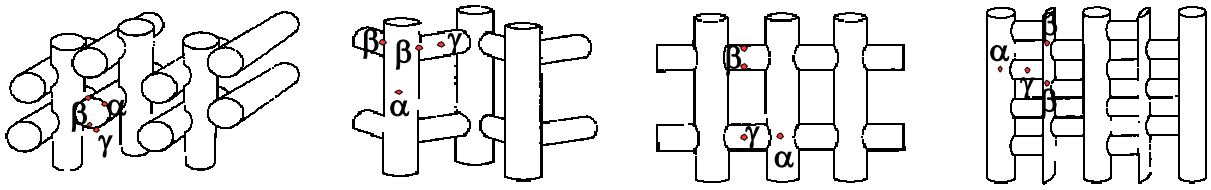

*BEA	MFI	FER	MOR
12 – 5.5 x 5.5 Å **12 –** 7.6 x 6.4 Å	**10 –** 5.3 x 5.6 Å **10 -** 5.1 x 5.5 Å	**10 –** 4.2 x 5.4 Å **8** – 3.5 x 4.8 Å	**12 –** 6.5 x 7.0 Å **8 –**2. x 5.7 Å

Scheme 1 Location of Co ions in zeolites (12,10,8 means number of T atoms in the channel ring)

Oxidative dehydrogenation and ammoxidation of paraffins over Co zeolites by molecular oxygen. Effect of Co ion species

Analysis of the state of Co ion species in the most active Co-*BEA zeolites (via ex-situ and in-situ UV-Vis and FTIR at the reaction conditions) led us to the conclusion that the cobalt ions at low concentrations are present in the zeolite as single Co ions. At Co/Al > 0.35 Co-ligand species are also exchanged resulting in Co-oxo species and at the "over-exchange" level (Co/Al > 0.5) cobalt oxide-like species are formed. In ethane oxidation (Figure 1) the single Co ions catalyse predominantly its oxidative dehydrogenation, and the Co-oxo species increase mostly oxidation to CO_x, while Co oxide-like species are less active per Co ion. In ethane ammoxidation a strong adsorption of ammonia on Co ions dramatically increases the ethane conversion and yield of (ethene + acetonitrile), and suppresses combustion activity over Co-oxo species [3]. We speculate that the substantial positive effect of ammonia is

a result of an electron density transfer from ammonia to molecular oxygen coordinated to Co ions followed by ammonia oxidation to NO_x involved then in paraffin oxidation to olefin, representing first step for acetonitrile formation (see Scheme 2).

A decrease in paraffin conversion with added ammonia over Co-MOR and Co–FER supports our suggestion on the dramatic effect of reaction space available in the inner zeolite volume on the acitivity of Co ions in (ammo)oxidation of paraffins.

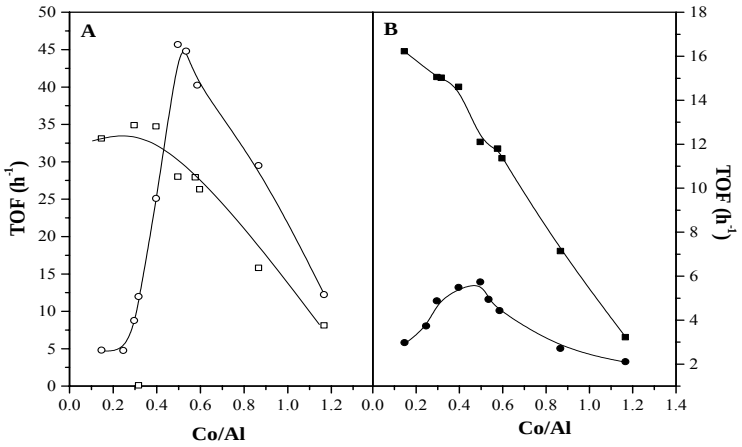

Figure 1 Dependence of TOF (turn-over-frequency) values on Co/Al molar ratio in the Co-*BEA catalysts at 450°C and F = 100 ml/min, 5 vol. % ethane, 6.5 vol. % oxygen, TOF related to (A) O - ethane conversion in oxidation, □- ethane conversion in ammoxidation, (B) ● - ethene yield , ■ - sum of ethene and acetonitrile yield,

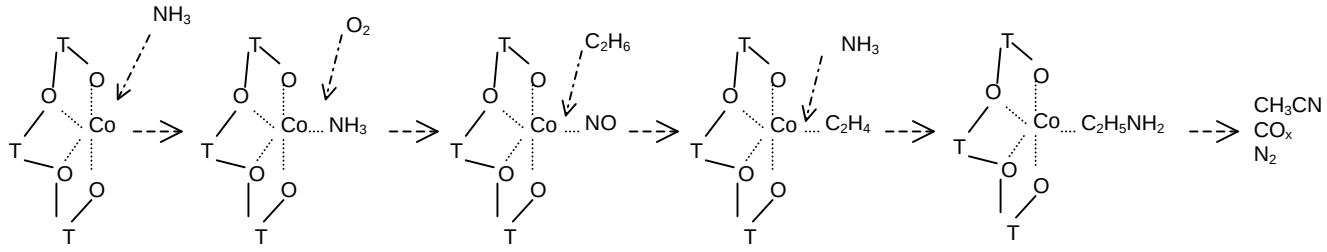

Scheme 2 Suggested mechanism of ethane ammoxidation

Higher concentration of ammonia in the feed considerably affects yields of nitriles. It supports ammonolysis of acrylonitrile (if formed from propene) and oxidation of acetonitrile to CO_x.

Oxidation of propane over Fe-zeolites by nitrous oxide and oxygen

The results of propane oxidation over Fe-zeolites (starting from trace concentrations) supported the revised conclusion that the active sites for N_2O oxidation are exclusively Fe ions and not protons or Al-Lewis sites. It follows that trace concentrations of Fe are responsible for the apparent redox activity of H-zeolites.

Iron in zeolites exhibits extremely low ability to activate molecular oxygen for the C_3H_8/O_2 reaction, leading to low yields of propene and carbon oxides, regardless of the Fe species structure. Nitrous oxide, used as oxidant gives higher propene yield together with low concentration of propanol, propanal, methane, ethane, ethene, C_4 and C_6 hydrocarbons as products of cracking and oligomeration reactions.

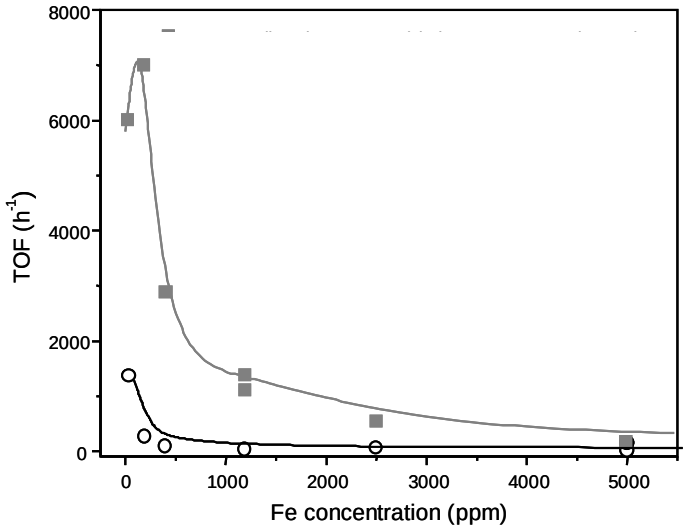

Figure 2 Dependence of TOF (turn-over-frequency) values on Fe concentration in the Fe-MFI catalysts at 450°C and F = 100 ml/min, 5 vol. % propane, 6.5 vol. % oxygen, 10 vol. % N_2O, ○ - propane oxidation by molecular oxygen, ■ - propane oxidation by nitrous oxide

The result emphasizes the decisive role of Fe structures present in the zeolite already at low concentration in the level of impurities in the generation of active sites for oxidation of propane by N_2O (see Figure. 2). Fe-zeolites contain in all instances a spectrum of different Fe species, as indicated by EPR spectroscopy. Reaction kinetic tests suggest that very small part of the well-isolated Fe-species is extremely active in propane oxidation by nitrous oxide following the propane - propanol – propene - propanal – CO_x reaction pathway. As steaming of Fe-zeolites increases substantially the activity of Fe-zeolites, a contribution of Al species removed from the framework might play a significant role [4-6].

Oxidation of propane over Co(Fe)-zeolites by molecular oxygen and nitrous oxide.

Propane oxidation over Co(Fe)-zeolites containing exchanged Co ions and trace concentration of Fe, by using a mixture of molecular oxygen and nitrous oxide, compared to molecular oxygen, leads to much higher propane conversion and yield of propene. Moreover, presence of oxygen and nitrous oxide exhibit a synergetic effect (see Figure 3) [7]. We suggest that specific Fe active centres in the zeolite decompose nitrous oxide into molecular nitrogen and atomic oxygen, and enable its insertion into a hydrocarbon molecule. On contrary, the Co ions catalyse nitrous oxide decomposition to molecular oxygen and nitrogen, but do not stabilize atomic oxygen. They catalyze oxidative dehydrogenation of paraffin to olefins by molecular oxygen. Thus nitrous oxide (a harmful by-product in, e.g., adipic acid plants) added to a stream of oxygen could be exploited for enhancement of selective transformation of paraffins to olefins over Co(Fe)-zeolites.

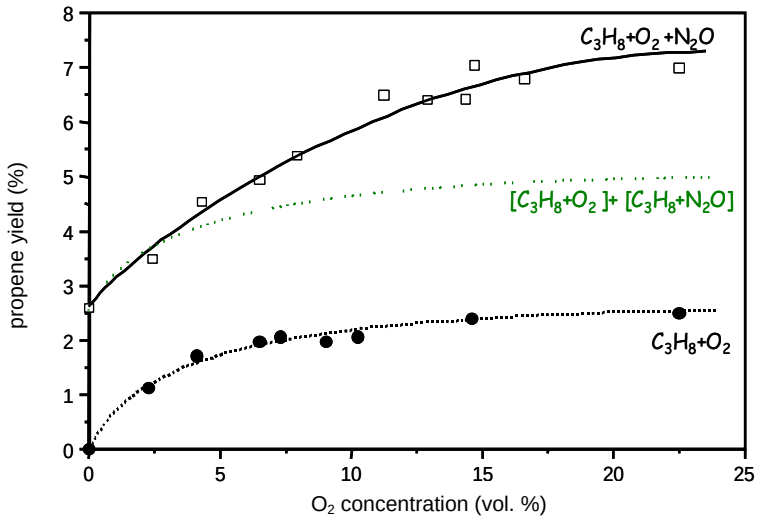

Figure 3 Dependence of propene yield on O_2 concentration over Co*-BEA at 450°C and F = 100 ml/min, 5 vol. % propane, 10 vol. % N_2O, 6.5 vol. % oxygen, ● - oxidation of propane by molecular oxygen, □- oxidation of propane by molecular oxygen and nitrous oxide, … - sum of propene yield after theoretical sum of propene yield from oxidation of propane by molecular oxygen and propene yield of propane oxidation by nitrous oxide

Conclusions

Metallo-zeolites, with the well established redox activity in NO_x reactions, belong also to promising candidates as catalysts for selective transformation of ethane and propane to

corresponding olefins, nitriles or other oxygenates. Understanding of their structure and performance by using molecular oxygen and nitrous oxide brings about a challenge for finding new reaction routes leading to the demanded products.

The present study represents contribution to understanding of some structural effects of metallo-zeolites and thus shows capability and shortcomings of metallo-zeolites with respect to the structure of metal ion species, inner free volume architecture of crystalline structure and application of various reactants (O_2, N_2O and NH_3). The main results are as follows.

(i) It has been found that single Co ions in zeolites, in contrast to Co-oxo and Co oxide-like species leading to complete oxidation, are responsible for selective oxidation of ethane and propane to olefins. Substantially higher activity of Co ions in *BEA and MFI zeolites compared with those in MOR and FER structures is attributed to a high level of accessibility of the most populated β-type Co ions coordinated to the framework in open channels of *BEA zeolite and at intersection of the straight and sinusoidal channels of MFI structure to reaction intermediates.

(ii) Presence of ammonia at the ammoxidation of paraffins results in a strong adsorption of ammonia on Co ion species. Ammonia bound to Co(II) ions increases substantially the rate of paraffin oxidation, and the selectivity and yields of olefins and nitriles. We speculate that the surprising increase of paraffin conversion and high conversion of ammonia to nitrogen might be due to coordination of ammonia and oxygen to the Co ions, oxidation of ammonia to NO_x increasing the rate of paraffin oxidation and leading to molecular nitrogen, and at the same time ammination of olefin formed to alkylamine, which is further oxidized to nitrile.

(iii) Formation of acetonitrile in the ammoxidation of propane is according to the literature caused by Markovnikov rule during the interaction of propene on the secondary carbon. However, it has been found that a surplus of ammonia enhances ammonolysis of acrylonitrile and further oxidation of nitriles to CO_x. Thus optimization of the ammonia concentration to support ammination and suppress nitriles oxidation is necessary.

(iv) As Fe species are present in trace concentrations in zeolites, the observed activity with respect to nitrous oxide decomposition and transfer of an oxygen atom to a paraffin molecule can be explored for selective oxidations. Only a minor part of Fe ion species in Fe-zeolites is extremely active in this oxygen transfer reaction. However, so far there is no conclusion on the structure of this highly active site.

(v) The product composition for series of Fe-zeolites suggests that the oxidation of propane with N_2O over Fe-zeolites follows the reaction pathway from

$$propane + O \rightarrow propanol - H_2O \rightarrow propene + O \rightarrow propanal \rightarrow CO_x$$

(vi) At the ammoxidation of propane with N_2O, ammonia is strongly adsorbed on the Fe active sites necessary for N_2O decomposition and O atom transfer, as no effect (either positive or negative) was observed on the paraffin ammoxidation with nitrous oxide.

(vii) Co(Fe)-zeolites have been revealed as bifunctional catalysts with respect to their function in oxidation of paraffins with molecular oxygen and nitrous oxide. Co ions are suggested to be active in oxidation of paraffins by molecular oxygen to olefins, their Co-oxo species in complete oxidation to carbon oxides. Specific Fe ions (a minor part from Fe species in zeolites) bear an ability to decompose nitrous oxide and transfer an oxygen atom to a hydrocarbon molecule. Moreover, there is some synergetic effect of oxygen and nitrous oxide. It implies a possibility for application of Co(Fe)-zeolites in paraffin oxidation for industrial streams containing both oxygen and harmful nitrous oxide.

References

[1] R. Bulánek, K.Novoveská, B. Wichterlová: Appl. Catal. A: General **235** (2002) 181.

[2] R. Bulánek, K. Novoveská: Pol. J. Chem. **78** (2004) 149.

[3] K.Novoveská, R. Bulánek, B. Wichterlová: Sci.Pap. Univ. Pardubice Ser. **A 9** (2003) 111.

[4] R. Bulánek, B. Wichterlová, K. Novoveská, V. Kreibich: App. Catal. A: **264** (2004) 13.

[5] K. Novoveská, R. Bulánek, B. Wichterlová: Catalysis Today **100** (2005) 315.

[6] R. Bulánek, J. Adam, K. Novoveská, Z. Sobalík, B. Wichterlová: Stud. Surf. Sci. Catal. **158** (2005) 1977.

[7] R. Bulánek, K. Novoveská: React. Kin. Catal. Lett. **80** (2003) 337.

Content

Chapter I

INTRODUCTION

Chapter II

AIM

Chapter III

EXPERIMENTAL

Chapter IV

RESULTS

Chapter V

DISCUSSION

Chapter VI

CONCLUSIONS

Chapter VII

APPENDICES

I.1. Selective oxidation and ammoxidation of paraffins

Nowadays, oxygenates (e.g. maleic anhydride, acrylic acid, furan) and nitriles (acrylonitrile, acetonitrile) are produced from unsaturated hydrocarbons[1]. As the unsaturated hydrocarbons belong to costly raw materials, there is an urgent need for their replacement by cheaper source or new industrial processes leading to these highly requested chemicals. Selective oxidation of light paraffins might be a solution of this important challenge. The advantage in the use of alkanes as alternatives to traditional processes is their low cost (propane is 5-6 times cheaper compared to propene[2]). Moreover, alkanes are less toxic or noxious reactants compared to alkenes and aromatics. Their direct selective oxidation could be used for replacement of energy-demanded processes like dehydrogenation or steam-cracking of paraffins. Light alkanes are obtained as by-products in petroleum processing and as components of natural gas. So far only less than 10 % of natural gas is consumed in chemistry and the rest is consumed in energy production.

Table.I.1 Processes and development of selective oxidation of light alkanes[3]

Raw Material	Product	Stage of development
methane	methanol	pilot plant
methane	syngas	pilot plant
methane	ethene	pilot plant
ethane	acetaldehyde	research
ethane	acetic acid	research
ethane	ethene	research
propane	acrolein	research
propane	propanol	research
propane	propene	research
n-butane	maleic anhydride	process
n-butane	butadiene	process
isobutene	isobutene	research
isobutene	t-butylalcohol	research

Selective oxidations of olefins account of more than 60 % of chemicals and intermediates synthesized via catalytic processes. About 25 % of most important organic chemicals is produced by olefin selective oxidations. The only oxidation industrial processes

using light alkanes are oxidation of butane to maleic anhydride and to butadiene over V-P-O type catalysts[4]. Nevertheless, the effort to optimise the catalyst structures still continues [5,6] (Table I.1).

Thus, two types of processes could be employed to convert light alkanes to requested oxygenates. One way is a direct conversion of alkanes to oxygenates or nitriles, the second one represents two-step process including oxidative dehydrogenation of alkanes to olefins followed by conversion of alkenes to demanded products.

I.1.1 Oxidative dehydrogenation of paraffins

Light alkenes are produced by catalytic dehydrogenation of alkanes at high temperatures, but alkane conversion is limited by thermodynamic equilibrium. Oxidative dehydrogenation of alkanes removes hydrogen from the system, shifting thus the equilibrium completely to the oxidized products. But the products of the selective oxidations, as alkenes, alcohols, aldehydes and organic acids are more reactive than the respective alkanes. This requires tailoring of highly selective catalysts providing activation of alkanes in the presence of alkenes or other oxygenates.

Generally, the selectivity in hydrocarbon oxidation by molecular oxygen is mainly controlled by the state of oxygen species present within the catalyst. With mixed metal oxide systems, like, e.g., Fe-Mo-O, Bi-Mo-O and V-P-O, according to Mars-van Krevelen mechanism[7], the lattice oxygen represents the species responsible for selective oxidations.

Numerous studies have been reported on the oxidative dehydrogenation of propane. High catalytic activity and selectivity in oxidative dehydrogenation was obtained over metal mixed oxide catalysts. These catalysts were based on vanadium (V-Sb-O, V-P-O and V-Mo-O) or molybdenum mixed oxides (Mo-Ni-O, Mo-Co-O)[8,9,10,11]; additional components were Mg or Nb. In the last decade, zeolites or zeolite-like materials were tested as catalyst in this reaction too[12]. The main advantage of zeolitic materials is the possibility to stabilize isolated metal ion sites inside the crystalline matrices. It was found that metal ions exchanged in zeolites, as Co, Cu, Fe and Mn ions in MFI structure[13], were also to some extent active in ethane and propane oxidation with molecular oxygen to corresponding alkenes. A great attention has been paid to catalytic behaviour of vanadium ions supported on zeolitic materials. However, the activity is rather low compared to mixed oxides [11,14,15].

Thus, the activity of both mixed metal oxides and metallo-zeolites in oxidative dehydrogenation of paraffins is still low for industrial application. There is, therefore, a need for tailoring of new catalyst structure for oxidative dehydrogenation of paraffins, highly selective to corresponding alkenes.

I.1.2 Ammoxidation of paraffins

Nitriles are base chemicals for production of polymers, dyes and solvents. Highly demanded are acetonitrile and acrylonitrile, which might be produced by ammoxidation of ethane and propane, respectively.

Nowadays acrylonitrile and acetonitrile are manufactured from unsaturated hydrocarbons – propene and ethene, respectively. The most extended production of acrylonitrile is pursued by SOHIO process (about 90 % of the world production[16]) employing of U-Sb-O or Mo-Bi-O catalysts at 370°C [17].

Development of catalysts for the direct ammoxidation of propane to acrylonitrile over mixed metal oxides based on V-Sb-O[18,19], V-Bi-O[20,21,22], V-Ga-O and Sb-Ga-O[8,23,24] or Mo-V-O[3,25,26] represented a breakthrough in ammoxidation of light paraffins. However, the reaction temperature (500 - 550°C) is 100-150°C higher compared to ammoxidation of propene. Nevertheless, the yield achieved was 35 % at 60 % conversion over the V-Sb-Al-O catalyst [8], and over $V_{0.3}Te_{0.23}MoO_x$ catalyst the yield was 55 % at 87 % of conversion[27]. However, even by addition of trace concentrations of other metals, the yields obtained are still low for industrial production.

Reaction mechanism suggested for propane ammoxidation to acrylonitrile over metal oxide catalysts consists of oxidative dehydrogenation of propane to propene as the first step. It is assumed that acrylonitrile is formed from propene either by direct interaction of allyl complex with adsorbed ammonia or by ammination of aldehyde. “Allyl mechanism” prevails over acid catalysts, whereas the aldehyde pathway predominates over base catalysts [8].

Direct ammoxidation of ethane was tested over series of metal mixed oxides, and the highest catalytic activity exhibited Nb-Sb-O[28,29], Mo-Sc-O[8] and Mo-Cr-O[8] catalysts. However, these systems were not highly selective. Aliev *et al.* [29] found over Cr-Nb-Mo-O catalyst (350 - 500°C) only 10 % selectivity to acetonitrile at 18 % of ethane conversion.

In a marked contrast to propane ammoxidation, the reaction mechanism of ethane ammoxidation does not involve ethene as an intermediate. With mixed V-Mo oxides,

ammonia as a strong reductant forms coordinatively unsaturated reduced molybdenum ions, which bind the active oxygen species. It is assumed that these oxygen species split ethane C-H bond with formation of neutral or positively charged alkyl group. Ammonia then directly reacts with those alkyl groups to surface amine or imine followed by its oxidations to nitrile[8].

In the last decade several reports on the activity of catalysts based on molecular sieves in ammoxidation of hydrocarbons were published[30]. Ammoxidation of ethanol and acetaldehyde to acetonitrile over vanadium on silicoaluminium phosphates were studied[31]. These systems were assumed to replace conventional Sb-V-P-O/Al_2O_3 catalyst.

Armor and Li[32,33] reported high activity in ethane ammoxidation over ion exchanged Co-zeolites. They used Co-zeolites of various topologies of MFI, *BEA, FAU (USY, X, Y), LTA, FER and MOR structures. The highest activity in ammoxidation of ethane to acetonitrile exhibited Co-MFI and Co-*BEA catalysts. The rate of acetonitrile formation over these Co-zeolites was 1 –2 orders higher than over the optimum metal oxide catalysts. The mechanism of ammoxidation of ethane to acetonitrile over Co-zeolites, suggested by Armor and Li[34], involves oxidative dehydrogenation of ethane to ethene as the first step, which afterwards reacts with strongly adsorbed ammonia with formation of ethylamine followed by its dehydrogenation to acetonitrile. By using IR spectroscopy, Wichterlová *et al.* [35] confirmed formation of ethylamine over Co-zeolites as a decisive and thermally stable intermediate. Like with ethane, Co-MFI and Co-*BEA zeolites showed the high activity in propane ammoxidation, but acetonitrile was formed[34]. Derouane *et al.*[36,37] were the only ones who obtained acrylonitrile in ammoxidation of propane over Ga-MFI catalyst but in a very low concentration at high contact time. Thus the activity was of orders lower compared to V-Sb-O oxide-type catalysts.

I.2 Zeolites

I.2.1 Topology and composition of zeolites

Chemical composition of a zeolite is given by formula:

$$M_{2/n}O{\cdot}Al_2O_3{\cdot}SiO_2{\cdot}v\ H_2O$$

where *n* is a valence of cation *M* and *s* ranges from 2 to ∞, and *v* gives the degree of hydration of a zeolite. Structurally the zeolites are complex, crystalline inorganic polymers based on an extending three-dimensional framework of TO_4 tetrahedra (where T is Al or Si).

Formula of zeolites based on crystallographic unit cell is represented by:

$$M_{x/n}[(AlO_2)^-_x(SiO_2)_y] \cdot zH_2O$$

where *n* is a valence of cation *M*, *x*, *y* and *z* are numbers of alumoxane, siloxane units and water molecule per unit cell, respectively.

Structural unit of zeolites is tetrahedron TO_4 (T = Si,Al), where the central atom T is coordinated to four oxygen atoms. Bridging oxygens, which enclose the central atom, connect individual tetrahedra and they are located in vertexes of corresponding tetrahedra. Two adjacent T atoms are connected only by one oxygen bridge; hence there is no connection by edge or by area of a tetrahedron. These tetrahedra are ordered into 4-12 membered rings combined into three-dimensional structure formed by a system of channels and cavities in various arrangements. Topologies differ from each other by channel ordering size of pores and presence of cavities[16].

The number of aluminum tetrahedra in the framework determines negative charge of the framework, which is compensated by inorganic (NH_4^+, Na^+, Li^+, K^+, Ca^{2+}, Ba^{2+}, Cs^{2+}, transition metal cations) or organic cations (e.g. amines used as templates) in extra-framework positions.

The framework composition is controlled by the Loewenstein rule excluding Al-O-Al sequences. Thus, the minimum Si/Al ratio equal to 1 can be achieved, but there is no limit at high Si/Al values (up to ∞). The concentration of Al in the framework determines its negative charge and thus ability to charge balance metal cations, ammonium ions or protons.

The other presumptions for zeolite synthesis are Dempsey rule[38], determining that alumoxane AlO_2^- units occupy the most distant positions to each other, and Takaishi rule forbidding two Al atoms located in one 5-member ring[39]. The six-membered rings can contain two aluminium atoms (Al pairs) in one framework zeolite ring as confirmed by both the theory and the experiment[40,41]. Occurrence of single Al atoms or aluminum pairs in six or eight –membered framework rings enables bonding of polyvalent cations and affects properties of metal cations in cationic sites[42]. Therefore, analysis of distribution of aluminium in the framework has started to be in the centre of interest. Wichterlová *et al.* [43,44] identified distribution of Al pairs in the rings of cationic sites of MFI zeolites of different compositions. Dědeček *et al*.[45,46] showed how the conditions of synthesis of MFI zeolites and the process of zeolite dealumination affect Al distribution.

In general there is a great variety of zeolite structures with various channel systems and ordering. Zeolites of ZSM-5, mordenite, ferrierite and beta structures (according to IUPAC nomenclature MFI, MOR, FER and *BEA topology, resp.) represent the most applied

zeolites in novel catalytic processes. Their framework is composed mainly from pentasil rings interconnected into 6- and 8- membered rings. The maximum concentration of aluminium in the framework, which can be achieved in these zeolites, corresponds to Si/Al ratios of 12, 6, 6 and 13 for MFI, MOR, FER and *BEA, respectively. The sizes of the channel, chemical formulas and structures of these zeolites are shown in Figures I.1- I.4.

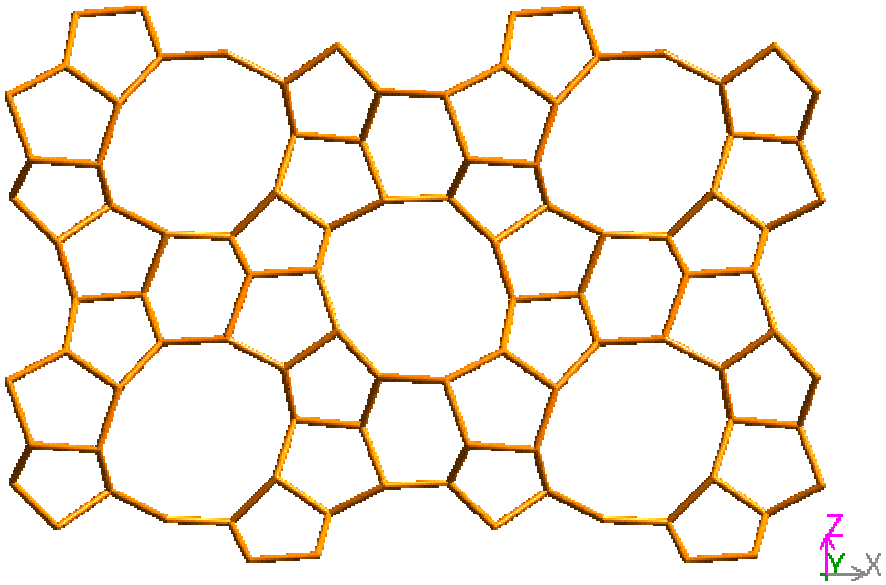

Figure I.1 Structure of ZSM-5 (MFI) - $Na_n[Al_nSi_{96-n}O_{196}]$~16 H_2O (Si/Al>12), ring-openings: **10 –** 5.3 x 5.6 Å, **10 –** 5.1 x 5.5 Å,

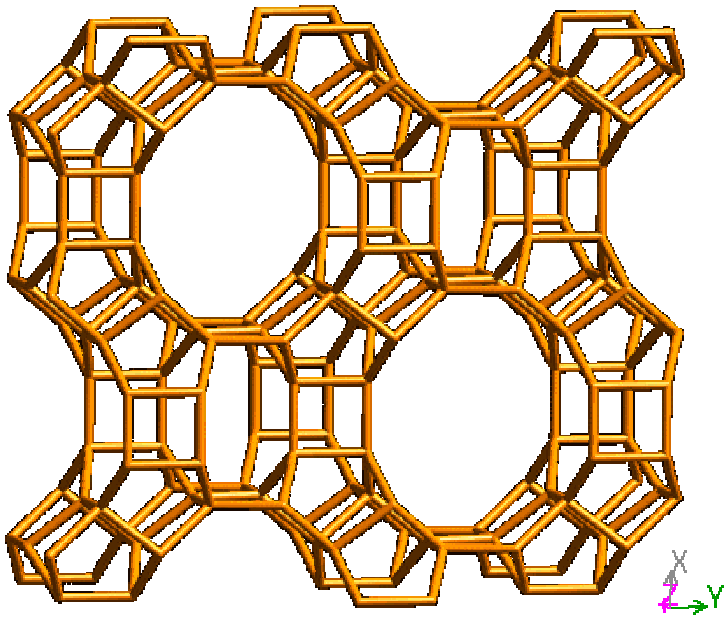

Figure I.2 Structure of mordenite (MOR) - $Na_8[Al_8Si_{40}O_{96}]$~24 H_2O (Si/Al=6-∞), ring-openings: **12 –** 6.5 x 7.0 Å **8 –** 2.6 x 5.7 Å

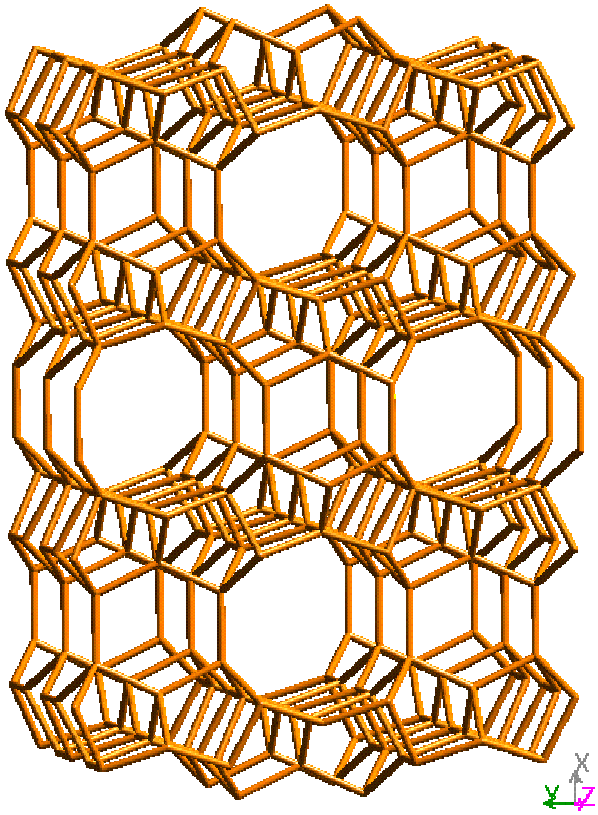

Figure I.3 Structure of ferrierite (FER) - $Na_2Mg_2[Al_6Si_{30}O_{72}].18\ H_2O$ (Si/Al=6-∞), ring-openings: **10 –** 4.2 x 5.4 Å **8 –** 3.5 x 4.8 Å

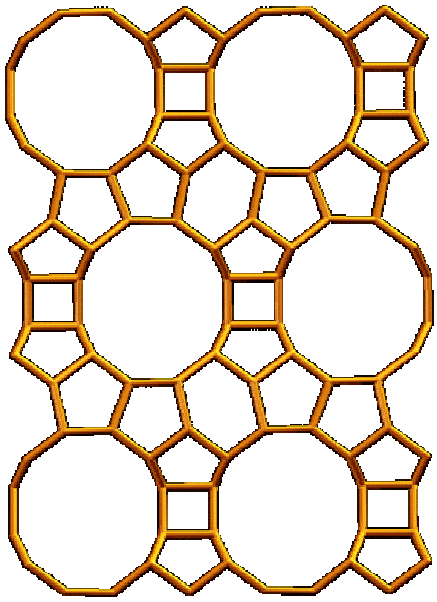

Figure I.4 Structure of beta (*BEA) - $Na_n[Al_nSi_{96-n}O_{196}]$~16 H_2O (Si/Al=13-∞), ring-openings: **12 –** 5.5 x 5.5 Å**12 –** 7.6 x 6.4 Å

I.2.2 Properties and utilization of zeolites

The dimension and architecture of channels and cavities control one of the important properties of zeolites –molecular sieving -, because the size of pores is comparable with the kinetic diameter of organic molecules. Therefore, a suitable choice of the zeolite - molecular sieve - structure can exclude some reactants or products (or even intermediates) from a given catalytic reaction.

Fundamental catalytic properties are controlled by composition of the zeolite, as concentration of active metal/metal ion sites and protonic acidic sites. Zeolites might contain some cations in the framework positions, e.g. Fe [47], Ga [48], In [49] and a wide range of metal ions in extra-framework positions (both mono-, di- and trivalent cations). If located in cationic sites they are atomically dispersed and usually exhibit open coordination sphere, resulting in high accessibility and reactivity of these cations to reactants. Moreover, the presence of negatively charged electric field of the surrounding framework, significantly modifies redox properties, which in combination with acidic sites provide metallo-zeolites with unique catalytic behaviour, non-attainable with solids based on metal or mixed metal oxides [50]. Therefore, zeolites, zeotype molecular sieves and other microporous materials are successfully utilized in adsorption, separation and heterogeneous catalytic processes. Their world production reaches about one million tons per year. Zeolites are used in 80 % as ion-exchangers, 8 - 10 % as adsorbents and 10 - 12 % as catalysts[29,51].

Since 1962 H-forms of zeolites are used as acid-base catalysts e.g. petroleum cracking over X and Y zeolites. Other processes employing shape-selective properties of zeolites are, e.g., production of ethylbenzene, disproportionation of toluene to benzene and xylenes, isomerization of xylenes [52], and transalkylation reactions. Zeolite based catalysts containing ion-exchanged transition metal ions are expected to find application in processes of redox catalysis, e.g. decomposition of NO [53] and N_2O, selective catalytic reduction of NO [54] and selective oxidations of paraffins[55].

I.2.3 Metallo-zeolites related to catalysis

Transition metal ions could be present in several types of species in extra-framework positions in zeolites, as shown in Figure I.5. Metal ions could be bound as “bare” ions, dimers with bridging oxygen, oxo-like species or supported small oxide clusters; if the latter are

present they are usually formed by precipitation on the crystal catalyst surface. The presence of different types of individual metallo-species and the framework cation (guest–host) interactions provide extraordinary redox properties of cations not found for metal oxide systems.

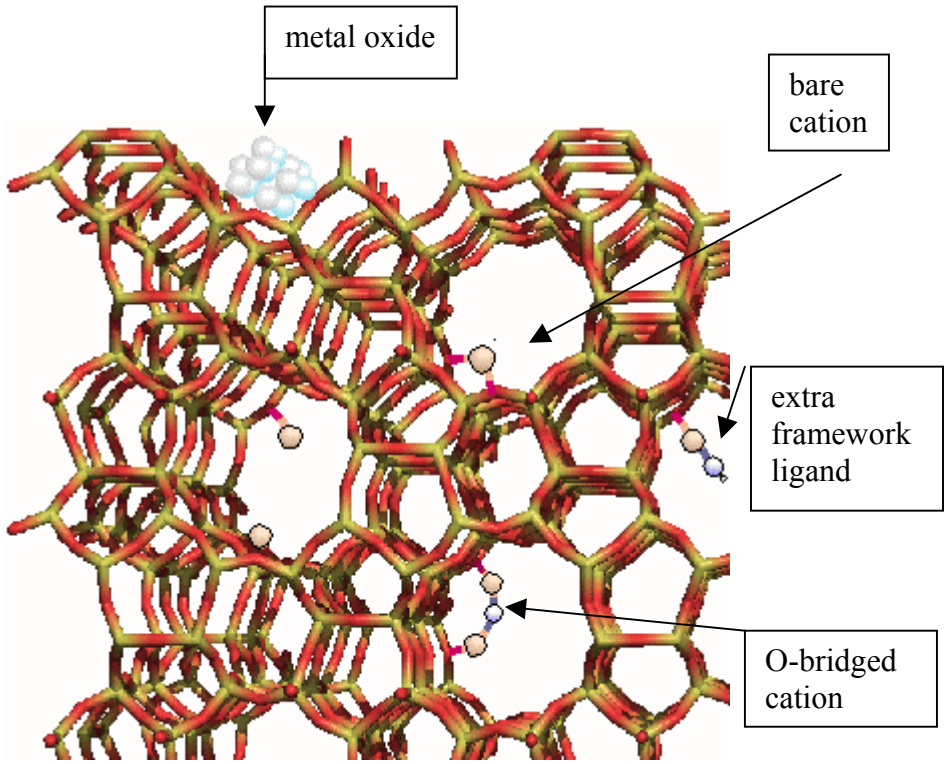

Figure I.5 Transition metal ions in extra-framework positions present in zeolite

Among metal cations, highly interesting with respect to redox behavior and catalytic function, have appeared namely Co, Cu and Fe ions[56]. The divalent state of Co is highly stable, persisting oxidation by molecular oxygen and reduction by hydrogen even at high temperatures[57]. With respect to catalytic reactions, Wichterlová et al. studied cobalt-zeolites in selective catalytic reduction of NO by methane in excess of oxygen on cobalt ions located in zeolites of MFI, FER, MOR, CHA and *BEA[58,59,60]. For the purpose of analysis of the activity of the individual Co ions they determined three different types of coordination of cobalt ions in zeolites of MFI[61], FER[62], *BEA[63] and MOR[64] structures by means of a set of spectral techniques involving UV-Vis-NIR and FTIR spectroscopy, and EXAFS[65]. Three different Co ion types denoted as α, β and γ types were found in the each zeolite in different population. The α-type Co ions are coordinated to four oxygens on the wall of main channel, β-type Co ions are coordinated to four oxygens in deformed 6-member (8-membered in MOR) ring and γ-type Co ions are coordinated in the boat shape site[66]. The positions of

cobalt ions in zeolite rings are shown in Figure I.6 and the positions in the structures of individual topologies are shown in Figure I.7.

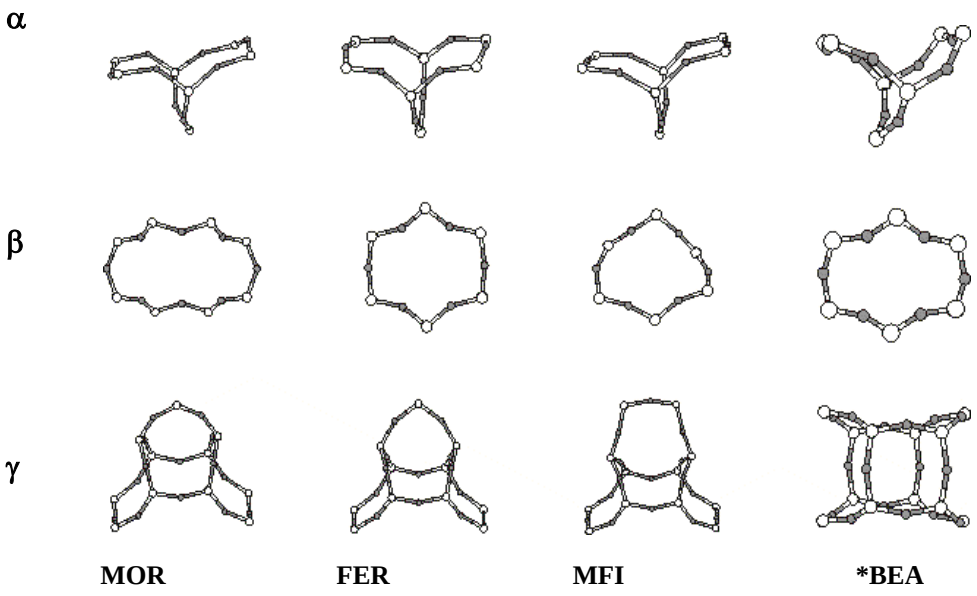

Figure I.6 Cobalt coordination in the framework rings

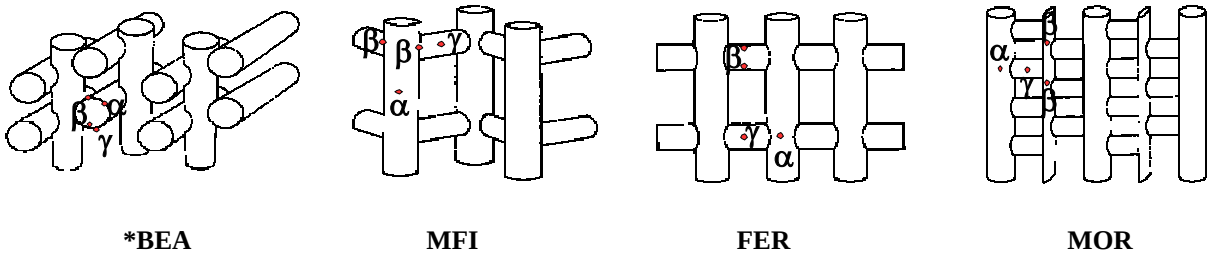

Figure I.7 Cobalt ion positions in the zeolite structures

Copper ions in Cu-MFI[54,67] is the most active catalyst in NO decomposition in the temperature range from 350 - 550°C. Cu-zeolites were also suggested as catalysts in selective catalytic reduction by light paraffins in the excess of oxygen[72], because they exhibit high activity at lower temperatures compared to other metallo-zeolites. Copper ions could be introduced into zeolite as divalent cation, balanced by Al pairs in the framework, or as monovalent Cu(II) complexes adjacent to single Al atom. In contrast to cobalt cations copper exhibits redox behaviour during these reactions, and it can be easy oxidized by oxygen and

reduced by both carbon oxide and hydrogen. Bulánek[68]discussed copper behaviour in oxidation of hydrocarbon and reducibility of copper. Hydrogen reduces divalent copper step by step up to metallic state and carbon oxide as an inferior reducing agent forms predominantly monovalent copper from divalent cation [69,70].

Fe ions introduced in zeolites can be in a divalent or trivalent state. The Fe(III) ions could be stabilized as metal-ligand complexes (as OH^- or O^-). Redox behaviour of iron species was observed during the catalytic experiments. Iron was easily oxidized by molecular oxygen, nitrous oxide and nitric oxide. Moreover, during the reaction with N_2O iron exhibited qualitatively new, catalytic behaviour. Easy decomposition of nitrous oxide leads to formation of atomic oxygen, which is a highly selective oxidant providing insertion of an oxygen atom into a hydrocarbon molecule[71]. The most successful catalyst and corresponding process has been developed for benzene hydroxylation with nitrous oxide to phenol over Fe-MFI catalyst by Panov`s group and scaled up by Monsanto Co [72]. Panov *et al.* [73,74,75,76] have also shown that, e.g., methane can be oxidized with N_2O to methanol, but at the temperature needed for the desorption of methanol, it is further oxidized to carbon oxides.

Although that the hydroxylation activity of H-MFI (with trace concentrations of iron) and Fe-MFI catalysts has at first been attributed to the protonic and Al-Lewis sites[77], it has then been evidenced[78,79] that low concentration of Fe in H-MFI zeolites plays a decisive role in the oxidation reactions. Particularly, the Fe ions released from the zeolite framework into the extra-framework positions at high calcination temperatures or by the zeolite steaming exhibit extremely high activity[79]. Low concentration of iron also prevents formation of bulk iron oxide, which might, on the other hand, enhance hydrocarbon combustion. The concentration of the so-called α-oxygen formed by N_2O decomposition in the zeolite, correlated well with the concentration of Fe in the zeolite. Mössbauer and EXAFS studies of Fe zeolites revealed presence of the dinuclear Fe complexes bearing bridging oxygen atoms[80]. However, a clear straightforward correlation between the concentration of these sites and zeolite hydroxylation activity was not found so far. Thus the question if the active site is represented by a dinuclear (Fe-O-Fe) or mononuclear (Fe-O) species is still open.

I.3 Approaches for analysis of the structure of metallo-zeolite catalyst and its function in catalysis

In general there are several spectral and diffraction techniques, which might be applied for analysis of the crystalline structure of zeolites, structure of metal ion species and reactivity of the metallo-zeolites catalysts. Nevertheless, to obtain relevant information on the structure of potential active sites an appropriate combination of selected techniques has to be used. The selection of techniques depends on the type and nature of the solid catalyst and expected active sites.

With metallo-zeolite catalysts the crystalline structure of a zeolite phase is determined by powder XRD and the degree of crystallinity can be estimated from the intensity of XRD patterns and the intensity of characteristic skeletal IR vibrations. The structure and surrounding of the potential active sites, i.e. metal ion and/or metal-oxo species, and protonic sites can be analyzed via determination of their coordination and/or via information obtained through adsorption of probe molecules. The coordination of metal ion centers is reflected in d-d electronic transitions and that of metal-oxygen type species in charge transfer transitions. They both can be advantageously monitored by the spectra in UV-Vis region. If metal ions in zeolites are coordinated in the cationic sites, then they perturb framework T-O-T bonds, reflected in characteristic IR spectra. Further methods like electron spin resonance - ESR (if metal ions or their complexes are paramagnetic) and Moessbauer spectroscopy (e.g. for Fe species) could provide additional information on the valence state and coordination of the cations. Extended X-ray Absorption Spectroscopy (EXAFS) yields metal-oxygen and metal-metal distances and coordination numbers of the cations, but the method provides average values for a given metal ion in the solid material, and hardly can distinguish the individual sites. X-ray photoelectron spectroscopy (XPS) is a method selective to surface and sub-surface layers (ca 50 Å). Therefore, it provides information rather on the surface oxide-like species in zeolites than on the metal ion species located inside the channels of the zeolite. As examples of using these techniques in analysis of the structure of metallo-zeolite catalysts are given in Refs. 60-65, 76 and 81.

Usually the approaches for studying catalyst structure and from that related structure of potential active sites employ the spectral and diffraction techniques for catalysts pretreated at certain conditions at high temperatures, but thereafter measured at "*ex-situ*" conditions usually at temperatures close to ambient one in vacuum or in a given atmosphere. However, the last development in selected spectroscopy techniques, i.e. their equipment with the high-

temperature through-flow cells and on-line connected dosing system for reactants and product analysis, enables to monitor the spectra at "*in-situ*" conditions of the true catalytic reactions. This represents a dramatic step ahead in providing for knowledge of the state of catalysts under the given performance of the catalytic reaction. Moreover, using, e.g., step changes in concentration of the individual reactants yields information distinguishing between the surface non-reactive deposits and real reaction intermediates. Thus, there are now available additional information contributing to understanding of the structure of sites, reaction intermediates and reaction mechanism at the conditions of the catalytic reaction.

The overview shows that there is a need for development of catalyst structure for both oxidative dehydrogenation to olefins and ammoxidation to nitriles of C_2 and C_3 paraffins. One way could be via development of highly mixed metal oxides. The other system showing some potential is based on transition metal ions in zeolite matrices. In such solids, the properties of metal ions can be tuned by metal ion coordination, guest-host interactions between cation species and the matrix, and the structure of metal ion species. With the advanced diffraction and spectral techniques presently available some progress can be expected in tailoring of metallo-zeolite catalysts based on the understanding of their structure and functioning on a molecular level.

I.4 References

[1] G.Centi, F. Cavani, F. Trifiro; Selective Oxidation by heterogeneous catalysis, Kluwer Academic , New York 2001.

[2] G. Centi, R.K. Grasselli, F. Trifiro; Catal. Today **13** (1992) 661.

[3] F.Trifiro Proceeding 3rd EFCATS School on Catalysis (2004).

[4] G.Emig, F. Martin; Catal. Today **1** (1987) 447.

[5] Y. Takita, T. Hashiguchi, H. Matsunosako; Bull. Chem. Soc. Jpn **61** (1988) 3737.

[6] J. Haber, R. Tokarz, M. Witko; Abstr. Pap. Am. Chem. Soc. **211** (1996) 207.

[7] A. Bielanski, J. Haber, Oxygen in Catalysis, Marcel Dekker, New York (1996) 139.

[8] H.H. Kung; Adv. Catal. **40** (1994) 1.

[9] F. Cavani, F. Trifiro; Catal. Today **24** (1995) 307.

[10] D.L. Stern, R.K. Grasselli; Stud. Surf. Sci. Catal. **110** (1997) 367.

[11] D. Levin, J.Y. Ying; Stud. Surf. Sci. Catal. **110** (1997) 367.

[12] P. Concepcion, J.M. Lopez Nieto, J. Peréz Pariente; Catal. Lett. **19** (1993) 558.

[13] K. Nowinska, A. Waclaw, A. Izbinska; Appl. Catal. A: General **243** (2003) 225.

[14] M.L. Pena, A. Dejoz, V. Fornés, F. Rey, M.I. Vazquez, J.M.Lopez Nieto; Appl. Catal. A: General **209** (2001) 155.

[15] M. Okamoto, L. Luo. J.A. Labinger, M.E. Davis; J. Catal. **192** (2000) 128.

[16] J.C. Védrine; 1st EFCATS School on Catalysis, Praha, (2001).

[17] J.D. Idol; US Patent 2904 580: Chem. Abstr. **54** 5470f (1959).

[18] S. Albonetti, G. Blackhard, P. Burattin, S. Masetti, F. Trifiro; Stud. Surf. Sci. Catal. **110** (1997) 403.

[19] J. Nilsson, S.R. Landa-Canoras, S. Hansen, S. Andersson; Stud. Surf. Sci. Catal. **110** (1997) 413.

[20] Y.C. Kim, W. Ueda, Y. Moro-Oka; Stud. Surf. Sci. Catal. **55** (1990) 491.

[21] Y.C. Kim, N. Miwa, W. Ueda, Y. Moro-Oka; Catal. Sci. technol. **1** (1990) 439.

[22] G. Minow, K.H. Schnabel, G. Ohlmann; React. Kinet. Catal. Lett. **22** (1983) 399

[23] S.Y. Burylin, Z.G. Osipova, V.D. Sokolovskii, I.P. Olenkava, B.V. Kalinkin, B.V. Paskis; Kinet. Katal. **30** (1989) 1251.

[24] S.Y. Burylin, Z.G. Osipova, V.D. Sokolovskii; Kinet. Katal. **24** (1983) 639.

[25] Y.C. Kim, W. Ueda, Y. Moro-Oka; Catal. Today **13** (1992) 673.

[26] J.P. Bartek, A.T. Guttmann; US Patent 4 797 381: Chem. Abstract **110**: 142305s (1989).

[27] K. Oshama, A. Kayo, T.K. Umezana, K. Kigono,I. Sawagki; EP 529 853: Chem. Abstract **119**: 139968r (1992).

[28] R. Catani, G. Centi; J. Chem. Soc.; Chem. Commun. (1991) 1081.

[29] S.M. Aliev, V.D. Sokolovskii, G.B. Boreskov; USSR Patent SU 738 657: Chem. Abstract **93**: 121053y (1980).

[30] G. Centi, P. Jírů, F. Trifiro; Stud. Surf. Sci. Catal. **44** (1989) 247.

[31] S.J. Kulkarni, R.R. Ramachandra, M. Subrahmanyaam, A.V. Rama Rao; J. Chem. Soc., Chem. Commun. (1994) 273.

[32] Y. Li, J.N. Armor; J. Chem. Soc.; Chem. Commun. (1997) 2013.

[33] Y. Li, J.N. Armor; J. Catal. **173** (1993) 511.

[34] Y.Li, J.N. Armor; J. Catal. **176** (1998) 495.

[35] B. Wichterlová, Z. Sobalík, Y.Li, J.N. Armor; Proceedings 12th International Congress on Catalysis, Granada (2000), Stud. Surf. Sci. Catal. **130B** (2000) 869.

[36] A.H.S.B. Derouane, P. Pal, H. He, E.G. Derouane; Catal. Today **64** (2001) 129.

[37] A.H.S.B. Derouane, G. Centi, P. Pal, E.G. Derouane; Topics Catal. **15** (2001) 161.

[38] S.T. Wilson; Stud. Surf. Sci. Catal. **58** (1991) 137.

[39] T.Takaishi, M. Kato; Zeolites **15** (1995) 689.

[40] M. Hunger, M.W. Anderson, A. Ojo, H. Pfeifer; Microporous Mater. **1** (1993) 17.

[41] K.P. Schroeder, J. Sauer; J. Phys. Chem. **97** (1993) 6578.

[42] B. Wichterlová, J. Dědeček, Z. Sobalík; Proceedings 12th International Zeolite Conference, Baltimore (1998) p. 941, Mat. Res. Soc. Warrendale (1998).

[43] J. Dědeček, D. Kaucký, B.Wichterlová, O. Gonsiorová, Phys. Chem. Chem. Phys., **21** (2002) 5406-5413.

[44] J. Dědeček, D. Kaucký, B. Wichterlová, Chem. Commun., **11** (2001) 970-971.

[45] V. Gábová, J. Dědeček, J. Čejka; Chem. Commun. **10** (2003) 1196

[46] J. Dědeček, V. Gábová, B. Wichterlová: Stud. Surf. Sci. Catal. **142** (2002) 1817.

[47] G.I. Panov, A.K. Uriarte, M.A. Rodkin, V.I. Sobolev; Catal. Today **41** (1998)365.

[48] J.J.Kim, S.J. Lee, J.S. Yu; Bull. Korean Chem. Soc. **21** (2000) 544.

[49] J. Halasz, Z. Konya, A. Fudala, A. Béres, I. Kirisci; Catal. Today **31** (1996) 293.

[50] J.N. Armor; Micropor. Mesopor. Mat. **22** (1998) 451.

[51] Ullman's Encyclopedia of Industrial Chemistry, 5th edition, vol. A 28. VCH Weinheim (1996).

[52] N.S. Gnep, J. Tejada, M. Guisnet; Bull. Soc. Chim. Fr. **I** (1982) 5.

[53] M. Iwamoto, H. Furukawa, Y. Mine, F. Uemura, S. Mikuriya, S. Kagawa; J. Chem. Soc., Chem. Commun. (1986) 1272.

[54] M. Iwamoto, H. Yahiro, S. Shundo, Y. Yu-u, N. Mizuno; Shokubai (Catalyst) **32** (1990) 430.

[55] A. Aucejo, M.C. Burguet, A. Corma, V. Fornes; Appl. Catal. **22** (1986) 187.

[56] T. Sun, M.L. Trudeau, J.Y. Ying: J. Phys. Chem. **100** (1996) 13662.

[57] E.M. El-Malki, D. Werst, P.E. Doan, W.M.H. Sachtler: J. Phys. Chem. **104** (2000) 5924.

[58] D. Kaucký, J. Dědeček, A. Vondrová, Z. Sobalík, B. Wichterlová; Collect. Czech. Chem. Commun. **63** (1998) 1781.

[59] D. Kaucký, A. Vondrová, J. Dědeček, B. Wichterlová; J. Catal. **194** (2000) 318.

[60] J.Dědeček, D. Kaucký, B. Wichterlová; Topics Catal. **18** (2002) 283.

[61] J. Dědeček, D. Kaucký, B. Wichterlová; Micropor. Mesopor. Mater. **35** (2000) 483.

[62] D. Kaucký, J. Dědeček, B. Wichterlová; Micropor. Mesopor. Mater. **31** (1999) 75.

[63] J. Dědeček, L. Čapek, D. Kaucký, Z. Sobalík, B. Wichterlová; J. Catal. **211** (2002) 198.

[64] J. Dědeček, B. Wichterlová; J. Phys. Chem. **103** (1999) 1462

[65] L. Drozdová, R. Prins, J. Dědeček, Z. Sobalík, B. Wichterlová; J. Phys. Chem. B **106** (2002) 2240.

[66] W.J. Mortier; Compilation of Extra-Framework Sites in Zeolites, Butterwords, London, 1982.

[67] B. Wichterlová, J. Dědeček, Z. Sobalík, A. Vondrová, K. Klier; J. Catal **169** (1997) 194.

[68] R.Bulánek, B. Wichterlová, Z. Sobalík, J. Tichý; Appl. Catal. B: Environmental **31** (2001) 13.

[69] R. Bulánek, P. Čičmanec, P. Knotek, D. Nachtigallová, P. Nachtigall; PCCP, **6** (2004) 2003.

[70] O. Bludský, P. Nachtigall, P. Čičmanec, P. Knotek, R. Bulánek; Catal. Today **100** (2005) 385.

[71] K.A. Dubkov, V.I. Sobolev, E. Talsi, M.A. Rodkin, N.H. Watkins, A.A. Steinman, G.I. Panov; J. Mol. Catal. A **123** (1997) 155.

[72] A.K. Uriarte, M.A. Rodkin, M.J. Gross, A.S. Kharitonov, G.I. Panov; in 3rd World Congress on Oxidation Catalysis (R.K. Grasselli, S.T. Oyama, A.M. Gaffney and J.E. Lyon, eds.) Stud. Surf. Sci. Catal. **110** (1997) 857.

[73] G.I. Panov, A.S. Kharitov, V.I. Sobolev; Appl. Catal. A: General **98** (1993) 1.

[74] G.I. Panov, A.K. Uriarte, M.A. Rodkin, V.I. Sobolev; Catal. Today **41** (1998) 365.

[75] G.I. Panov, G.A. Sheveleva, A.S. Kharitonov, V.N. Romannikov, L.A. Vostrikova; Appl. Catal.A: General **82** (1992) 31.

[76] G.I. Panov, V.I. Sobolev, A.S. Kharitonov; J. Mol. Catal. **61** (1990) 85.

[77] V.I. Zholobenko, I.N. Senchenya, L.M. Kustov, V.B. Kazansky; Kinet. Catal., **32** (1991) 151.

[78] P. Kubánek, B. Wichterlová, Z. Sobalík; J. Catal. **211** (2002) 109.

[79] J. Pérez-Ramírez, F. Kapteijn, G. Mul, J.A. Moulijn, A.R. Overweg, A. Doménech, A. Ribera, I.W.C.E. Arends; J. Catal. **207** (2002) 113.

[80] P. Marturano, L. Drozdová, A. Kogelbauer, R. Prins; J. Catal. **192** (2000) 236.

The study has been aimed at analysis of the structure and reactivity of Co- and Fe-zeolites and exploitation of this knowledge for understanding of the oxidation and ammoxidation of low chain paraffins to olefins, aldehydes and nitriles by molecular oxygen and/or nitrous oxide. The main questions have concerned the effect of the nature and type of metal ion species and topology of zeolite matrix on the catalyst activity. It has been expected that such study would contribute to understanding of the function of metallo-zeolite catalysts in oxidation of paraffins by both molecular oxygen and atomic oxygen formed via N_2O decomposition, and thus to contribute to a design of a new type of oxidation catalysts and reaction routes.

Besides reaction kinetic measurements, the UV-Vis and FTIR spectroscopy techniques have been mainly employed to obtain information on the state, structure and behaviour of potential active sites and surface reaction intermediates. For selected cases of oxidation and ammoxidation of paraffins *in-situ* UV-Vis and *in-situ* FTIR spectra of Co zeolites were monitored at true reaction conditions to obtain more realistic picture on the cobalt state and reaction intermediates. While UV-Vis spectra provided information on the unusual coordination of the individual Co ions at various structural sites and the Co-oxo species, FTIR spectra yielded information on the perturbations of the framework T-O-T bonds adjacent to the individual Co ions at structural sites as well as on the reactant molecules and reaction intermediates sorbed on the surface.

III.1 Catalyst preparation

III.1.1 Parent H-zeolites

Na-MFI zeolite (Si/Al 22.6 and 12.5) was kindly provided by the Institute of Oil and Hydrocarbon Gases, Slovnaft, Slovakia. Na,K-FER and NH_4-MOR were purchased from TOSOH Co., Japan. NH_4-MFI was prepared from Na-MFI zeolite by repeated ion exchange with 1 M NH_4NO_3 solution (10 g of a zeolite per 150 ml of solution at 80 °C over night). NH_4-FER was prepared from Na,K-FER by the repeated exchange with 1 M NH_4NO_3 solution at 70 °C (1000 ml of solution per 20 g of a zeolite). Both zeolites were after ion exchange washed several times with distilled water, filtered and dried on an open air at room temperature (RT). NH_4-*BEA with Si/Al ratio 13 was kindly provided by the Research Institute of Inorganic Chemistry, Inc., Unipetrol (CZ). NH_4-*BEA zeolite with Si/Al ratio 12.4 was purchased from PQ Corp., USA, and NH_4-*BEA zeolite with Si/Al ratio 17.6 was synthetized according to the procedure given elsewhere [1,2]. Si/Al ratios and concentration of iron are given in Table III.1.

Table III.1 Si/Al ratio and concentration of Fe in parent zeolites

Parent zeolite	Si/Al	Fe (ppm)
H-MFI	22.6	550
	12.5	300
H-*BEA	13.0	450
	12.4	400
	17.6	600
H-FER	9.5	300
	8.6	350
H-MOR	9.4	400

III.1.2 Cu-zeolites

Cu ions were introduced by ion exchange of the NH_4-forms of MFI, *BEA, and FER zeolites with copper (II) nitrate and copper (II) acetate solutions. After ion exchange, the solids were thoroughly washed with redistilled water, filtered and dried on air at RT.

Conditions of preparation of zeolites and their chemical compositions are given in Table III.2. The samples are marked as copper-zeolite-Si/Al molar ratio-Cu/Al molar ratio-Cu content in wt. % (e.g. Cu-*BEA-13.5-0.3-1.6).

Table III.2 Conditions of preparation and chemical composition of the Cu-zeolites

Sample	Time (h)	T (°C)	Solution	m_{zeol}/V_{sol} (g/ml)	Cu wt. %
Cu-MFI-22.6-0.28-1.1	12	25	0.01M $CuCl_2$	1/20	1.1
Cu-*BEA-13.5-0.3-1.6	12	25	0.01M $Co(Ac)_2$	1/250	1.6
Cu-FER-9.5-0.25-2.2	24	25	0.001M $Co(Ac)_2$	1/1000	2.3

III.1.3 Co-zeolites

Co ions were introduced by ion exchange of the NH_4-forms of MFI, *BEA, MOR and FER zeolites with cobalt (II) nitrate and cobalt (II) acetate solutions. After ion exchange, the solids were thoroughly washed with redistilled water, filtered and dried on air at RT.

Conditions of preparation of zeolites and their chemical compositions are given in Table III.3. The samples are marked as cobalt-zeolite-Si/Al molar ratio-Co/Al molar ratio-Co content in wt. % (e.g. Co-*BEA-13.0-0.5-2.6).

Table III.3 Conditions of preparation and chemical composition of the Co-zeolites and results of TPR experiments (average oxidation number)

Sample	repetion x time (h)	T (°C)	Solution	m_{zeol}/V_{sol} (g/ml)	Co wt. %	n_e/n_{Co}*
Co-*BEA-13.1-0.15-1.0	1x6	25	0.05M $Co(NO_3)_2$	1/160	1.0	2.08
Co-*BEA-12.4-0.25-1.8	1x8	25	0.01M $Co(Ac)_2$	1/67	1.8	1.97
Co-*BEA-13.1-0.30-1.8	1x12	25	0.05M $Co(NO_3)_2$	1/100	1.8	2.06
Co-*BEA-13.1-0.32-2.0	2x8	60	0.01M $Co(NO_3)_2$	1/80	2.0	nd
Co-*BEA-12.3-0.40-2.1	2x12	25	0.01M $Co(NO_3)_2$	1/100	2.1	nd
Co-*BEA-13.0-0.50-2.7	2x12	60	0.05M $Co(NO_3)_2$	1/80	2.7	2.11

Co-*BEA-13.0-0.6-3.1	3x7	70	0.05M $Co(NO_3)_2$	1/100	3.1	1.91
Co-*BEA-11.9-0.60-3.2	2x12	25	0.01M $Co(NO_3)_2$	1/100	3.2	1.91
Co-*BEA-13.1-0.87-4.7	2x7	70	0.05M $Co(Ac)_2$	1/71	4.7	1.93
Co-*BEA-13.1-1.17-7.8	3x12	70	0.01M $Co(Ac)_2$	1/100	7.8	2.44
Co-*BEA-13.8-0.5-2.8	1x12	25	0.05M $Co(NO_3)_2$	1/100	2.8	nd
	1x24	25	0.1M $Co(NO_3)_2$	1/100		
Co-*BEA-17.6-0.39-1.7	1x12	25	0.05M $Co(NO_3)_2$	1/16		
	1x24	25	0.075M $Co(NO_3)_2$	1/16	1.7	nd
	1x48	25	0.1M $Co(NO_3)_2$	1/16		
Co-MFI-12.5-0.23-1.6	1x7	70	0.05M $Co(Ac)_2$	1/16	1.6	nd
	1x17	25	0.05M $Co(Ac)_2$	1/16		
Co-MFI-12.5-0.42-2.9	2x12	70	0.05M $Co(Ac)_2$	1/16	2.9	nd
Co-MFI-12.5-0.55-3.8	3x12	70	0.1M $Co(Ac)_2$	1/16	3.8	nd
Co-FER-9.4-0.23-1.0	1x2	60	0.05M $Co(NO_3)_2$	1/83	1.0	nd
	1x4	60	0.05 M $Co(NO_3)_2$	1/83		
Co-FER-8.6-0.42-3.6	5x10	70	0.01M $Co(Ac)_2$	1/16	3.6	nd
Co-MOR-9.4-0.48-2.1	1x2	60	0.05M $Co(NO_3)_2$	1/50	2.1	nd
	1x4	60	0.05M $Co(NO_3)_2$	1/50		

*n_e/n_{Co} – number of electrons per Co ion consumed at H_2-TPR, see part III.3

III.1.4 Fe-zeolites

H-MFI zeolites (originally NH_4-MFI) with different iron content and treated at various conditions were used. NH_4-MFI (Si/Al = 28) with only trace concentration of Fe (30 ppm) and NH_4-MFI (Si/Al = 28) with 1200 ppm Fe (mostly in the framework) were prepared in the laboratory by hydrothermal synthesis by using of tetraethylorthosilicate, aluminum nitrate and iron nitrate, as sources of silicon, aluminium and iron by using procedure described in Ref. 3. The synthesized zeolites were thoroughly washed by distilled water, dried, and calcined in a stream of dry oxygen at 500 °C for 6 h to remove the template. The NH_4 forms of zeolites were prepared by repeated three-times ion exchange of the calcined material with 0.5 M NH_4NO_3 at 25 °C. NH_4-MFI zeolite (Si/Al = 12.5, 190 ppm Fe) was provided by the Research Institute of Inorganic Chemistry, Inc., CZ. The NH_4-MFI zeolite (Si/Al = 28, 1200 ppm Fe) and that of NH_4-MFI zeolite (Si/Al = 12.5, 190 ppm Fe) were treated in a stream of

oxygen containing 30 % water vapor at temperature 600°C for 6 h (hydrothermally treated zeolite, denoted as HT). In addition a part of the steamed zeolite (Si/Al = 28, 1200 ppm Fe) was transformed into Na form by repeated (3x) ion exchange using 0.1 M NaCl solution at 25 °C.

The chemical composition of zeolites was determined by Wavelength-dispersive X-Ray Fluorescence Spectroscopy (WD XRF) and by Inductively Coupled Plasma Optical Emission spectrometry (ICP OES) or by Atomic Absorption Spectrometry (AAS) after zeolites dissolution. Conditions of preparation of zeolites and their chemical compositions are given in Table III.4.

Table III.4 Chemical composition, treatment condition and acid site concentration of Fe-HMFI zeolite

Catalyst	Composition		Treatment[a]	Acid site concentration (mmol/g)	
	Si/Al	Fe (ppm)		Brønsted	Lewis
FeH-MFI-30-C	28.0	30	C, 480 °C	0.37	0.06
FeH-MFI-190-C	12.5	190	C, 480 °C	0.52	0.21
FeH-MFI-190-HT	12.5	190	HT, 600°C	0.08	0.11
FeH-MFI-1200-HT	28.0	1200	HT, 600 °C	0.07	0.08
FeNa-MFI-1200-HT	28.0	1200	HT, 600°C	0.05	0.04

[a] C-calcined, HT- hydrothermally treated, steamed.

III.2 Catalytic tests

Catalytic tests of ethane and propane oxidation and ammoxidation were carried out in a through-flow apparatus with integral fixed-bed micro-reactor. Apparatus consisted of a mixing line containing cylinders with gases (O_2, C_3H_8, C_2H_6, He, NH_3 and N_2O) provided by Technoplyn Linde a.s. and mass flow-controllers, a micro-reactor in a rheostatic oven and gas chromatograph (CHROM 5, Laboratorní přístroje, Praha) connected on-line to micro-reactor outlet (see Scheme III.1).

III.2.1 Oxidation and ammoxidation of paraffins by oxygen

The reaction runs of oxidative dehydrogenation and ammoxidation of paraffins over Co-, Cu- and H-zeolites were carried out at atmospheric pressure and the data correspond to

the steady-state conditions. Feed composition was 5 vol. % of a hydrocarbon (propane or ethane), 6.5 vol. % of O_2 and rest of helium for alkane oxidative dehydrogenation, and 5 vol. % of hydrocarbon (propane or ethane), 6.5 vol. % of O_2, 10 vol. % of NH_3 and rest of helium for ammoxidation of paraffins. Helium as an inert carrier gas was used. The catalysts were pretreated before each reaction run in a flowing gas mixture containing 6.5 vol. % of O_2 in He at 450 °C for 1 h. Typically a total flow rate was 100 ml/min with the catalyst weight 0.2 g. Flow rates of the individual gases were controlled by mass flow controllers (Elmet, CZ). The reactions were measured in the temperature range from 350 to 500 °C by step-by-step increasing temperature. The steady-state product composition for each temperature was reached within 1 h.

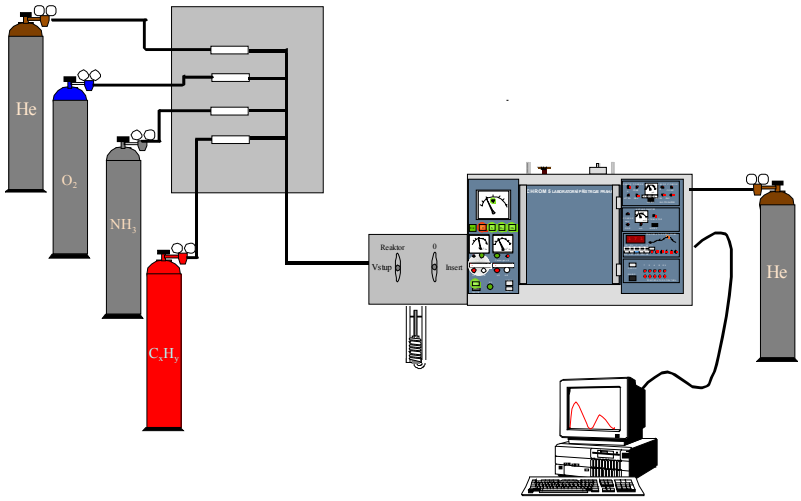

Scheme III.1 Apparatus for catalytic tests connected on-line with GC and computer

III.2.2 Oxidation of propane by nitrous oxide and molecular oxygen

Oxidation of propane was also measured in the presence of nitrous oxide and and a mixture of nitrous oxide with oxygen over Co- and FeH-zeolites in the temperature range from 400 to 490°C by step-by-step increasing temperature. The composition of the reaction mixture was C_3H_8/N_2O 5/10 vol. % and $C_3H_8/O_2/N_2O$ 5/6.5/0-14 vol. % in helium. A total flow rate was 100 ml/min and catalyst weight 0.2 g. Catalyst was pretreated in an oxygen flow at 450°C for 1 h before each reaction run. The steady-state conditions for each temperature and feed composition were reached within 1h.

III.2.3 Oxidation/ammoxidation of acrylonitrile and acetonitrile

Experiments of the reaction of acetonitrile or acrylonitrile with oxygen and ammonia in the stream were carried out at 450 °C over 0.2 g of Co-MFI-12.5-0.42-2.9 sample. Nitriles were injected into the reaction mixture by means of a saturator kept at 25 °C. The reaction mixture composed of 6.5 vol. % of O_2, 0.4 vol. % of acrylonitrile or acetonitrile, and the concentrations of ammonia ranged from 0 to 14 vol. %. An effect of N_2O on the ammoxidation of propane was investigated at 450 °C over 0.2 g of Co-MFI-12.5-0.42-2.9 sample by addition of 1 vol.% of N_2O to the standard reaction mixture.

III.2.4 Columns

For product analysis a set of columns was used. The typical chromatograms are shown in Figure III.1 – III.6.

Column "CARPOK N 1:1" (Porapak N and Carboxen 1000 with ratio 1:1, length 1200 mm and internal diameter 3 mm) was used to separate reactants and products in ammoxidation of C_3 hydrocarbons. The following temperature program was used: 25°C (0 min) – 10 °C/min – 120 °C (0 min) – 10 °C/min – 180 °C (12 min). The products and reactants of ammoxidation of ethane were separated on the column CARPOK N 1:5 (5/6 Porapak N and 1/6 Carboxen 1000, length of 1200 mm with diameter 3 mm), temperature program: 25°C (0 min) – 20 °C/min – 120 °C (4 min) – 10 °C/min – 180 °C (14 min). The separation of permanent gases (O_2, N_2, CO, CH_4) was pursued at temperature 25 °C on the column MOLSITO (molecular sieve 5A, 2500 mm length with internal diameter 3 mm). The products of oxidative dehydrogenation over Cu-, Co- and parent H-zeolites were separated on column CARPOK Q 1:2 (1/3 Porapak Q and 2/3 Carboxen 1000, length of 1200 mm with diameter 3 mm), temperature programm: 25°C (2 min) – 10 °C/min – 120 °C (0 min) – 20 °C/min – 215 °C (12 min). Analysis of the products of paraffins oxidation with nitrous oxide, i.e. hydrocarbons, related oxygenates, carbon dioxide and N_2O were separated on packed column of Porapak Q and Porapak S (PQS) by using of the temperature program: 40°C (18 min) – 5 °C/min – 150 °C (18 min) – 50 °C/min – 230 °C (32 min).

Reaction products of ammoxidation of propane and ethane were CO_2, H_2O, N_2, CO, N_2O, CH_4, ethene, propene and acetonitrile. A mass balance based on carbon was ranging from 95 –100 %. No other products were detected. The main products of oxidative dehydrogenation over Cu-, Co- and parent H-zeolites were CO, CO_2, H_2O, CH_4, ethene and

propene. The mass balance of oxidative dehydrogenation was ranging from 98 –100 %. The oxidative dehydrogenation of propane with N_2O over Fe-zeolites yielded in addition xylenes, benzene, aldehydes and alcohols.

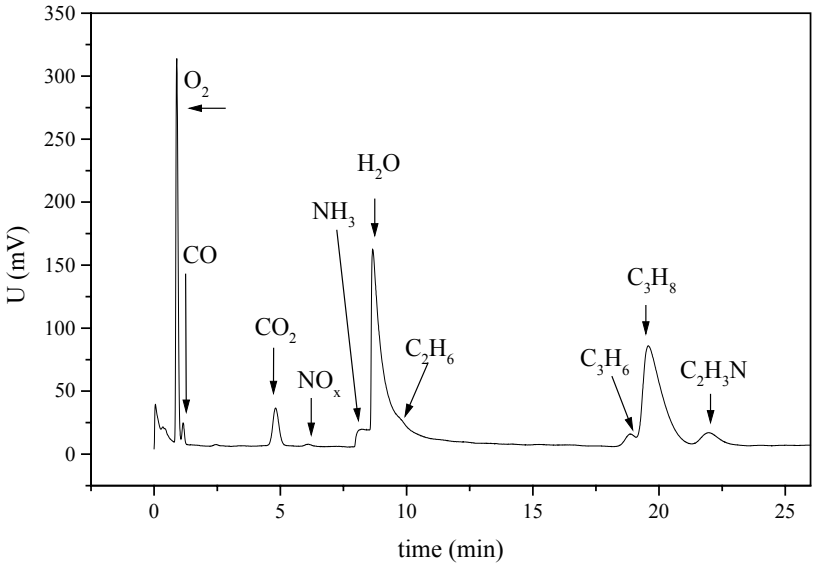

Figure III.1 Typical chromatogram of CARPOK N 11 (Carboxen 1000 + Porapak N (1:1 ratio)), 1200 mm, temperature program: 25°C – 10°C/min - 120°C - 10°C/min - 180°C

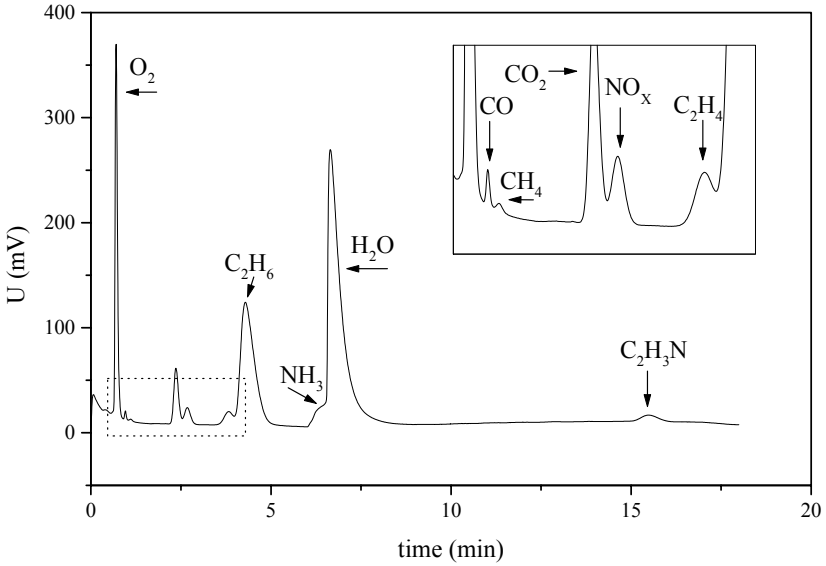

Figure III.2 Typical chromatogram of CARPOK N 15 (Carboxen 1000 + Porapak N (1:5 ratio)), 1200 mm, temperature program: 25°C – 20°C/min - 120°C (4 min) - 10°C/min - 180°C

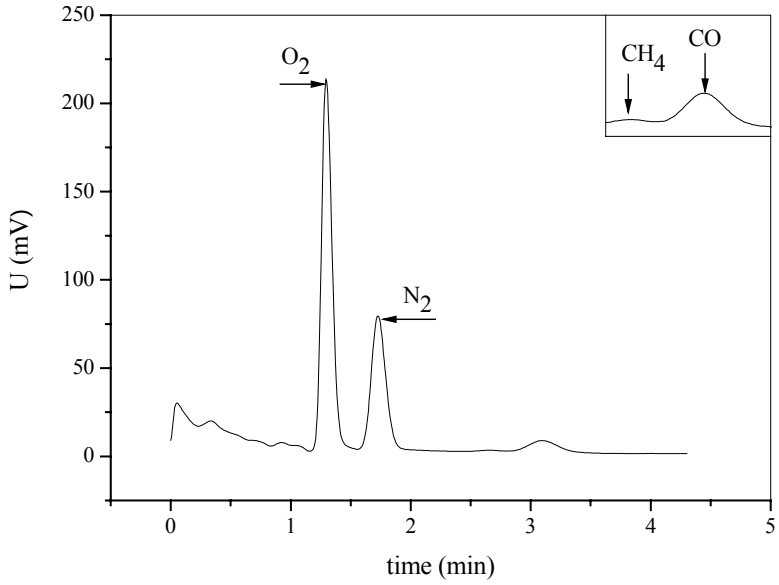

Figure III.3 Typical chromatogram of MOLSITO (molecular sieve 5A (1:5 ratio)), 3500 mm, temperature program: 25°C

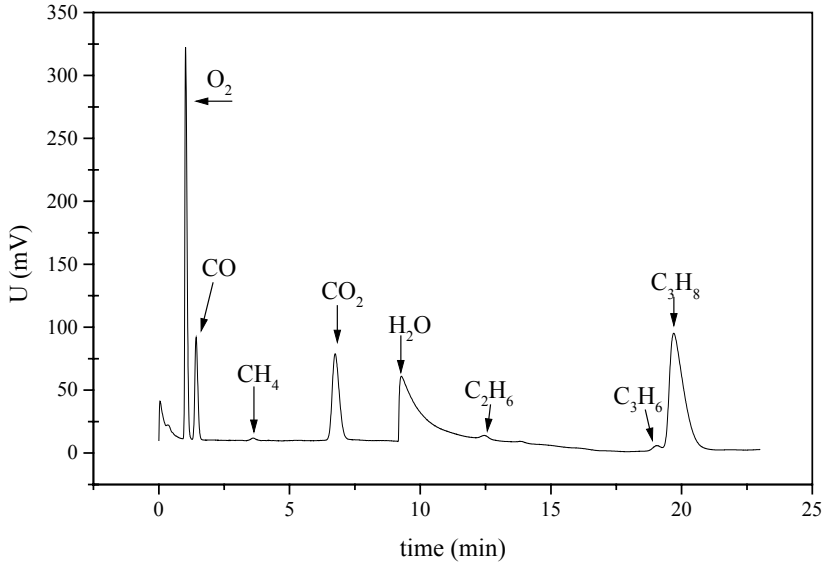

Figure III.4 Typical chromatogram of CARPOK Q 12 (Carboxen 1000 + Porapak Q (1:2 ratio)), 1200 mm, temperature program: 25°C (2 min) – 10°C/min - 120°C - 20°C/min - 210°C

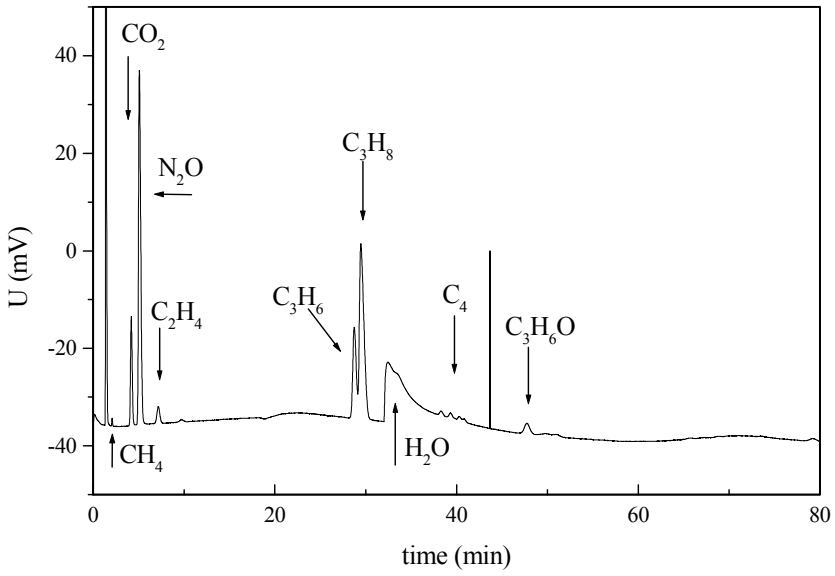

Figure III.5 Typical chromatogram of PQS (Porapak Q + Porapak S (1:1 ratio)), 3500 mm, temperature program: 40°C (18 min) – 5°C/min - 130°C (18 min) - 5°C/min - 230°C (32 min) TCD detector

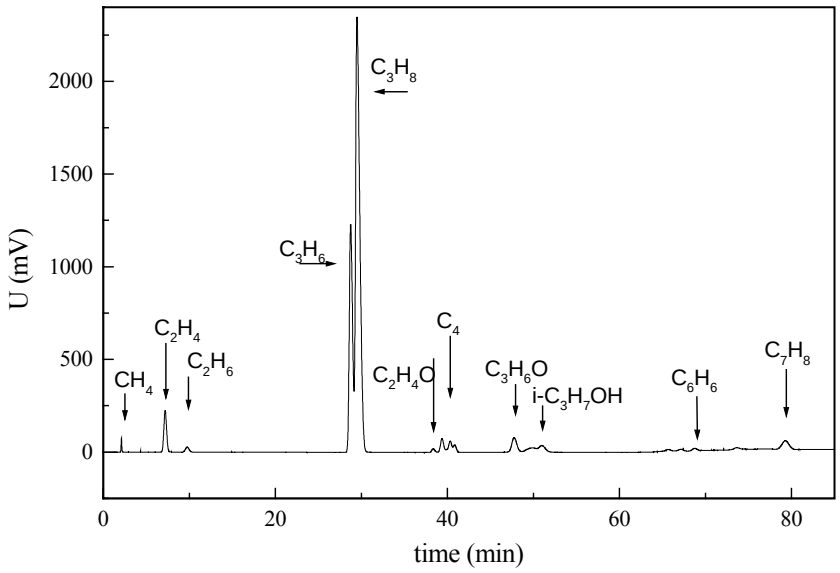

Figure III.6 Typical chromatogram of PQS (Porapak Q + Porapak S (1:1 ratio)), 3500 mm, temperature program: 40°C (18 min) – 5°C/min - 130°C (18 min) - 5°C/min - 230°C (32 min) FID detector

The reactions were described by hydrocarbon conversion (X_i), selectivity (S_i) to the individual products and yield (Y_i) of the individual products, defined as:

$$X_i = \left(1 - \frac{a_i * n_i}{\left(\sum a_j * n_j\right) + a_i * n_i}\right) * 100 \quad (1)$$

$$S_j = \frac{a_j * n_j}{\sum a_j * n_j} * 100 \quad (2)$$

$$Y_j = \frac{a_j * n_j}{\left(\sum a_j * n_j\right) + a_i * n_i} * 100 \quad (3)$$

where n_i is molar amount of reactant in the outlet, a_i is the stoichiometric coefficient of the element in the reactant, a_j is the stoichiometric coefficient of the element in the product and n_j is the molar amount of the product in the outlet of the reactor . Values are given in percentage.

The activity of the samples was expressed by turn over frequency (TOF) at 450 °C. This value reflects the number of reacted molecules over one metal atom in a zeolite. The temperature 450 °C was chosen as the conversion reached values up to 25 %. The TOF value is defined as:

$$TOF = \frac{n_i^0 * X_i * N_A}{\frac{W * w_{Co} * N_A}{M_{Co}}} \quad (4)$$

where n_i^0 is the molar amount of key reactant at the inlet of the reactor, X_i - conversion of the reactant, N_A - Avogadro‘s constant, W - weight of the catalyst, w_{Co} – weight concentration of the metal in the zeolite and M_{Co} is molar weight of the metal.

III.3 Temperature-programmed techniques

The apparatus for temperature programmed desorption and reduction by hydrogen is given in Scheme III.2. The apparatus consisted of the line containing cylinders with gases (O_2, He, H_2/Ar and hydrocarbons, provided by Technoplyn Linde a.s.), gas mass-flow controllers, micro-reactor, and connected TCD detector (Labio Praha) and Mass spectrometer

(Omnistar GDS, Balzers Pfeiffer). All capillaries were heated to 100°C to prevent condensation of water. Water formed during the sample reduction by hydrogen was removed by cooling trap in front of the TCD detector.

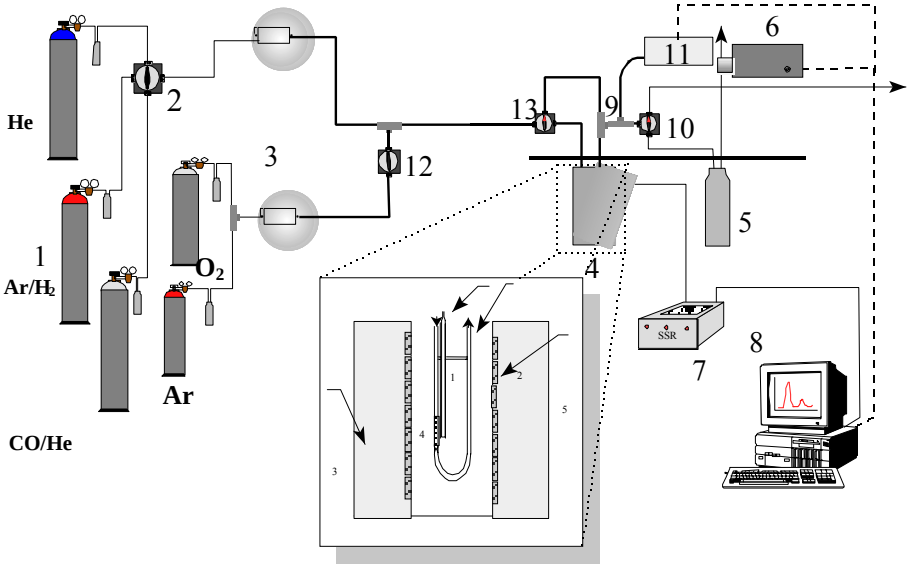

Scheme III.2 Apparatus for temperature programmed techniques, 1- cylinders with gases, 2- valve for choosing the gas, 3- flow controller, 4- oven, 5- freezing traps, 6- TCD detector (Labio), 7- SSR rele, 8- computer with programme controlling the oven, MS and data collection, 9- Swagelok T-fitting, 10- three-ways valves, 11- MS OmniStar, 12 – valve to side branch, 13 – valve to by-pass,

With TP reduction by hydrogen a 100 mg of sample was first dehydrated and oxidized at 500°C for 1 h in flow oxygen and then cooled to ambient temperature in flowing helium. The reduction of samples was carried out in 5 vol. % of hydrogen in argon from 25°C to 1100°C (the maximum temperature was kept for 20 min) with a heating rate of 10°C/min. The gas containing hydrogen was dried in a freezing trap kept at temperature of solid CO_2 and ethanol mixture. Mass fractions at 2, 18, 32 and 40 were monitored every 3 s, i.e. at 0.5 °C step).

III.4 FTIR spectroscopy

The IR spectra were collected in the range from 4000 to 400 cm^{-1} with resolution of 2 cm^{-1} by using an FTIR spectrometer PROTEGE 460 (Nicolet Instrument Corporation) equipped with an MCT/B detector, which was kept at a temperature of liquid nitrogen. Thin

transparent self-supported wafers of catalysts (5 – 7 mg/cm^2) were heated in vacuum at 450°C for 3 hours. Spectra of evacuated zeolites were collected at ambient temperature. The collected spectra of samples were normalized per 5 mg/cm^2 and deconvoluted into Gaussian curves. Final data processing was carried out using the MicroCal Origin 6.1 Software (MicroCal Software, Inc. USA).

In-situ FTIR experiments during oxidative dehydrogenation of ethane, hydrocarbons adsorption, ammonia oxidation and ammoxidation reaction were carried out over Co-FER, and Co-*BEA catalysts at 450°C. The catalyst in the form of a thin self-supporting wafer (ca 10 mg/cm^2) was placed in the stainless steel flow-through IR cell-reactor (In-Situ Research Instruments, Inc.) with NaCl windows. Before each reaction run the sample was calcined in a stream of O_2/He (45 vol. % O_2) for 1 h at 450°C. Composition of the individual reactants, controlled by mass-flow controllers, was 10 vol. % NH_3, 6.5 vol. % O_2, 5 vol. % hydrocarbon (ethane, ethene) and rest was helium. Total feed was held at 100 ml/min. Some experiments were performed in a pulse regime, where O_2, ethane (or ammonia) were continuously fed, and pulses of ammonia (or ethane, resp., 1 vol. %) were applied.

The in-situ FTIR spectra were measured in transmittance mode on the Nexus 670 e.s.p. FTIR spectrometer (Thermo Nicolet Co.) equipped with DTGS KBr detector. The resolution of the spectrometer was 2 cm^{-1} with 32 spectra recorded per second. The spectrum of calcined sample (recorded in a stream of oxygen at a given temperature) was subtracted from the monitored spectra recorded at *in-situ* conditions of the catalytic reaction. The spectra were continuously recorded during the reaction and processed with Microcal Origin 4.1.

III.5 UV-Vis spectroscopy

The UV-Vis spectra were collected in the range from 4000 to 50 000 cm^{-1} with resolution of 2 cm^{-1} by using an UV-Vis spectrometer Perkin Elmer Lambda 19. Before the measurements of the spectra the grained samples were pretreated in a vacuum 10^{-2} Pa at 480 °C for 3 h and cooled to RT. The samples were then transferred under vacuum to a quartz cell and sealed. Spectra of evacuated zeolites were collected at RT. The collected spectra were deconvoluted into Gaussian curves. Final data processing was carried out using the MicroCal Origin 6.1 Software (MicroCal Software, Inc. USA).

Before the measurements of the spectra the samples were pretreated in a vacuum 10^{-2} Pa at 480 °C for 3 h and cooled to RT. After dehydration the pressure of 500-600 Torr of dried reactants was fed onto a catalyst. The adsorption took 20 min, then the sample was

measured, following by evacuation at room temperature measurement, desorption at 100, 200, 300, 400 and 450 °C with individual collection of spectra. Spectra of adsorbed reactants were collected at ambient temperature.

In-situ UV-Vis experiments during the oxidative dehydrogenation of ethane, ammonia oxidation and ammoxidation reactions were carried out over all zeolites investigated (Co-FER, Co-MOR, Co-MFI and Co-*BEA catalysts) at 450° by the using Harrick through flow cell with the catalyst in the form of grains overlaid by a thin wafer (ca 50 mg). Before each reaction run the sample was calcined in a stream of O_2/He (45 vol. % O_2) for 1 h at 450°C. Composition of the reactants, controlled by mass-flow controllers, was 10 vol. % NH_3, 6.5 vol. % O_2, 5 vol. % hydrocarbon (ethane, ethene) and rest was helium. Total feed was kept on the value of GHSV corresponding to the catalytic tests.

Spectra were collected in time of 0, 10, 30 and 60 min. The collected spectra were deconvoluted into Gaussian curves. Final data processing was carried out using the MicroCal Origin 6.1 Software (MicroCal Software, Inc. USA).

III.6 Chemical composition and structure

XRD pattern of samples before and after the reaction tests or H_2-TPR experiment were obtained with diffractometer D8 ADVANCE (Bruker AXS) using Cu anode (λ = 0.1544390 nm) at 2θ from 5° to 80° at room temperature.

The chemical composition of zeolites was determined by Wavelength-dispersive X-Ray Fluorescence Spectroscopy (WD XRF) and by Inductively Coupled Plasma Optical Emission spectrometry or by Atomic Absorption Spectrometry after zeolites dissolution.

III.7 References

[1] M.J. Eapen, KS.N. Ready, V.P. Shiralkar; Zeolites **14** (1994) 295.

[2] P. Kubánek, B. Wichterlová, Z. Sobalík; J. Catal. **211** (2002) 109.

The results describe behaviour of Cu-, Co- and Fe-zeolites in paraffins oxidation and ammoxidation to olefins and nitriles, resp. With the most active and selective Co-zeolites the effect of zeolite matrix topology and metal ion concentration is analyzed. As it has appeared that N_2O has provided enhancement of paraffin oxidation, moreover, it represents a possible intermediate in ammoxidation reaction. As Fe is present in all zeolites in trace concentrations as impurity**,** the attention has been devoted to paraffin oxidation by O_2 and N_2O over Co- and Fe-zeolites

IV.1 Activity of metallo-zeolites in oxidation of ethane and propane with molecular oxygen

IV.1.1 Parent H-zeolites

At given conditions parent H-*BEA, H-MFI, H-FER and H-MOR exhibited only low conversion of propane and only to carbon oxides as shown in Table IV.1. Carbon balance was calculated to be 96 %. Nevertheless that the conversions did not exceed 3.4 %, there should be present some active redox sites. As H-MFI and H-*BEA zeolites contained trace concentrations of iron (see Table III.1 and III.4), this activity of H-zeolites was attributed to trace concentration of Fe species, present in all zeolite samples.

Table IV.1 Oxidation of propane over parent H-zeolites at 450°C, w_{cat} = 200 mg, F = 100 ml/min, 5 vol. % propane, 6.5 vol. % oxygen

sample	X %		S %			Y %
cation-matrix-Si/Al	C_3H_8	O_2	CO	CO_2	C_3H_6	C_3H_6
H-MFI-12.5	3.2	14.7	59.2	40.8	0.0	0.0
H-*BEA-13.0	3.4	15.3	57.4	42.6	0.0	0.0
H-FER-9.5	0.9	8.1	58.7	41.3	0.0	0.0
H-MOR-9.4	0.6	6.8	63.9	36.1	0.0	0.0

IV.1.2 Cu-zeolites

The activity of Cu-zeolites in propane oxidation was compared at 450°C and the results are given in Table IV.2. All Cu-zeolites investigated exhibited low selectivity to propene, and surprisingly some selectivity to ethene, indicating oligomerization and cracking

reactions. The turn-over-frequency (TOF) values per Cu ion related to hydrocarbon conversion indicate that the most active Cu sites are located in MFI structure, while those in FER and *BEA exhibit comparable activity. Relatively high propane conversion, high selectivity to carbon dioxide and TOF values indicates that the Cu ions are highly active in complete paraffin oxidation.

Table IV.2 Oxidation of propane over Cu-zeolites at 450°C w_{cat} = 200 mg, F = 100 ml/min, 5 vol. % propane, 6.5 vol. % oxygen

sample matrix-Si/Al-Cu/Al-w_{Cu}	X %		S %						Y %	TOF_{total} (h^{-1})
	C_3H_8	O_2	CO	CO_2	CH_4	C_2H_4	C_2H_6	C_3H_6	C_3H_6	
Cu-MFI-22.6-0.28-1.1	24.6	97.9	24.7	71.0	0.0	3.2	0.0	1.1	0.3	24.2
Cu-*BEA-13.5-0.3-1.6	13.3	55.9	11.8	82.2	0.0	6.0	0.0	0.0	0.0	13.1
Cu-FER-9.5-0.25-2.2	28.6	98.6	25.0	60.7	0.6	13.7	0.0	0.0	0.0	14.1

IV.1.3 Co-zeolites

In general, Co-zeolites exhibited lower oxidation activity compared to Cu-zeolites, and reached higher selectivity and yield of propene. Compared to Fe-zeolites, the activity of Co-zeolites was higher. Therefore, as Co-zeolites among Cu-, Fe- and Co-zeolites exhibited the highest yields to olefin products we centred our attention to these zeolites. The effect of concentration of oxygen, contact time and temperature on paraffins oxidation was investigated over the active Co-*BEA zeolite sample.

It has been shown that increasing concentration of oxygen in the feed increases conversion of propane decreasing propene selectivity, while the propene yield is nearly constant above 6 % of oxygen (see Figure IV.1).

The effect of contact time on the conversion of propane, selectivity to the products at C_3H_8/O_2 molar ratio 1:1, shown in Figure IV.2, exhibited a typical feature. Increasing W/F increases conversion of propane and increases selectivity to CO and CO_2 on the account of decreasing propene selectivity.

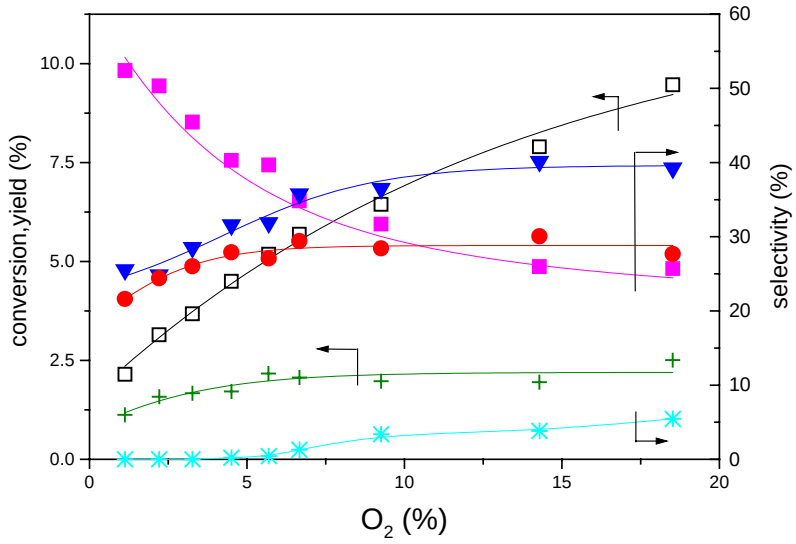

Figure IV.1 The influence of oxygen concentration on the oxidation of propane over catalyst Co-*BEA-12.4-0.25-1.8 at 450°C, w_{cat}= 200 mg, F = 100 ml/min, 5 vol. % propane, 1-18 vol. % oxygen; ◘- conversion of propane, ■ - selectivity to propene,● - selectivity to carbon dioxide, ▼ -selectivity to carbon monoxide, ✻ - selectivity to ethene, + - yield of propene

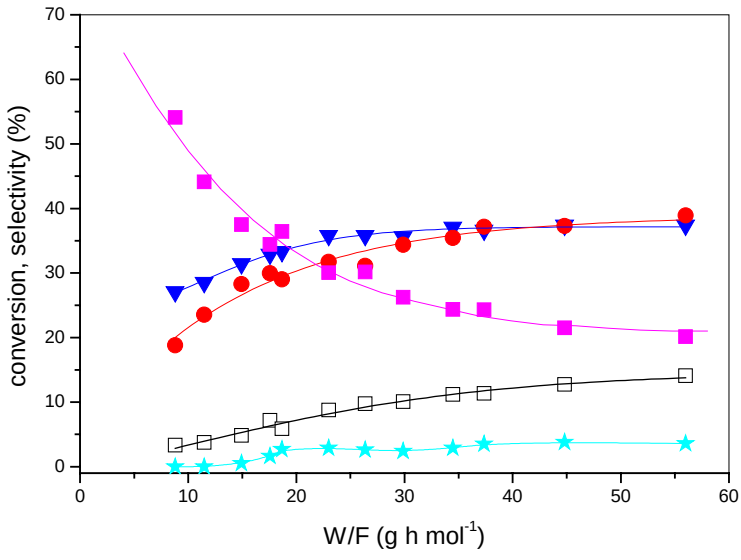

Figure IV.2 The influence of the W/F ratio on the oxidation of propane over Co-*BEA-12.4-0.25-1.8 at 450°C, w_{cat}= 200 mg, F = 100 ml/min, 5 vol. % propane, 5 vol. % oxygen; ◘- conversion of propane, ■ - selectivity to propene,● - selectivity to carbon dioxide, ▼ -selectivity to carbon monoxide, ✻ - selectivity to ethene

The temperature dependence of propane and ethane oxidation over the most active Co-*BEA-17.6-0.39-1.7 zeolite is shown in Figures IV.3 and IV.4. The dependence of conversion and selectivity on temperature exhibit similar features for all the Co-zeolites investigated. Typically for paraffin oxidation, the conversion of paraffin and oxygen increases sharply with temperature, while selectivity to corresponding olefins decreases. With increasing temperature increases also selectivity to CO_2, while the selectivity to CO remains at higher temperature nearly constant. This indicates that the main source of CO_2 is oxidation of more reactive olefins compared to paraffins. Higher propene selectivity was achieved with Co-zeolites where ethene and methane concentrations were low, and thus oligomerization and cracking of propene can be assumed to be limited. Slightly higher selectivity in ethene indicates understandably that propene is more reactive for both oxidation and oligomerization/cracking reactions.

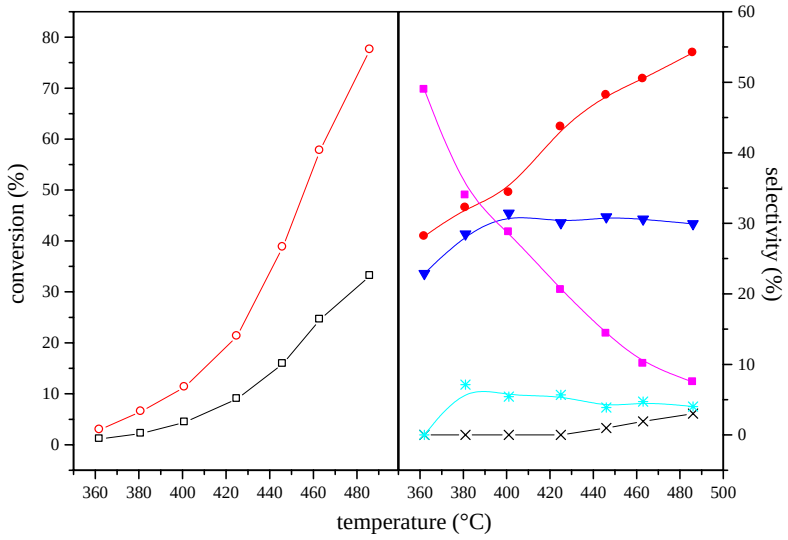

Figure IV.3 Oxidation of propane in dependence on temperature over Co-*BEA-17.6-0.39-1.7, w_{cat} = 200 mg, F = 100 ml/min, 6.5 vol. % oxygen, 5 vol. % propane, ○ -conversion of oxygen, □- conversion of propane, ■ - selectivity to propene, ● - selectivity to carbon dioxide, ▼ -selectivity to carbon monoxide, ✳ - selectivity to ethene, × - selectivity to methane

From this analysis of the effect of reaction conditions on the product distribution in paraffin oxidation, we selected suitable conditions for the investigation of the effect of zeolite topology and structure of Co ions on the oxidation of paraffins. These studies were carried out at conditions of 6.5 vol. % O_2, 5.0 % of a hydrocarbon, temperature of 450 °C and W/F = 15 g.h. mol^{-1}.

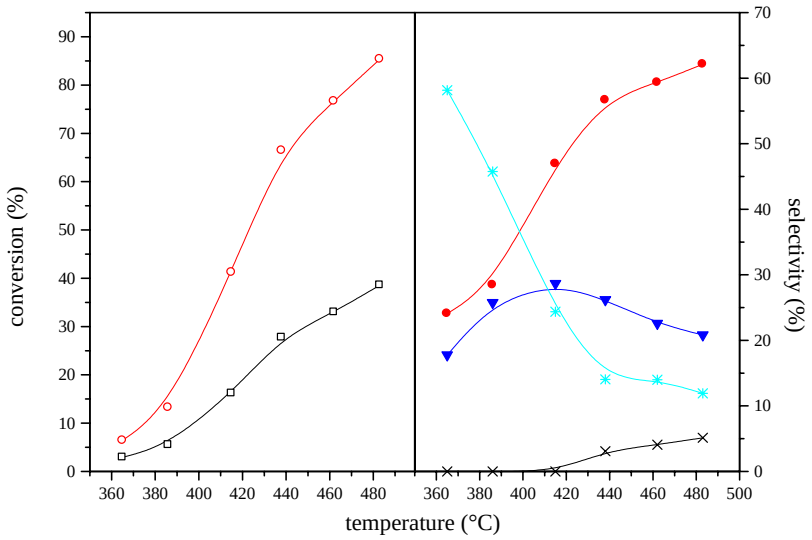

Figure IV.4 Oxidation of ethane in dependence on temperature over Co-*BEA-17.6-0.39-1.7, w_{cat} = 200 mg, F = 100 ml/min, 6.5 vol. % oxygen, 5 vol. % ethane, ○ -conversion of oxygen, □- conversion of ethane, ● - selectivity to carbon dioxide, ▼ -selectivity to carbon monoxide, ✳ - selectivity to ethene, × - selectivity to methane

IV.1.3.1 Co-zeolites with various framework topology

Oxidation of ethane and propane was carried out over a set of samples with exchanged cobalt ions in zeolites of *BEA, MFI, FER and MOR topologies. Among the products of propane oxidation propene, ethene, methane and carbon oxides were detected (Tables IV.3 and IV.4).

The effect of zeolite topology on propane conversion was clearly manifested. Co-*BEA and Co-MFI zeolites showed much higher activity compared to Co-FER and Co-MOR as follows from conversion and TOF values (see Table IV.3), particularly for the samples where presence of single exchanged Co ions can be assumed (Co/Al up to ca 0.4, see below).

Table IV.3 Oxidation of propane over Co-zeolites at 450°C w_{cat} = 200 mg, F = 100 ml/min, 5 vol. % propane, 6.5 vol. % oxygen

Sample matrix-Si/Al-Co/Al-w_{Co}	X %		S %						Y %	TOF total (h^{-1})	TOF C3H6 (h^{-1})
	C_3H_8	O_2	CO	CO_2	CH_4	C_2H_4	C_2H_6	C_3H_6	C_3H_6		
Co-*BEA-12.4-0.25-1.8	6.4	18.4	31.4	26.2	0.0	0.0	0.0	41.5	2.6	14.0	5.8
Co-*BEA-13.8-0.50-2.8	10.9	34.0	35.1	38.8	0.0	2.5	0.0	23.0	2.5	15.6	3.6
Co-*BEA-17.6-0.39-1.7	17.5	42.8	30.2	49.0	0.8	3.7	2.0	13.5	2.4	35.0	4.7
Co-MFI-12.5-0.23-1.6	7.5	21.4	40.6	42.6	0.0	0.0	0.0	16.7	1.3	17.9	3.0
Co-MFI-12.5-0.42-2.9	8.5	22.0	34.7	48.5	0.0	2.6	0.0	13.6	1.2	11.1	1.5
Co-MFI-12.5-0.55-3.8	9.8	33.1	28.1	48.9	0.4	7.3	0.0	15.5	1.5	9.8	1.5
Co-FER-9.4-0.23-1.0	1.5	5.9	33.3	20.8	13.2	13.9	0.0	18.8	0.3	5.7	1.1
Co-FER-8.6-0.42-3.6	3.1	13.0	37.1	62.3	0.0	0.0	0.0	0.0	0.0	3.5	0.0
Co-MOR-9.4-0.48-2.1	3.3	13.0	40.3	36.4	0.0	0.0	0.0	23.3	0.8	6.2	1.4

Also a comparison of the propene yield and corresponding TOF values showed the sequence: *BEA > MFI > MOR ~ FER.

With oxidative dehydrogenation of ethane main products were ethene and carbon oxides. Similarly like with propane, Co-MFI and Co-*BEA zeolites exhibited much higher ethane conversion in comparison with that of Co-FER and Co-MOR. TOF values per Co ion reacted to ethane conversion and ethane yield indicate much higher activity of these ions in *BEA and MFI zeolites compared to those in FER and MOR frameworks.

Table IV.4 Oxidation of ethane over Co-zeolites at 450°C w_{cat} = 200 mg, F = 100 ml/min, 5 vol. % ethane, 6.5 vol. % oxygen

Sample matrix-Si/Al-Co/Al-w_{Co}	X %		S %				Y %	TOF total (h^{-1})	TOF C3H6 (h^{-1})
	C_2H_6	O_2	CO	CO_2	CH_4	C_2H_4	C_2H_4		
Co-*BEA-12.4-0.25-1.8	5.2	19.2	23.2	16.3	0.0	60.5	3.2	11.4	6.9
Co-*BEA-13.8-0.50-2.8	7.3	27.9	25.2	12.2	0.0	62.6	4.6	10.4	6.5
Co-*BEA-17.6-0.39-1.7	30.1	71.3	24.2	57.8	4.3	13.7	4.1	60.2	8.2
Co-MFI-12.5-0.23-1.6	5.2	24.3	37.7	7.6	0.0	54.7	2.8	12.4	6.8
Co-MFI-12.5-0.42-2.9	18.2	39.8	32.0	43.8	2.6	21.6	3.9	23.7	5.1
Co-MFI-12.5-0.55-3.8	21.8	60.9	28.5	45.8	4.6	21.1	4.6	21.7	4.6

Co-FER-9.4-0.23-1.0	0.8	3.3	21.7	0.0	0.0	78.3	0.6	3.0	2.3
Co-FER-8.6-0.42-3.6	3.7	23.9	20.4	23.5	0.0	56.1	2.1	4.2	2.3
Co-MOR-9.4-0.48-2.1	2.2	8.3	17.0	6.7	0.0	76.2	1.7	4.1	3.1

III.1.3.2 Effect of Co concentration

The effect of Co concentration in zeolites was investigated in oxidation of ethane over Co-*BEA and Co-MFI zeolites, as given in Tables IV.5 and IV.6.

Table IV.5 Oxidation of ethane over Co-*BEA zeolites at 450 °C. w_{cat} = 200 mg, F = 100 ml/min, 5 vol. % ethane, 6.5 vol. % oxygen

Sample matrix-Si/Al- Co/Al-w_{Co}	X (%)		S (%)				Y %	TOF total	TOF C2H4
	C_2H_6	O_2	CO	CO_2	CH_4	C_2H_4	C_2H_4	(h^{-1})	(h^{-1})
Co-*BEA-13.1-0.15-1.0	1.1	58.3	13.3	10.8	0.0	75.9	0.8	3.6	2.7
Co-*BEA-12.4-0.25-1.8	2.1	52.4	27.2	10.1	0.0	62.7	1.3	4.7	2.9
Co-*BEA-13.1-0.30-1.8	3.6	89.8	30.9	13.3	0.0	55.8	2.0	7.7	4.3
Co-*BEA-13.1-0.32-2.0	9.8	90.5	36.0	21.5	0.0	42.5	4.2	19.8	8.4
Co-*BEA-12.3-0.34-2.1	6.6	91.1	31.2	24.0	0.0	44.8	3.0	12.2	5.5
Co-*BEA-13.0-0.50-2.7	31.8	94.7	25.5	60.1	1.9	12.5	4.0	45.6	5.7
Co-*BEA-13.0-0.51-3.1	35.1	96.6	24.5	62.2	2.4	11.0	3.9	44.7	4.9
Co-*BEA-11.9-0.50-3.2	32.5	98.5	26.8	60.6	0.6	11.0	3.6	40.2	4.4
Co-*BEA-13.1-0.87-4.7	36.0	87.4	22.9	65.3	2.7	9.1	3.3	30.2	2.7
Co-*BEA-13.1-1.17-7.8	24.0	86.1	22.3	59.2	2.2	17.1	4.1	12.1	2.0

With increasing Co concentration in zeolites increased conversion of ethane with exception of the sample with the highest Co concentration. But the TOF values per Co ion showed different results. The dependence of ethane oxidation expressed in TOF values on cobalt loading is shown in Figure IV.5. It is clearly seen that the Co ions in zeolites with low cobalt concentration exhibited low TOF values for total oxidation, but with increasing Co loading above Co/Al 0.3, the activity dramatically increased up to Co/Al ratio = 0.5, and above this concentration steadily decreased. The TOF related to ethene increased up to Co/Al 0.4-0.5 and then decreased with Co loading. TOF values for CO_x formation showed similar dependence as total TOF in ethane conversion (Figure IV.5).

Dependence of the activity of Co-MFI catalysts on Co loading is given in Table IV.6. The increasing conversion was observed with increasing Co loading accompanied by decreasing selectivity to ethene. Understandably, the yield of ethene increased with cobalt concentration. Total TOF values exhibited similar feature as those over Co-*BEA zeolites.

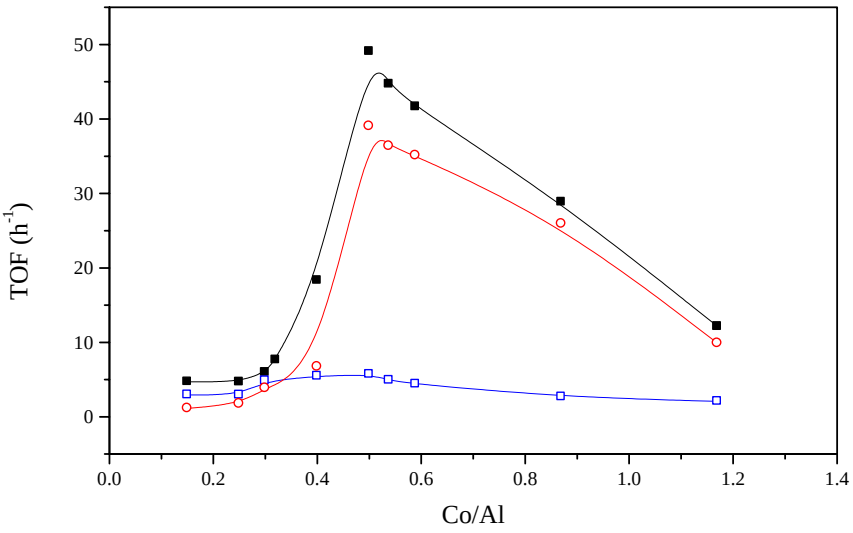

Figure IV.5 Dependence of TOF values on Co/Al molar ratio in Co-*BEA at reaction temperature 450°C. w_{cat} = 200 mg, F = 100 ml/min, 6.5 vol. % oxygen, 5 vol. % ethane ■ - TOF related to conversion of ethane, ○ - TOF related to sum of selectivity to CO_X, □ - TOF related to ethene selectivity, F = 100 ml/min, 5 vol. % ethane, 6.5 vol. % oxygen,

Table IV.6 Oxidation of ethane over Co-MFI zeolites at 450 °C. w_{cat} = 200 mg, F = 100 ml/min, 5 vol. % ethane, 6.5 vol. % oxygen

Sample matrix-Si/Al-Co/Al-w_{Co}	X %		S %				Y %	TOF total	TOF C2H4
	C_2H_6	O_2	CO	CO_2	CH_4	C_2H_4	C_2H_4	(h^{-1})	(h^{-1})
Co-MFI-12.5-0.23-1.6	5.2	24.3	37.7	7.6	0.0	54.7	2.8	12.4	6.8
Co-MFI-12.5-0.42-2.9	18.2	39.8	32.0	43.8	2.6	21.6	3.9	23.7	5.1
Co-MFI-12.5-0.55-3.8	21.8	60.9	28.5	45.8	4.6	21.1	4.6	21.7	4.6

Ethane oxidation over Co-*BEA zeolites was also investigated at various temperatures (Figures IV.6 A-D). A simple comparison of the ethane conversion and the yields of the individual products indicate that the reaction scheme might follow parallel-consecutive mechanism. Such dependences did not provide any suggestions on the activity of various species present in Co-*BEA of various Co concentrations. However, if we plotted, regardless

of reaction temperature, yields of CO_x and ethene vs. ethane conversion two different dependences were obtained for zeolites with Co/Al <0.4 and Co/Al >0.4 (see Figure IV.7A and IV.7B). These results indicate that various Co ion species in *BEA zeolite are present and exhibit different oxidation activity.

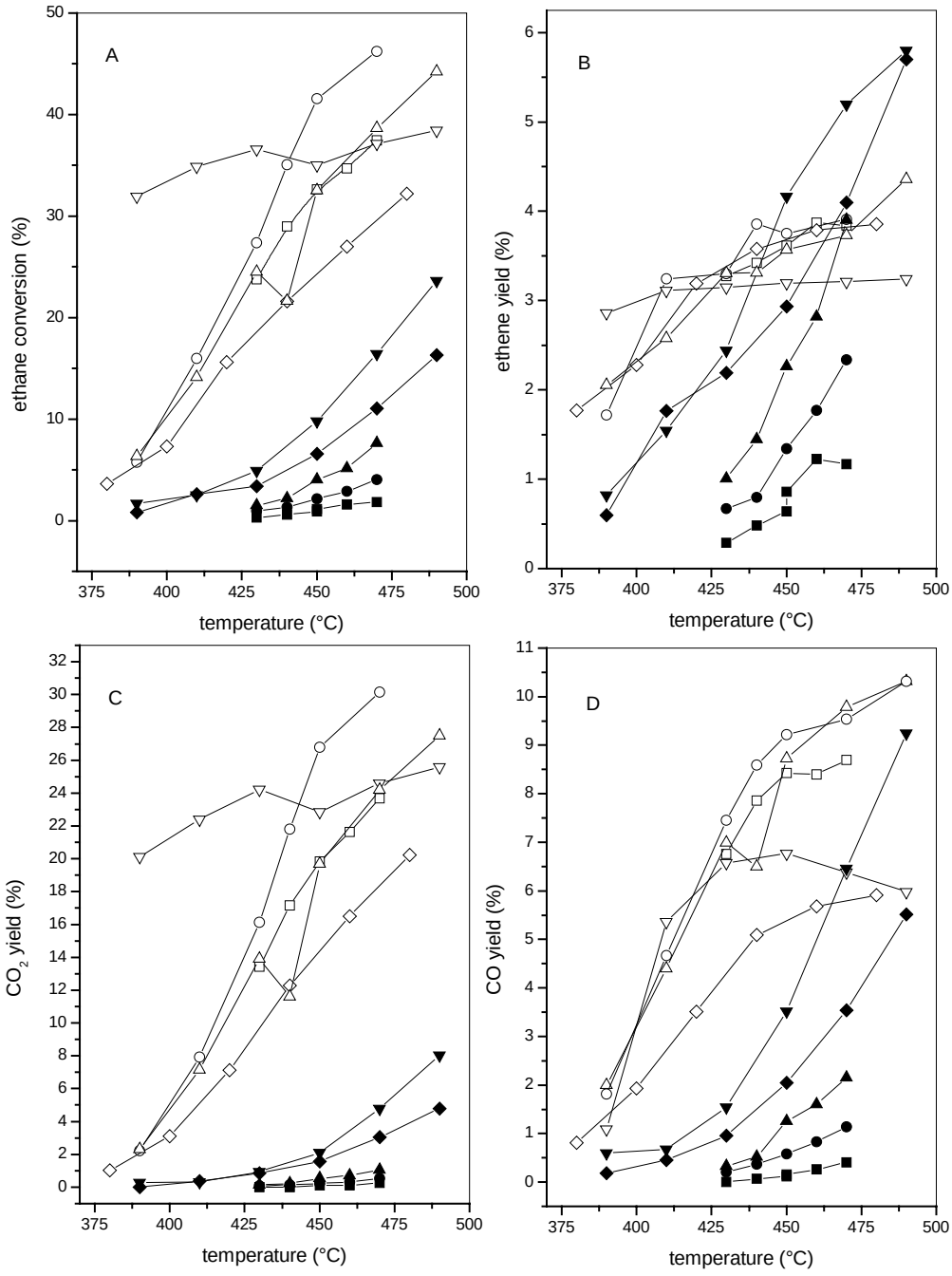

Figure IV.6 A-D Dependence of ethane conversion (A), ethane yield (B) and carbon oxides yield (C,D) on temperature over Co-*BEA zeolites. w_{cat} = 200 mg, F = 100 ml/min, 6.5 vol. % oxygen, 5 vol. % ethane; ■ - Co/Al = 0.15; ● - Co/Al = 0.25; ▲ - Co/Al = 0.30; ▼ - Co/Al = 0.32; ◆ - Co/Al = 0.40; □ - Co/Al = 0.50; ○ - Co/Al = 0.58; △ - Co/Al =0.60; ▽ - Co/Al = 0.87; ◇ - Co/Al = 1.14;

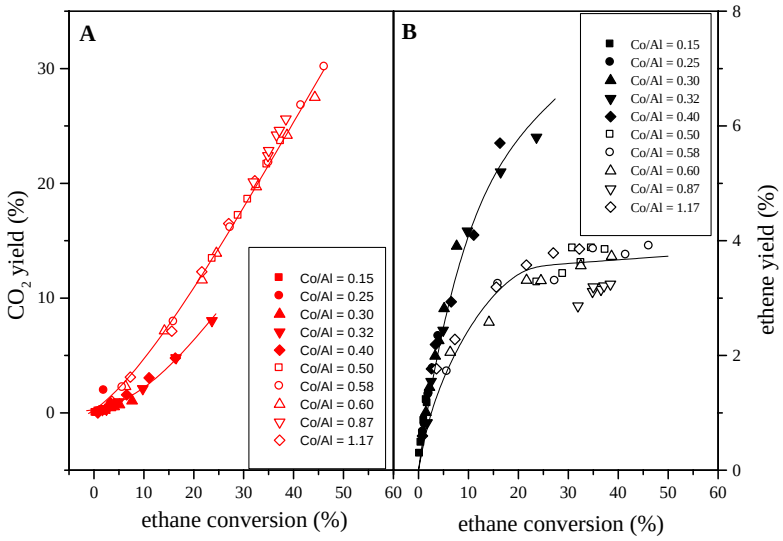

Figure IV.7 A Dependence of carbon dioxide yield on ethane conversion over Co-*BEA. (full symbols – samples with Co/Al < 0.5, open symbols – samples with Co/Al > 0.5), w_{cat} = 200 mg, F = 100 ml/min, 6.5 vol. % oxygen, 5 vol. % ethane

Figure IV.7 B Dependence of ethene yield on ethane conversion. over Co-*BEA (full symbols – samples with Co/Al < 0.5, open symbols – samples with Co/Al > 0.5), w_{cat} = 200 mg, F = 100 ml/min, 6.5 vol. % oxygen, 5 vol. % ethane

IV.1.3.3 Effect of nitrous oxide on oxidation of propane

As N_2O can be formed during ammoxidation reaction, moreover, (see Chapter IV.2) represents quite different oxidant, we also investigated the effect of N_2O on propane oxidation. Figure IV.8 shows the dependence of nitrous oxide conversion at various feed compositions on temperature over Co-*BEA zeolite. It has been found that nitrous oxide is decomposed over Co-zeolites to molecular nitrogen and molecular oxygen. Oxygen addition into the feed did not influence the N_2O conversion in its decomposition. In the reaction of propane with N_2O its conversion was much lower. When oxygen was added to the feed of N_2O and propane, the N_2O conversion significantly increased. The results indicate that N_2O decomposition is not affected by oxygen presence, on the other hand presence of oxygen in the C_3H_8/N_2O mixture enhance N_2O conversion.

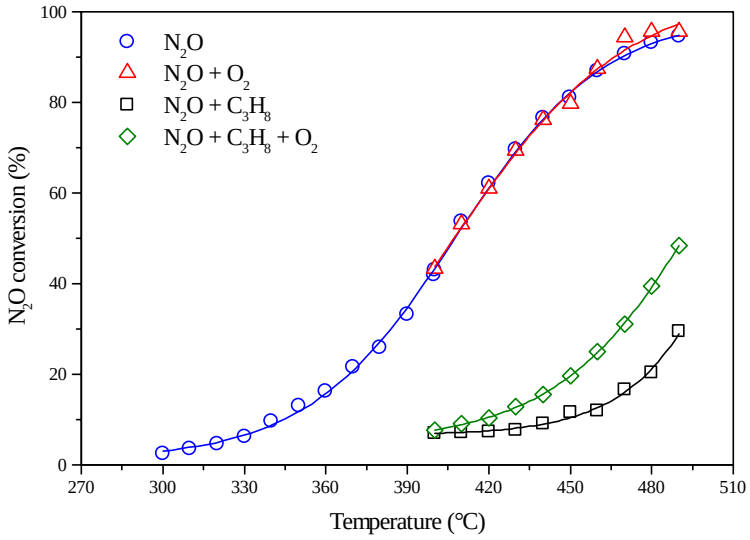

Figure IV.8 Conversion of N_2O to N_2 over Co-*BEA-12.4-0.25-1.8 zeolite in dependence on composition of the reaction mixture, m_{cat} = 0.2 g, F = 100 ml/min, 10 vol. % N_2O, 0-6.5 vol. % oxygen, 0-5 vol. % propane

The dependence of oxidation of propane by nitrous oxide on temperature is shown in Figure IV.9. Main products were propene, carbon dioxide and low concentration of carbon monoxide (selectivity < 5 %). Propane conversion increase from 2 to 9 % was accompanied by the decrease of selectivity to propene from 90 % to 30 %, which resulted in nearly constant yield of propene of about 2.5 %. No molecular oxygen was detected in the effluent gas.

Figure IV.10 depicts the effect of concentration of nitrous oxide in the N_2O/oxygen mixture at 450°C on propane oxidation. The data show that the conversion of propane depends on the N_2O/O_2 ratio. Conversion of propane dramatically increases with the increasing concentration of N_2O up to N_2O/O_2 ratio equal to ca 1, when the conversion reaches 14 % and then only slightly increases. After addition of 14 vol. % of N_2O to the reaction mixture of propane and oxygen there was observed a threefold higher propane conversion in comparison with that if only oxygen was fed. The selectivity to propene was independent on N_2O concentration. Selectivity to carbon dioxide slightly increased with increasing N_2O concentration herewith decreased the CO selectivity. These two reasons caused the increasing in the propene yield from 2 to 6 % at 450°C.

A comparison of propane oxidation by molecular oxygen, nitrous oxide and their mixture at 450°C is summarized in Table IV.7

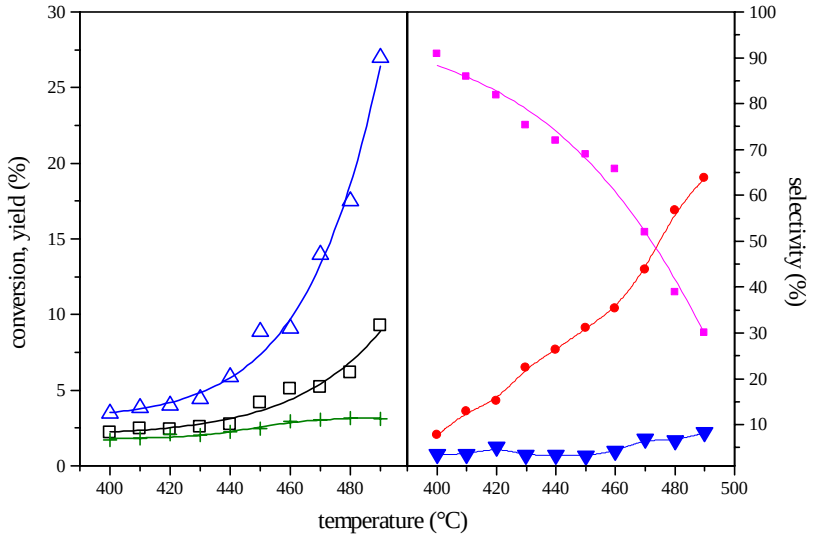

Figure IV.9 Oxidation of propane by N_2O as a function of temperature over Co-*BEA-12.4-0.25-1.8 zeolite at 450°C. w_{cat} = 200 mg, F = 100 ml/min, 5 vol. % propane, + 10 vol. % N_2O,. ◘- conversion of propane, + - yield of propene, △ - conversion of N_2O, ■ - selectivity to propene, ● - selectivity to carbon dioxide, ▼ - selectivity to carbon monoxide,

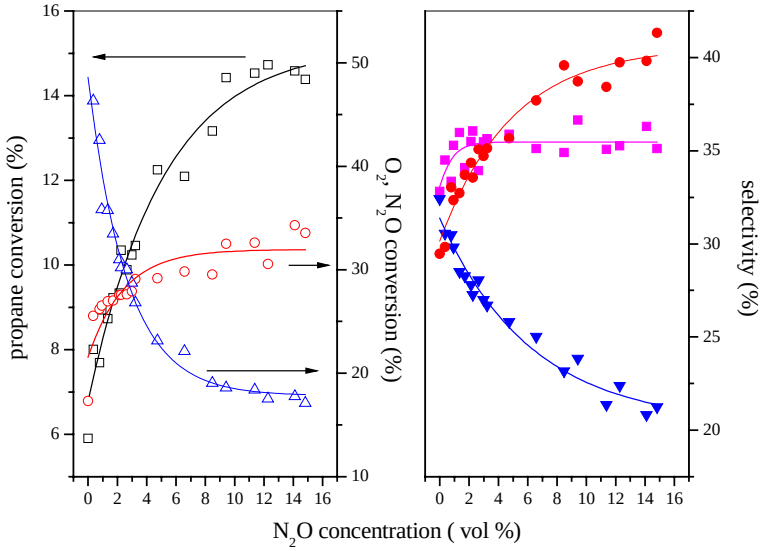

Figure IV.10 Influence of N_2O addition to propane/oxygen mixture over Co-*BEA-12.4-0.25-1.8 at 450°C. w_{cat} = 200 mg, F = 100 ml/min, 5 vol. % propane, 6.5 vol. % oxygen. ◘ - conversion of propane, △ - conversion of N_2O, O -conversion of oxygen, ■ - selectivity to propene, ● - selectivity to carbon dioxide, ▼ - selectivity to carbon monoxide

Table IV.7 Comparison of propane oxidation over Co-*BEA-12.4-0.5-1.8 zeolite at 450 °C, F = 100 ml/min and at propane conversion value of 5 %.

Reaction mixture	X (%)	S (%)			Y (%)	S^d (%)
	C_3H_8	C_3H_6	CO	CO_2	C_3H_6	C_3H_6
$C_3H_8 + O_2$[a]	5.9	33.6	32.3	34.1	2.0	35.7
$C_3H_8 + N_2O$[b]	3.8	68.0	2.3	29.7	2.6	52.3
$C_3H_8 + N_2O + O_2$[c]	13.9	37.5	22.0	40.5	5.2	71.1

[a] *Feed composition C_3H_8/O_2 – 5/6.5 vol. % , F = 100 ml/min*
[b] *Feed composition C_3H_8/N_2O – 5/10 vol. % , F = 100 ml/min*
[c] *Feed composition $C_3H_8/N_2O/O_2$ – 5/10/6.5 vol. % , F = 100 ml/min*
[d] *Selectivity to propene at identical conversion ($X_{propane}$ = 5 %)*

It is clearly seen that the substitution of molecular oxygen by nitrous oxide led to a slight decrease in propane conversion, nearly elimination of CO, but to a remarkable increase in selectivity to propene from 33.6 to a 68.0 % as well as in an increase in the propene yield. This also follows from propene selectivity values at identical propane conversion (last column in Table IV.7). The mixture of N_2O and O_2 resulted in two and half times higher conversion than if only oxygen was used and in four-times higher than that when only nitrous oxide was an oxidant. Selectivity to propene in N_2O/O_2 mixture was 37.5 %. But the conversion increased dramatically to 13.9 % and the yield increased up to 5.2 %. Also the selectivity to propene at comparable conditions substantially increased, see Table IV.7. The increase in propane conversion for the N_2O/O_2 mixture did not correspond to the sum of conversion of propane in oxidative dehydrogenations by oxygen and by nitrous oxide. Therefore, some synergy effect of oxygen and N_2O in this reaction was clearly manifested.

IV.1.4 Fe –zeolites

To explain the positive effect of N_2O on oxidative dehydrogenation of paraffins over Co-zeolites, which also contained trace concentration of Fe, behaviour of Fe-zeolites in oxidation with N_2O was investigated.

It is known that Fe-zeolites are connected with the extremely high activity of Fe ions in N_2O decomposition and oxidation benzene to phenol by N_2O, particularly for steamed zeolites exhibiting Fe ions as well as Al species in extra-framework positions[1,2]. Therefore,

we focus the attention to Fe-zeolites with respect to oxidation of propane by molecular oxygen, N_2O and their mixture

Catalytic activity of FeH-zeolites, expressed in terms of propane conversion, yield of propene and product selectivity with respect to hydrocarbons and oxygenates, is summarized in Table IV.8. All the investigated Fe-zeolites exhibited low activity in the oxidation of propane with molecular oxygen. The conversion of propane reached max. 3.4 % for the steamed zeolite (FeH-MFI-1200-HT) with maximum iron content. The main products were propene and carbon oxides. Selectivity towards propene reached 44.0 %, but the yield was only 1.5 %.

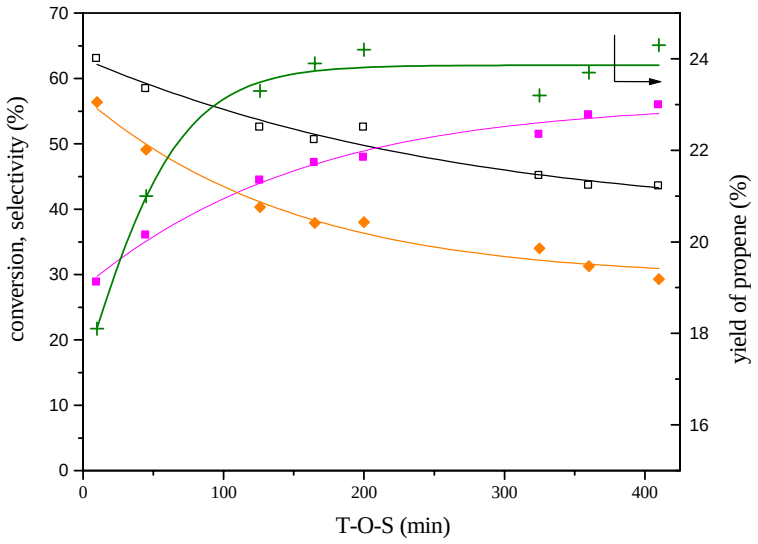

Figure IV.11 Dependence of the performance of FeH-MFI-1200-HT catalyst on time-on-stream at 450 °C. F = 100ml/min, w_{cat} = 200 mg, 5 vol. % propane, 10 vol. % N_2O. ☐ - conversion of propane, + - yield of propene, , ■ - selectivity to propene, ◆ - sum of selectivity towards oxygenates and products of propane oligomerization.

Propane oxidation with nitrous oxide led to a dramatic increase in propane conversion over FeH-MFI zeolites, particularly over the zeolites steamed at 600 °C, (3.4 vs. 43.5 % for FeH-MFI-1200-HT). The conversion notably increased from very low concentrations of Fe. An increase in the conversion was accompanied by a substantial increase in the selectivity to propene (44.0 vs. 55.9 %) and to the sum of aromatics and oxygenates (0 vs. 29.0 %); being again the highest with the steamed zeolites. Among the products appeared methanol, ethanol, propanol, propanal, phenol and acetone.

Also the products of propane cracking, i.e. methane, ethane and ethene appeared when N_2O was used. Moreover, N_2O presence in the reaction mixture caused formation of aromatics including benzene, toluene and phenol. It implies that using N_2O as oxidant compared to oxygen resulted in the higher propane conversions, higher selectivity to propene and in the appearance of aldehydes in the products as well as products of propane cracking and propene oligomerization. These effects were higher with increasing Fe content in the zeolite and with the zeolites steamed compared to those calcined in a dry oxygen.

However, the catalyst performance depended on the reaction time-on-stream (T-O-S), Figure IV.11. With decreasing propane conversion from 63.0 to 43.5 %, the selectivity to propene increased as well as the yield of propene, which reached ca 24 % within 100 min T-O-S and then remained nearly constant. On the other hand, the selectivity to the sum of oxygenates remained nearly constant with T-O-S (it changes from 24.6 to 26.4 %) as well as the selectivity to the sum of products of propane/propene cracking and oligomerization (7.1 %). The distribution of oxygenates was substantially changed with T-O-S. The selectivity to products of propane cracking/oligomerization substantially decreased from 10 to 2.6 %. Aromatics nearly disappeared within T-O-S, and accordingly decreased the selectivity to phenol.

Oxidation of propane with N_2O over Na form compared to H form of the steamed zeolite (FeNa-MFI-1200-HT contained trace concentration of Brønsted sites) was manifested in a slightly lower propane conversion, lower degree of deactivation with T-O-S, resulting in the higher selectivity to propene and constant yield of propene, as well as in a considerably lower selectivity to the sum of hydrocarbons excluding propene, oxygenates and phenol (see FigureIV.12). Stable reaction performance with respect to the products composition was achieved within 300 min.

Using a mixture of oxygen and nitrous oxide as oxidants compared to N_2O resulted with all the Fe-catalysts in an increase in propane conversion accompanied by a substantial increase in the selectivity to carbon oxides and a decrease in the propene selectivity, but not in substantial changes in the propene yields. The selectivity to and yields of oxygenates and aromatics decreased dramatically.

Table IV.8 Catalytic performance of Fe-zeolites with various content of Fe ions in propane oxidation at 450 °C. T-O-S = 400 min.

catalyst	$C_3H_8/O_2/N_2O$ (vol. %)	$X(C_3H_8)$ (%)	selectivity (%)															Y (C_3H_6)
			CO	CO_2	CH_4	C_2H_4	C_2H_6	C_3H_6	other [a]	C_3H_4	C_1OH*	C_2OH*	propanal	C_3OH*	phenol	C_6H_6	C_7H_8	
FeH-MFI-30-C	5/6.5/0	1.1	47.8	34.2	nd	nd	nd	18.0	nd	nd	nd	nd	nd	Nd	nd	nd	nd	0.2
	5/0/10	2.1	1.6	nd	nd	nd	nd	98.4	nd	nd	nd	nd	nd	Nd	nd	nd	nd	2.1
	5/6.5/10	3.2	33.4	24.3	nd	nd	nd	42.3	nd	nd	nd	nd	nd	Nd	nd	nd	nd	1.4
FeH-MFI-190-C	5/6.5/0	1.2	26.5	14.6	0.4	1.2	nd	57.3	nd	nd	nd	nd	nd	Nd	nd	nd	nd	0.7
	5/0/10	3.8	5.6	65.7	nd	2.0	nd	26.7	nd	nd	nd	nd	nd	Nd	nd	nd	nd	1.0
	5/6.5/10	6.8	8.7	63.7	0.3	<0.1	nd	27.3	nd	nd	nd	nd	nd	Nd	nd	nd	nd	1.9
FeH-MFI-190-HT	5/6.5/0	1.6	26.4	14.1	nd	nd	nd	59.4	nd	nd	nd	nd	nd	Nd	nd	nd	nd	0.9
	5/0/10	10.2	0.9	1.5	0.2	2.3	0.2	83.1	2.8	nd	0.2	1.9	1.7	2.7	0.8	0.5	1.2	8.5
	5/6.5/10	15.8	10.5	9.8	0.8	3.5	0.5	61.9	0.2	nd	1.1	4.1	2.2	3.0	<0.1	1.0	1.5	9.8
FeH-MFI-1200-HT	5/6.5/0	3.4	31.9	22.4	nd	1.7	nd	44.0	nd	nd	nd	nd	nd	Nd	nd	nd	nd	1.5
	5/0/10	43.5	2.8	4.7	0.7	4.6	1.8	55.9	0.4	0.1	0.4	5.6	5.7	12.7	2.0	0.9	1.7	24.3
	5/6.5/10	51.7	21.4	20.6	0.7	5.3	0.8	39.7	2.8	0.1	2.0	2.1	1.7	2.2	0.3	0.1	0.2	20.5
FeNa-MFI-1200-HT	5/6.5/0	2.5	30.0	18.6	nd	3.6	nd	47.8	nd	nd	nd	<0.1	nd	Nd	nd	<0.1	<0.1	1.2
	5/0/10	39.2	2.7	5.0	0.5	4.8	2.4	58.2	0.2	nd	0.8	3.2	4.0	17.4	<0.1	0.2	0.5	22.9
	5/6.5/10	45.9	22.4	24.5	0.5	3.8	0.7	41.6	1.5	nd	1.3	1.2	1.0	1.5	nd	<0.1	<0.1	19.1

nd – not detected
a - sum of selectivity to unknown products (based on mass balance)
**C_1OH-methanol, C_2Oh-ethanol, C_3OH-propanol*
C – calcined
HT – hydrothermal treatment

Different T-O-S behavior of propane conversion was observed depending on the oxidation agents used (see Figure IV.13). With molecular oxygen no deactivation occurred, while with N_2O a substantial deactivation was found, being slightly slower with the Na-form compared to H-form of the Fe zeolite. This finding corresponds to the presence of acidic protonic sites, which catalyze cracking/oligomerization and aromatization and hydrogen transfer reactions (as seen from the product composition) leading to formation of aromatics and coke precursors.

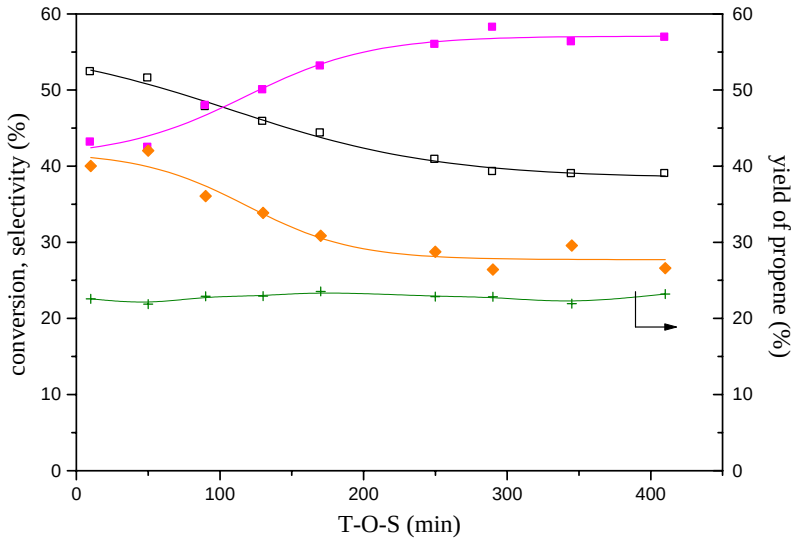

Figure IV.12 Dependence of the performance of FeNa-MFI-1200-HT catalyst on time-on-stream at 450 °C. F = 100 ml/min, w_{cat} = 200 mg, 5 vol. % propane, 10 vol. % N_2O. □ - conversion of propane, + - yield of propene, , ■ - selectivity to propene, ◆ - sum of selectivity towards oxygenates and products of propane oligomerization/cracking.

Moreover, the N_2O presence can initiate radical reactions. Participation of radicals in the oxidation process also supports formation of coke precursors. If, on the other hand, a mixture of oxygen and nitrous oxide was employed a lower deactivation in TOS was observed compared to the oxidation with nitrous oxide. A lower deactivation during the oxidation reaction with a mixture of N_2O and oxygen can be attributed to the oxidation of the reaction intermediates to carbon oxides by molecular oxygen.

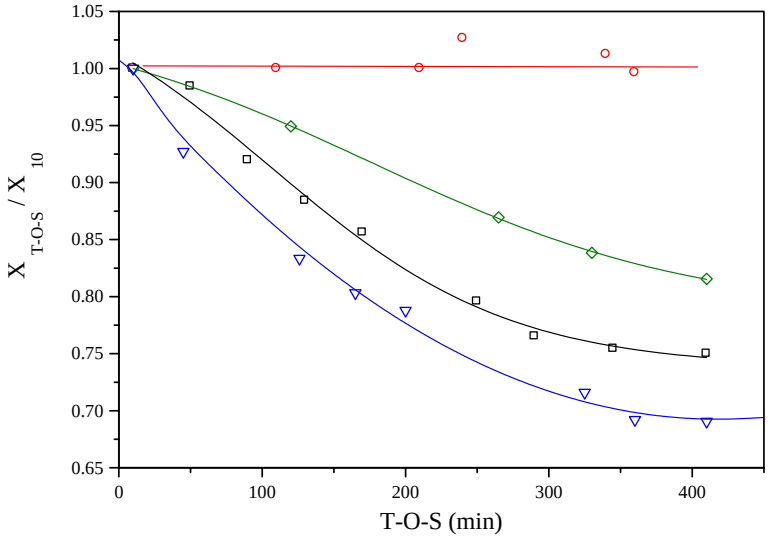

Figure IV.13 Deactivation of Fe-zeolites in oxidation of propane in dependence on time-on-stream. Deactivation is expressed as a ratio of actual propane conversion and conversion at T-O-S of 10 min. F = 100 ml/min, w_{cat} = 200 mg. FeNa-MFI-1200-HT: propane oxidation with ○ – oxygen, □ – N_2O, ◇ –oxygen and N_2O; ▽ - propane oxidation with N_2O over FeH-MFI-1200-HT.

IV.2 Activity of metallo-zeolites in ammoxidation of ethane and propane with molecular oxygen

IV.2.1 Parent H-zeolites

Samples of parent H-*BEA, H-MFI, H-FER and H-MOR exhibited conversion of propane only to carbon oxides and nitrogen as given in Table IV.9. Compared to oxidative dehydrogenation, the ammonia addition caused a decrease in propane conversion. No acrylonitrile, acetonitrile or propene was found. A hydrocarbon was converted to carbon oxides and ammonia only to nitrogen with selectivity 100 %. Carbon balance was calculated to be 98 %.

Table IV.9 Ammoxidation of propane over parent H-zeolites at 450°C, w_{cat} = 200 mg, F = 100 ml/min, 5 vol. % ethane, 6.5 vol. % oxygen, 10 vol. % ammonia

Sample	X %			S %				Y %
cation-matrix-Si/Al	C_3H_8	O_2	NH_3	CO	CO_2	C_3H_3N	N_2	C_3H_6
H-MFI-12.5	0.4	35.6	8.7	59.2	40.8	0.0	100.0	0.0
H-*BEA-13.0	0.5	37.3	9.1	53.4	46.6	0.0	100.0	0.0
H-FER-9.5	0.5	33.0	7.0	0.0	100.0	0.0	100.0	0.0
H-MOR-9.4	0.0	34.4	6.0	0.0	0.0	0.0	100.0	0.0

IV.2.2 Cu-zeolites

The activities of copper zeolites were compared at 450°C and the results are given in Table IV.10. All Cu-zeolites investigated exhibited high selectivity to propene, but acrylonitrile was not detected. Ammonia addition caused a significant decrease in propane and oxygen conversion. No acrylonitrile and only low selectivity to acetonitrile was found in contrast to substantial selectivity to propene. Ammonia was converted to dinitrogen with selectivity of 100 %. The turn-over-frequency (TOF) values related to a hydrocarbon conversion indicate that the most active Cu sites are located in *BEA structure, while those in FER exhibit 9x lower activity.

Table IV.10 Ammoxidation of propane over Cu-zeolites at 450°C, w_{cat} = 200 mg, F = 100 ml/min, 5 vol. % propane 6.5 vol. % oxygen, 10 vol. % ammonia

sample matrix-Si/Al-Cu/Al-w_{Cu}	X %			S %						TOF $_{total}$
	C_3H_8	O_2	NH_3	CO	CO_2	C_3H_6	C_2H_3N	C_3H_3N	N_2	(h^{-1})
Cu-MFI-22.6-0.28-1.1	3.7	41.1	7.7	10.8	26.2	56.4	6.6	0.0	98.0	3.6
Cu-*BEA-13.5-0.3-1.6	7.6	28.5	16.0	16.1	36.3	47.6	0.0	0.0	100.0	7.5
Cu-FER-9.5-0.25-2.2	1.7	47.8	18.8	7.9	66.4	25.7	0.0	0.0	100.0	0.8

IV.2.3 Co-zeolites

Dependences of conversion and selectivity in propane ammoxidation and ethane ammoxidation on temperature over the most active Co-*BEA-17.6-0.39-1.7 are shown in Figures IV.14 and IV.15. The dependences have similar features like those for paraffins oxidations (cf. Figures IV.3 and IV.4). Conversion of oxygen was higher in the ammoxidation reactions as it was consumed also in oxidation of ammonia to molecular nitrogen (high selectivity to N_2). Very low concentrations of NO_x were also detected. Surprisingly no acrylonitrile was formed although propene was among the products, but only acetonitrile appeared. Conversion of propane, oxygen and ammonia understandably increased with temperature, and the opposite trend has been observed for selectivity of acetonitrile, but propene and ethene selectivity slightly increased with temperature.

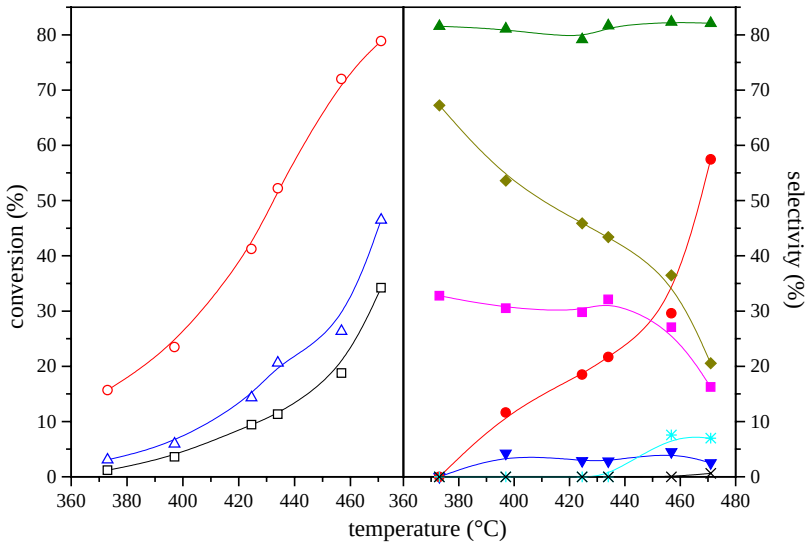

Figure IV.14 Ammoxidation of propane in dependence on temperature over Co-*BEA-17.6-0.39-1.7, w_{cat} = 200 mg, F = 100 ml/min, 6.5 vol. % oxygen, 5 vol. % propane, 10 vol. % ammonia, ○ -conversion of oxygen, □- conversion of propane, △ - conversion of ammonia, ▲- selectivity to nitrogen, ◆ - selectivity to acetonitrile, ■ - selectivity to propene,● - selectivity to carbon dioxide, ▼ -selectivity to carbon monoxide, ✳ - selectivity to ethene, × - selectivity to methane

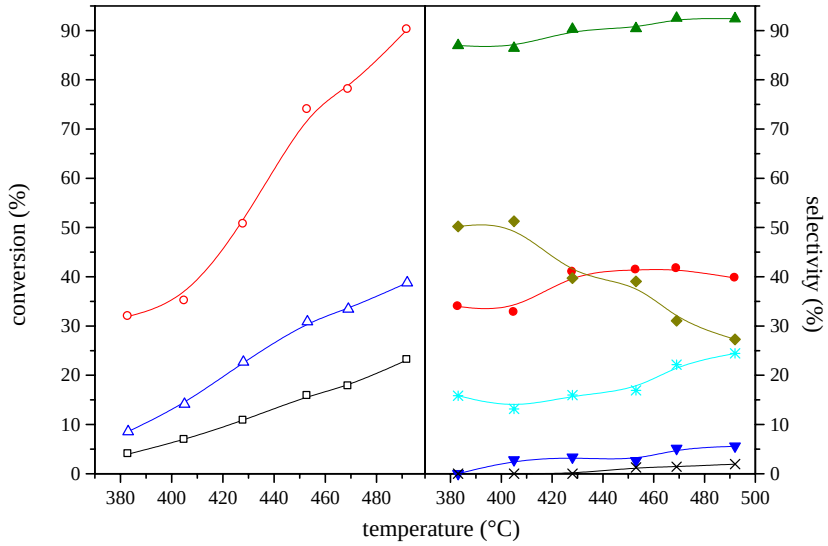

Figure IV.15 Ammoxidation of ethane in dependence on temperature over Co-*BEA-17.6-0.39-1.7, w_{cat} = 200 mg, F = 100 ml/min, 5 vol, % ethane, 6.5 vol. % oxygen, 10 vol. % ammonia, ○ -conversion of oxygen, □- conversion of propane, △ - conversion of ammonia, ▲- selectivity to nitrogen, ◆ - selectivity to acetonitrile, ● - selectivity to carbon dioxide, ▼ -selectivity to carbon monoxide, ✳ - selectivity to ethene, × - selectivity to methane

IV.2.3.1 Co-zeolites with various framework topology

To analyze the effect of zeolite topology, ammoxidation of ethane and propane was carried out over a set of samples with exchanged cobalt ions in MFI, *BEA, MOR and FER zeolites. The effect of zeolite topology on propane conversion was clearly manifested. Like for oxidative dehydrogenation Co-*BEA and Co-MFI zeolites showed much higher propane conversion and TOF values, compared to Co-FER and Co-MOR (Table IV.11). Also a comparison of the TOF values related to acetonitrile showed the sequence: *BEA > MFI >> FER ~ MOR.

Table IV.11 Ammoxidation of propane over Co-zeolites at 450°C, w_{cat} = 200 mg, F = 100 ml/min, 5 vol. % propane, 6.5 vol. % oxygen, 10 vol. % ammonia

Sample matrix-Si/Al-Co/Al-w_{Co}	X %			S %							TOF $_{total}$ (h^{-1})	TOF $_{C2H3N}$ (h^{-1})
	C_3H_8	O_2	NH_3	CO	CO_2	CH_4	C_2H_4	C_3H_6	C_2H_3N	N_2		
Co-*BEA-12.4-0.25-1.8	7.3	48.0	11.8	5.8	16.4	0.0	0.0	40.7	36.6	84.2	15.9	5.8
Co-*BEA-13.8-0.50-2.8	7.0	38.3	12.5	2.9	17.0	0.0	0.0	51.8	26.9	90.0	10.0	2.7
Co-*BEA-17.6-0.39-1.7	17.0	64.6	25.1	3.4	25.1	0.0	4.4	28.0	37.6	81.9	34.1	12.8
Co-MFI-12.5-0.23-1.6	14.0	73.7	30.2	4.0	22.3	0.0	1.5	38.6	27.9	90.8	33.3	9.2
Co-MFI-12.5-0.42-2.9	18.3	34.0	37.2	3.2	29.1	0.9	4.8	36.0	25.8	91.2	23.9	6.2
Co-MFI-12.5-0.55-3.8	12.8	61.7	27.9	0.1	22.6	0.1	3.0	46.5	23.8	93.0	12.8	3.0
Co-FER-9.4-0.23-1.0	0.8	23.7	4.8	0.0	15.8	0.0	26.6	57.5	0.0	100.0	3.18	0.0
Co-FER-8.6-0.42-3.6	0.5	25.4	8.3	0.0	93.9	0.0	0.0	6.2	0.0	100.0	0.6	0.0
Co-MOR-9.4-0.48-2.1	2.0	34.0	3.9	0.0	26.1	0.0	0.0	65.2	8.7	97.1	3.7	0.3

Table IV.12 Ammoxidation of ethane over Co-zeolites at 450°C, w_{cat} = 200 mg, F = 100 ml/min, 5 vol. % ethane, 6.5 vol. % oxygen, 10 vol. % ammonia

sample matrix-Si/Al-Co/Al-w_{Co}	X %			S %						TOF total (h^{-1})	TOF C2H3N (h^{-1})
	C_2H_6	O_2	NH_3	CO	CO_2	CH_4	C_2H_4	C_2H_3N	N_2		
Co-*BEA-12.4-0.25-1.8	11.1	52.4	19.3	12.4	28.2	0.0	13.3	46.1	86.4	45.0	20.7
Co-*BEA-13.8-0.50-2.8	11.8	59.4	21.2	7.6	30.5	0.0	15.4	46.6	86.8	16.8	7.8
Co-*BEA-17.6-0.39-1.7	14.4	69.5	29.0	3.0	40.8	0.1	17.9	38.2	90.5	28.8	11.0
Co-MFI-12.5-0.23-1.6	6.3	51.9	21.9	7.2	31.4	0.0	31.2	30.2	95.5	15.0	4.5
Co-MFI-12.5-0.42-2.9	17.2	72.2	31.4	3.3	39.5	0.0	31.4	25.8	95.7	22.4	5.8
Co-MFI-12.5-0.55-3.8	16.3	80.1	38.8	0.4	41.3	0.0	32.8	25.7	95.1	16.3	4.2
Co-FER-9.4-0.23-1.0	0.2	32.7	3.4	0.0	100.0	0.0	0.0	0.0	100.0	0.8	0.0
Co-FER-8.6-0.42-3.6	0.0	22.1	6.9	0.0	0.0	0.0	0.0	0.0	100.0	0.0	0.0
Co-MOR-9.4-0.48-2.1	0.5	36.8	4.4	0.0	100.0	0.0	0.0	0.0	100.0	0.9	0.0

IV.2.3.2 Effect of Co concentration

The effect of Co concentration in zeolites on ammoxidation of ethane is shown on Co-*BEA and Co-MFI zeolites, as given in Table IV.13 and in a part of Table IV.12.

Table IV.13 Ethane ammoxidation over Co-*BEA zeolites at 450 °C. w_{cat} = 200 mg, F = 100 ml/min, 5 vol. % ethane, 6.5 vol. % oxygen, 10 vol. % ammonia

sample matrix-Si/Al-Co/Al-w_{Co}	X %			S %						TOF total (h^{-1})	TOF C2H3N (h^{-1})
	C_2H_6	O_2	NH_3	CO	CO_2	CH_4	C_2H_4	C_2H_3N	N_2*		
Co-*BEA-13.1-0.15-1.0	8.0	58.3	15.9	8.7	42.2	0.0	10.2	38.9	93.4	33.0	13.1
Co-*BEA-12.4-0.25-1.8	14.6	55.9	15.0	5.8	48.6	0.0	6.4	39.2	93.2	33.6	13.2
Co-*BEA-13.1-0.30-1.8	16.3	89.8	31.8	4.8	51.3	0.8	15.2	28.0	94.7	34.8	10.0
Co-*BEA-13.1-0.32-2.0	16.7	90.5	30.6	3.1	58.9	0.0	10.4	27.6	95.3	33.8	9.3
Co-*BEA-12.3-0.34-2.1	18.6	91.1	31.0	4.8	49.4	0.9	13.4	31.5	93.5	34.6	10.9
Co-*BEA-13.0-0.50-2.7	18.8	94.7	34.8	2.9	52.8	1.1	15.3	27.9	95.2	27.9	7.6
Co-*BEA-13.0-0.51-3.1	21.8	96.8	33.9	0.0	48.9	1.4	20.9	28.9	94.3	27.8	8.0
Co-*BEA-11.9-0.50-3.2	21.2	98.5	33.1	0.9	54.6	1.3	16.2	27.0	94.6	26.2	7.1
Co-*BEA-13.1-0.87-4.7	19.2	87.7	31.6	1.5	52.1	1.1	16.7	28.6	93.5	15.7	5.2
Co-*BEA-13.1-1.17-7.8	15.9	86.2	29.7	0.0	60.1	0.4	18.2	21.6	95.7	8.0	1.7

*max $NH_3 \rightarrow$NOx was 2 %; *related to NH_3 conversion*

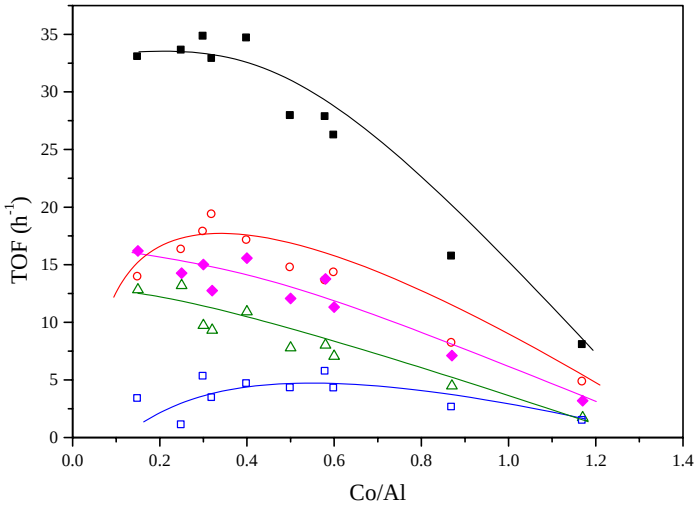

Figure IV.16 Dependence of TOF values in ethane ammoxidation on Co/Al molar ratio of Co-*BEA catalysts at reaction temperature 450°C. F = 100 ml/min, w_{cat} = 200 mg, 5 vol. % ethane, 6.5 vol. % oxygen, 10 vol. % ammonia ■ - TOF related to conversion of ethane, ○ - TOF related to CO_2, □ - TOF related to ethene, △ - TOF related to acetonitrile, ◆ - TOF related to sum of ethene and acetonitrile,

With increasing Co concentration in zeolites increased conversion of ethane up to Co/Al = 0.5 and then decreased. The TOF values per Co ion showed different dependence compared to oxidative dehydrogenation. The dependence of TOF for ethane ammoxidation on cobalt loading is shown in Figure IV.16. It is clearly seen that the activity of Co ions in *BEA zeolites with low cobalt concentration was high and nearly constant up to Co/Al = 0.4, and then declined. TOF related to ethene and to carbon dioxide was increasing with Co loading exhibited broad maximum about Co/Al 0.4 - 0.5. TOF related to acetonitrile decreased with Co/Al. Similarly to previous experiments over Cu-, H- and Co-MFI zeolites, the addition of ammonia caused the decrease in selectivity to carbon monoxide. But TOF values for acetonitrile formation showed similar dependence as total TOF in ethane conversion (Figure IV.16).

It is to be pointed out that in contrast to oxidative dehydrogenation the dependence of ethene or CO_2 yields on ethane conversion over Co-*BEA zeolites in ammoxidation for various cobalt concentrations shows only one dependence (Figure IV.18).

Similarly to oxidative dehydrogenation, the increasing conversion of ethane was observed with increasing Co loading. Selectivity to ethene was low (< 6 %) in the whole concentration range; it exhibited a broad maximum around Co/Al 0.5. A decrease in selectivity to acetonitrile was observed with increasing Co loading.

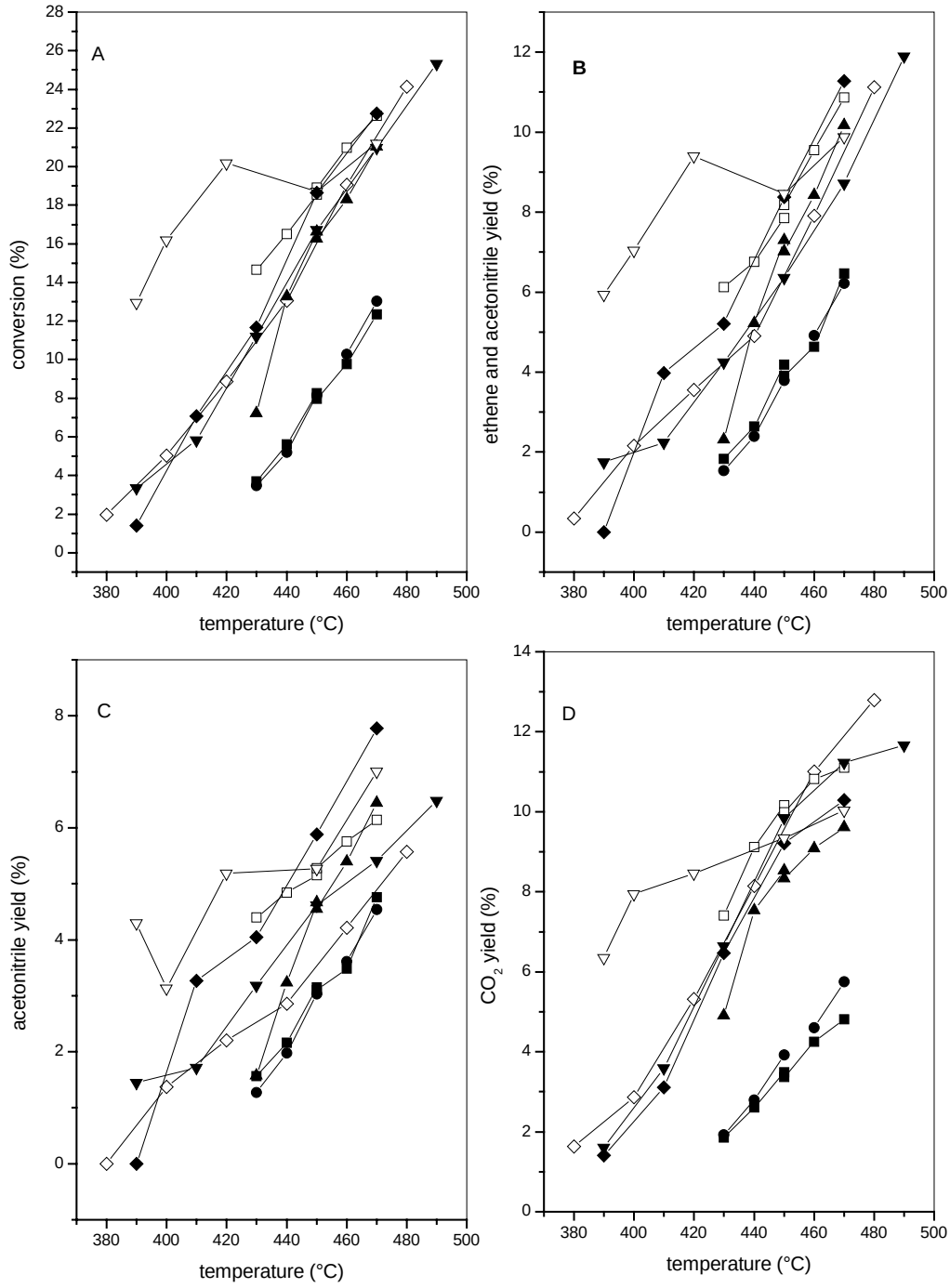

Figure IV.17 A-D Dependence of ethane conversion (A), ethane and acetonitrile yield (B), acetonitrile yield (C) and carbon dioxide yield (D) on temperature over Co-*BEA zeolites. w_{cat} = 200 mg, F = 100 ml/min, 6.5 vol. % oxygen, 5 vol. % ethane, 10 vol.% ammonia; ■ - Co/Al = 0.15; ● - Co/Al = 0.25; ▲ - Co/Al = 0.30; ▼ - Co/Al = 0.32; ◆ - Co/Al = 0.40; □ - Co/Al = 0.50; ▽ - Co/Al = 0.87; ◇ - Co/Al = 1.14;

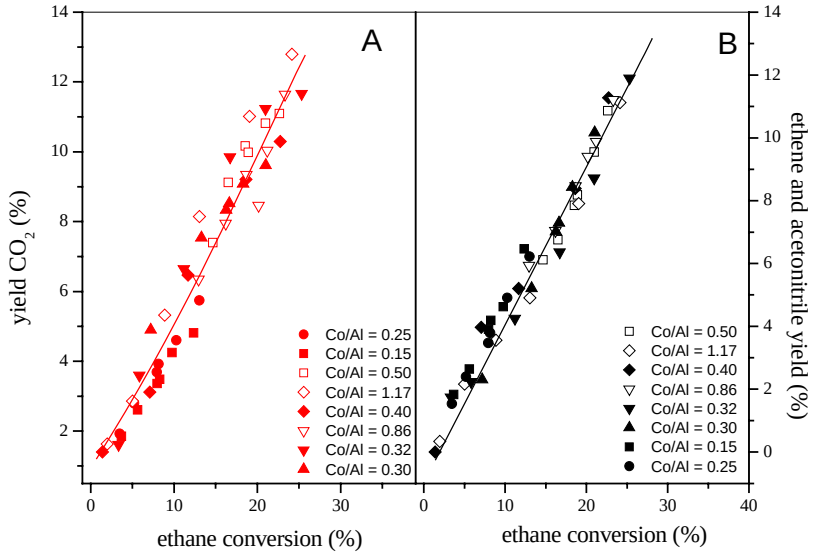

Figure IV.18 Ethane ammoxidation over Co-*BEA, F = 100 ml/min, 5 vol. % ethane, 6.5 vol. % oxygen, 10 vol. % ammonia; **A** Dependence of carbon dioxide yield on ethane conversion (full symbols – samples with Co/Al < 0.5, open symbols – samples with Co/Al > 0.5) **B** Dependence of ethene yield on ethane conversion (full symbols – samples with Co/Al < 0.5, open symbols – samples with Co/Al > 0.5)

IV.2.3.3 Reactivity of acrylonitrile and acetonitrile

To explain absence of acrylonitrile in the products of propane ammoxidation, reactivity of both acetonitrile and acrylonitrile was studied on the CoH-MFI-12.5-0.42 zeolite at 450 °C (see Figures IV.19 and IV.20, resp.). The conversion of acetonitrile in its oxidation (0.35 vol. % of acetonitrile, 6.5 vol. % of oxygen) was 37 %. The selectivity to CO was 38 % and to CO_2 achieved 62 % (Figure IV.19). All nitrogen of acetonitrile was converted to molecular nitrogen. Addition of ammonia to the reaction mixture (0.4 vol. % of acetonitrile, 6.5 vol. % of oxygen) up to 2 vol. % led to an increase in conversion of acetonitrile from 37 to 60 % and then the conversion levelled-off. The selectivity to CO_2 increased after addition of ammonia to 97 % and the selectivity to CO decreased to 2 %. Thus the most distinct changes were observed in the range from 0 to 2 vol. % of ammonia in the reaction mixture.

The reactivity of acrylonitrile in the presence of ammonia was investigated at similar conditions (0.4 vol. % of acrylonitrile, 6.5 vol. % of oxygen and concentrations of ammonia from 0 to 10 vol. %) (Figure IV.20). Without ammonia in the feed CoH-MFI zeolite exhibited acrylonitrile conversion about 7 %. Main products were CO_2, N_2 and low concentration of CO. Addition of ammonia up to 0.8 % to the reaction mixture led to a rapid increase in conversion of acrylonitrile. At ammonia concentration of 0.5 vol. %, conversion of acrylonitrile increased to

70 % and a new product – acetonitrile was formed with 76 % selectivity. Further increase in concentration of ammonia to 2.5 vol. % led to a decrease in selectivity to acetonitrile and to an increase in selectivity to carbon dioxide. Above this concentration of ammonia the conversion of acrylonitrile and the selectivity to acetonitrile (26 %) and carbon dioxide (73 %) were constant.

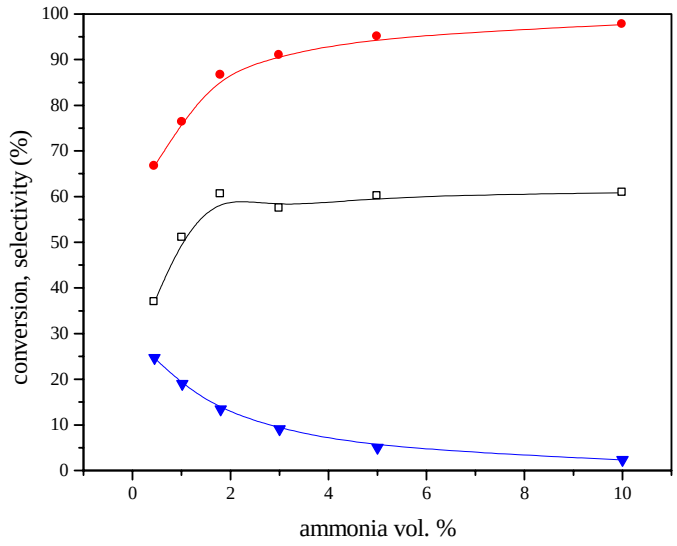

Figure IV. 19 Oxidation of acetonitrile in dependence on ammonia concentration over Co-MFI-12.5-0.42-2.9, w_{cat} = 200 mg, F = 100 ml/min, 0 - 10 vol. % ammonia, 0.35 vol. % acetonitrile, 6.5 vol. % oxygen, □- conversion of acetonitrile, ▼- selectivity to carbon monoxide, ● - selectivity to carbon dioxide,

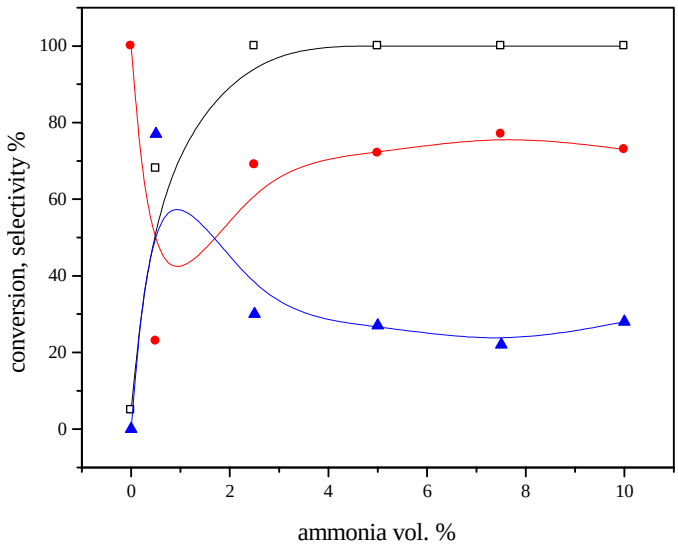

Figure IV.20 Oxidation of acrylonitrile in dependence on ammonia concentration over Co-MFI-12.5-0.42-2.9, w_{cat} = 200 mg, F = 100 ml/min, 0 - 10 vol. % ammonia, 0.45 vol. % acrylonitrile, 6.5 vol. % oxygen, □- conversion of acrylonitrile, ▲- selectivity to acetonitrile, ● - selectivity to carbon dioxide,

It is clearly seen that in ammonia presence acetonitrile is less reactive than acrylonitrile. Acrylonitrile is readily converted already at low ammonia concentration to acetonitrile, surprisingly no other products (CO, methane) were detected. Higher ammonia concentrations in the reaction stream supported oxidation of acrylonitrile (or acetonitrile as intermediate product) to CO_2 like in the case of acetonitrile.

IV.2.3.4 Effect of nitrous oxide on ammoxidation of propane

To evaluate the effect of possibly formed N_2O (although of very low concentration) on the conversion of hydrocarbons over Co-MFI and Co-*BEA zeolites in ammonia presence, 1 vol. % of N_2O was added to the reaction mixture. The results showed a small decrease in hydrocarbon conversions in both reactions, but no significant changes in the selectivity in ammoxidation reactions (see Table IV.15). It is in contrast to oxidative dehydrogenation, where substantial increase of paraffin conversion and ethene yield were observed with N_2O presence in the reactant stream. It follows that there is an important finding that while with both ethane and propane oxidation addition of N_2O caused an increase in paraffin conversion at the same selectivity to olefins (see Table IV.7), no such enhancement was observed at the ammoxidation reaction.

Table IV.15 Addition of N_2O to oxidation and ammoxidation of propane and ethane over Co-MFI-12.5-0.42-2.9 at 450°C, w_{cat} = 200 mg, F = 100 ml/min, 5 vol. % propane, 6.5 vol. % oxygen, 0/10 vol. % ammonia,

reaction	vol. % N_2O	X (%)	S (%)				
			CO	CO_2	C_2H_4	C_2H_3N	C_3H_6
propane ammoxidation	0	17.1	1.9	24.0	5.4	27.1	40.0
	1	16.0	1.8	24.4	3.1	25.9	44.7
ethane ammoxidation	0	8.1	0.0	26.4	41.4	32.3	-
	1	7.3	0.0	28.3	45.9	25.8	-

IV.3 UV-Vis spectroscopy

It is known that the exchanged Co ions in zeolites exhibit a divalent valent state[3]. Oxidation of these cations to Co(III) does not occur and the reduction of Co ions to metallic cobalt is difficult even in hydrogen at high temperatures.

IV.3.1 Ex-situ UV-Vis spectra of Co zeolites

IV.3.1.1 Dehydrated (deammoniated) Co-zeolites

In the previous work siting of Co ions in pentasil ring zeolites of MOR, FER, MFI and *BEA topology was suggested from the known local framework topologies, siting of non-transition metal ions, characteristic spectra of d-d transitions of Co(II) ions and related characteristic perturbation of framework T-O bonds induced by Co(II) ion bonding to the framework [3,4,5,6]. The wavenumbers of the band positions of d-d transitions in Vis spectra corresponding to the individual Co sites are given in Table IV.17. The positions and half-widths of the Vis bands were established for Co-zeolite samples exhibiting predominantly one type of the Co site. It was concluded that the cobalt ions exhibit three typical coordinations, corresponding to three structural sites, denoted as α, β and γ, but so far not reported in the literature for Co(II) complexes in solids (see Ref.3,4,5,6).

According to the known band positions, relatively broad spectra of Co-zeolites could be fitted (for illustration see Figure IV.21). It enabled to obtain quantitative analysis of cobalt ions in the individual sites (see Refs. 3,4,5,6). Quantitative analysis using absorption coefficients, revealed that the β sites are the most populated by Co ions in all pentasil ring zeolites (about 60-80%). The α–type (10-30 %) and particularly the γ-type Co-sites represent minor parts.

UV-Vis spectra were measured for a set of dehydrated samples with different concentrations of cobalt in the most active Co-*BEA zeolites (Figure IV.22). It is clearly seen that with all Co-*BEA zeolites, the highest intensity possesses the bands of the Co ions in β sites, followed by the Co ions in α sites. Number of Co-γ sites is very low.

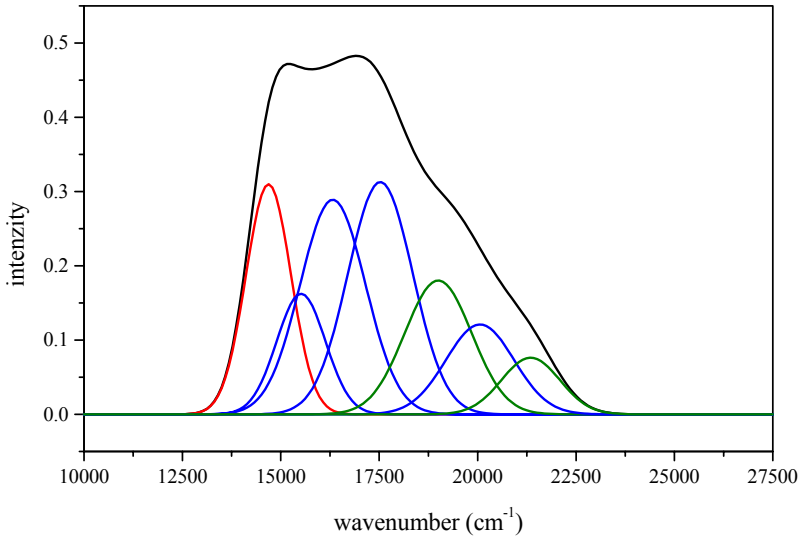

Figure IV.21 Example of UV-Vis spectrum of evacuated (10^{-5} Pa) Co-*BEA zeolite deconvoluted to the bands corresponding to α (—), β (—) and γ (—) type Co-sites.

Table IV.17 UV-Vis bands of the l α–, β–, γ– Co-sites in zeolites taken from Refs. 3,4,5 and 6

topology	Co-site	(cm^{-1})	(cm^{-1})	(cm^{-1})	(cm^{-1})
*BEA	α	14 600			
	β	15 500	16 300	17 570	21 700
	γ	18 900	20 100		
MFI	α	15 100			
	β	16 000	17 150	18 600	21 200
	γ	20 100	22 000		
FER	α	15 000			
	β	16000	17 100	18 700	20 600
	γ	20 300	22 000		
MOR	α	14 800			
	β	15 900	17 500	19 200	21 080
	γ	20150	22 050		

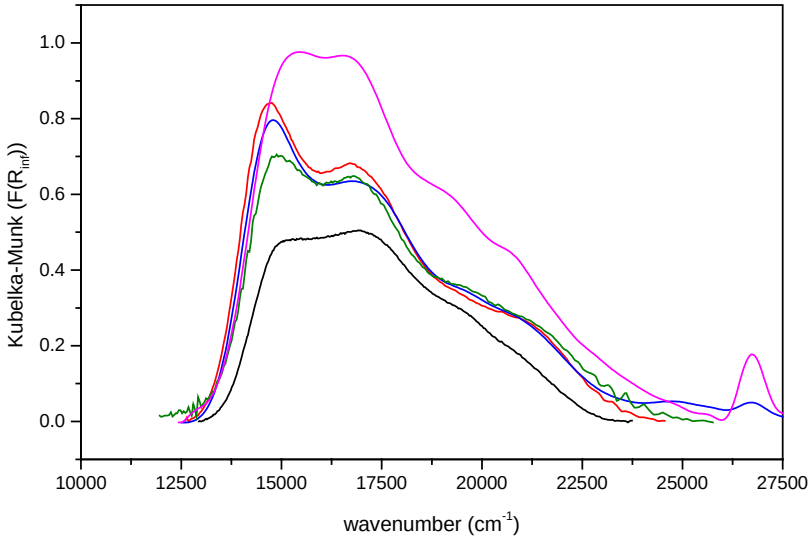

Figure IV.22 UV-Vis spectra of evacuated samples (10^{-5} Pa) with various Co loading in *BEA zeolite -— Co/Al 0.35, — Co/Al 0.5, — Co/Al 0.6, — Co/Al 0.84, — Co/Al 1.17

IV.3.1.2 Adsorption of oxygen, ethane, ethene and ammonia

The investigation of the interaction of the Co ions with the reactants – ethane, ethene, oxygen and ammonia – was done by adsorption of these gases at ex-situ experiments using UV-Vis spectroscopy. The spectra of the Co-*BEA with adsorbates are given in Figure IV.23. It was shown that adsorption of oxygen (dry) and ethane did not affect significantly the d-d transitions of the Co(II) ions in dehydrated Co-*BEA catalyst. Even at higher temperature with the presence of ethane or oxygen (300°C) no changes in the spectra were observed. On contrary, ethene interacted strongly with Co(II) ions and changed the spectrum feature, as reflected in both the spectra of Co-α and Co-β sites.

The most significant changes were obtained after exposure of the zeolite to ammonia at RT, Figures IV.23 and IV.24. The spectrum of ammonia adsorbed of Co(II) ions was preserved after evacuation at 100 ^{o}C, and even evacuation of the sample at 450 ^{o}C showed ammonia bonding to both Co-α and Co-β sites. Lowering of the intensity of the bands can indicate transformation of the Co-(NH_3)n complexes to the Co-NH_3 ones. Thus ammonia is strongly bound on both Co-α and Co-β sites at temperature of the ammoxidation reaction.

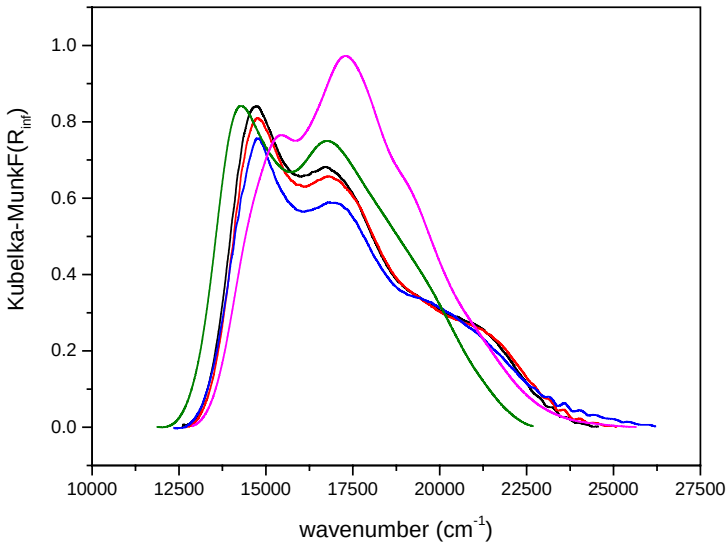

Figure IV. 23 Normalized UV-Vis spectra of dehydrated and evacuated (10^{-5}Pa) Co*BEA-13.1-0.5-2.6 (—), with oxygen (—), ethane (—), ethene (—), with ammonia (—)66.66 kPa and RT

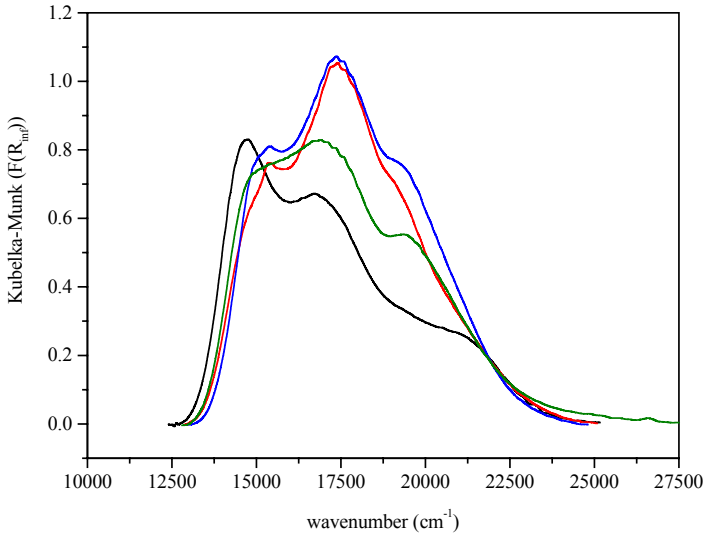

Figure IV. 24 UV-Vis spectra of dehydrated and evacuated (10^{-5}Pa) Co*BEA-13.1-0.5-2.6 (—), adsorption of ammonia (RT, 66.66 kPa) (—), and evacuation at 100°C (—), and at 470°C (—).

IV.3.2 In-situ Vis spectra of Co-zeolites

In-situ Vis spectra were monitored in the reactant streams at conditions comparable to those at the reaction kinetic test. The spectra changes were monitored after stepwise addition of the individual reactants into the stream of helium at reaction conditions (450°C). The UV-Vis spectum of Co-*BEA is shown in Figures IV.25. Already catalyst calcination (Co-*BEA-13.1-0.5-2.6) in an oxygen stream showed a change in Co(II) coordination compared to the evacuated sample in contrast to the adsorption of dry oxygen, which did not result in the change of the spectrum of the evacuated Co-beta zeolite. This change might be caused by adsorption of traces of water vapour present in an oxygen stream. Addition of ethane in an oxygen stream did not result in a further change of the Co spectrum, although gas product analysis revealed formation of low concentration of ethene and CO_x in the reactor outlet However, ammonia addition to this mixture or into He/ethane mixture provided (see Figure IV.25) a dramatic change of the spectrum feature. These results clearly show a strong adsorption of ammonia on Co(II) ions at both structural sites. Thus strong ammonia adsorption of Co sites dominates at the real conditions of the ammoxidation reaction.

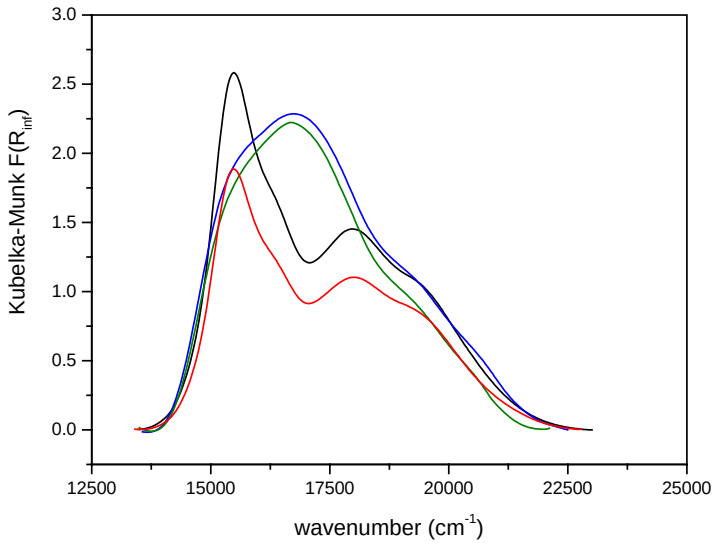

Figure IV. 25 In-situ UV-Vis spectra of Co*BEA-13.1-0.5-2.6 at 450°C, — calcination in an oxygen stream (6.5 vol. % O_2 in helium), — 5 vol. % ethane and 6.5 vol. %oxygen, — 10 vol. % ammonia and 5 vol. % ethane, — - 10 vol. % ammonia, 6.5 vol. % oxygen and 5 vol. %ethane

IV.4 FTIR spectroscopy

Recording of FTIR spectra of Co- and H-zeolites enabled to obtain information on the presence of bridging OH groups, perturbation of the framework T-O-T bonds by Co(II) ions coordinated to the framework, and adsorption of reaction intermediates.

IV.4.1 Ex-situ FTIR spectra over Co-zeolites

IR spectra were recorded for the most active Co-*BEA zeolites with cobalt concentrations up to an "over-exchange" level. The OH region of the IR spectra of dehydrated Co-zeolites (Figure IV.26 A) exhibited typical features for beta zeolites, with the dominant peak at 3748 cm^{-1} belonging to terminal Si-OH groups and relatively weak band at 3610 cm^{-1} of unperturbed Si-OH-Al groups. The hydroxyls bonded to extra-lattice aluminum, reflecting the structural defects, were observed as very weak peak[7] at 3660 cm^{-1}. As the IR band at 3610 cm^{-1}, reflecting the non-interacting OH groups, did not change its intensity during Co ion exchange, it indicates that these Si-OH-Al groups are not exchanged by divalent Co ions and they represent the groups originated from Al atoms of far distances in the framework. It follows that the Co ions are exchanged at sites originally exhibiting Lewis character and/or at interacting Si-OH-Al groups (seen in the IR spectrum as broad absorbance increase ranging from ca 3700 to 3300 cm^{-1}), representing close Si-OH-Al groups.

The IR spectra at the "transmission window" in the region of skeletal vibrations between 800 and 1000 cm^{-1} are shown in Figure IV.26 B. The samples with low cobalt loading exhibited an intensive band at 918 cm^{-1} with a weak shoulder around 908 cm^{-1}. These bands were ascribed to perturbation of framework T-O-T bond vibrations due to bonding of single Co ions (see Ref.8,9). With the increasing cobalt concentration the shoulder's intensity increased and finally it became dominant. These two bands were ascribed to the T-O-T vibrations affected by bonding of Co(II) ions in the α- (918 cm^{-1}) and β-sites (908 cm^{-1}), respectively, in the *BEA zeolite. The changes in intensity of the individual bands reflect the changes in population of the Co ions at the α- and β- cationic sites.

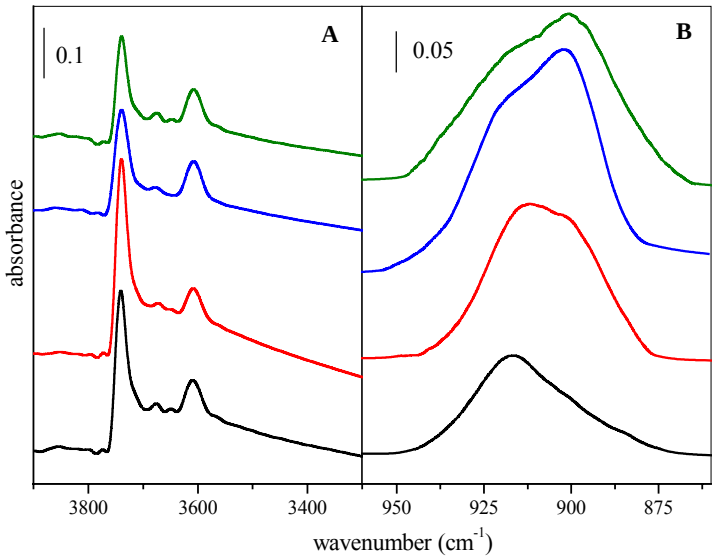

Figure IV.26 FTIR spectra of dehydrated Co-*BEA zeolites. The spectra are normalized to wafers density and the background is subtracted. **(A)** Region of hydroxyl groups, **(B)** perturbed skeletal vibrations (the spectrum of parent H-BEA zeolite was subtracted to obtain perturbation of T-O-T bonds caused by Co ions): —- Co-*BEA-13.1-0.15-0.95, —- Co-*BEA-13.0-0.32-1.95, —- Co-*BEA-13.0-0.87-4.69, —- Co-*BEA-13.1-1.17-7.8

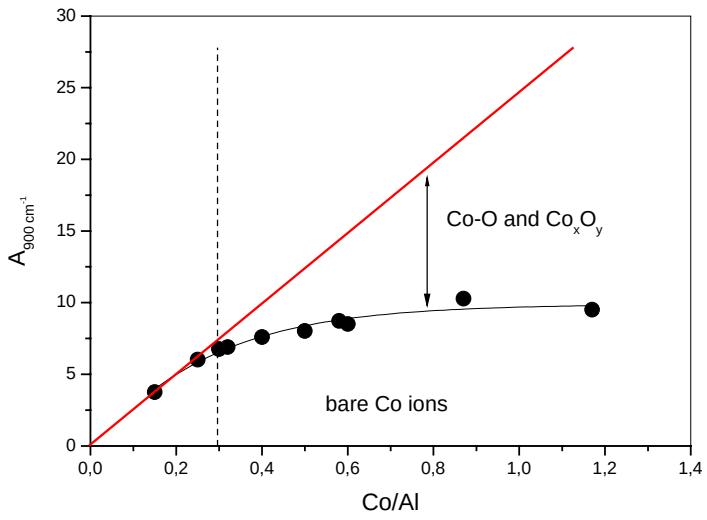

Figure IV.27 The dependence of integrated intensity of T-O-T vibrations on Co/Al. —- Theoretical value of ion exchange in zeolite

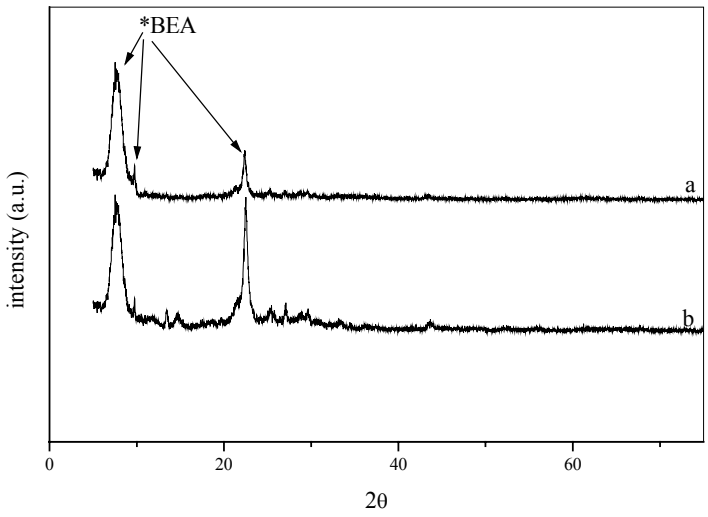

Figure IV.28 XRD pattern of Co-*BEA zeolites: a – Co-*BEA/13.1/1.17/7.8, b – Co-*BEA/13.0/0.30/1.84, 2θ values at 7.69, 9.77 and 22.33 correspond to the structure of *BEA zeolite.

The integrated intensity of the bands of perturbed T-O-T vibrations increased nearly linearly with increasing content of cobalt in cationic positions and at high Co content levelled-off (Figure IV.27). It indicates that besides single Co ions bound exclusively to the framework T-O bonds, some other Co species (Co-oxo or cobalt oxide like species), exhibiting very weak interaction with the framework T-O-T bonds and, therefore, not being reflected in the T-O-T vibrations, are present in the zeolite. Formation of so far unspecified Co oxide-like species can be represented also by well-dispersed cobalt oxide. If such oxide is present, it should be amorphous as no XRD signals corresponding to Co-oxides were found even in the highly loaded Co-zeolite with Co/Al = 1.17 (see Figure IV.28).

IV.4.2 In-situ FTIR spectroscopy over Co-zeolites

To analyse behaviour of surface reaction intermediates and Co ions during the catalytic reactions, the in-situ FTIR experiments were carried out over Co-*BEA and Co-FER zeolites. It must be noted that the reaction conditions were similar to those of the kinetic tests as for the feed composition and temperature is concerned.

Table IV.18 summarizes vibration band positions of the individual groups. Compared to the samples measured at RT the vibration positions are shifted to lower wavenumbers due

to higher temperature (450°C). The IR spectra of the catalyst surface under the conditions of the individual reactions are shown in Figures IV. 29 – IV.35.

Table IV.18 Band positions and their attribution, according to Refs. 9,10,11

wavenumber (cm^{-1})	groups
3587	Si-OH-Al
3733	terminal Si-OH
3333, 3272 and 3189	tertiary, secondary and primary NH
3135, 3035	vinyl
2975 and 2935	CH_x
2187	CN
1622	NH_4^+ or $(M\text{-}O)_2$=NO
1592 and 1350	C=C
1425	$M\text{-}NO_2$
908 and 918	T-O-T due to Co(II)

IV.4.2.1 Reactions at steady-state conditions over Co-*BEA and Co-FER zeolites

The presence of ethane or ethene in the helium stream caused a small decrease in intensity of Si-OH-Al groups (3587 cm-1) over Co-*BEA-12.4-0.25-1.8, given in Figure IV.29. Adsorption of ethane was manifested by the bands at 2975 and 2935 cm^{-1} of CH_x vibrations. Adsorption of ethene was accompanied by formation of the band at 3135 cm^{-1}, ascribed to vinyl groups, and a band with maximum at 1592 cm^{-1}, ascribed to C=C vibrations. Absorption bands of C=C groups exhibited lower intensity with Co-FER-8.6-0.23-1.0 (not shown in the Figure) compared to those for the Co-*BEA sample. It is expected that oligomerization of ethene on the surface took place.

During oxidation of hydrocarbons over Co-*BEA-12.4-0.25-1.8 no new bands appeared in the spectra of adsorbed hydrocarbons recorded at 450°C compared to those observed with only adsorbed hydrocarbons (see Figure IV.30 A). The adsorption of a hydrocarbon was very fast as seen from the time dependence of the intensity, shown in Figure IV.30 B. The region of 1700-1300 cm^{-1} exhibited only low intensity band around 1592 cm^{-1}, corresponding to ethene formed during the reaction. The spectra of the same reaction obtained over Co-FER-8.6-0.23-1.0 are shown in Figure IV.31 A. On contrary to Co-*BEA zeolite, much lower intensity of the bands of C=C vibration in the region 1700-1300 cm^{-1} was

observed. This corresponds to the lower activity of Co-FER compared to Co-BEA zeolite in oxidative dehydrogenation of both ethane and propane (see Tables IV.3 and IV.4).

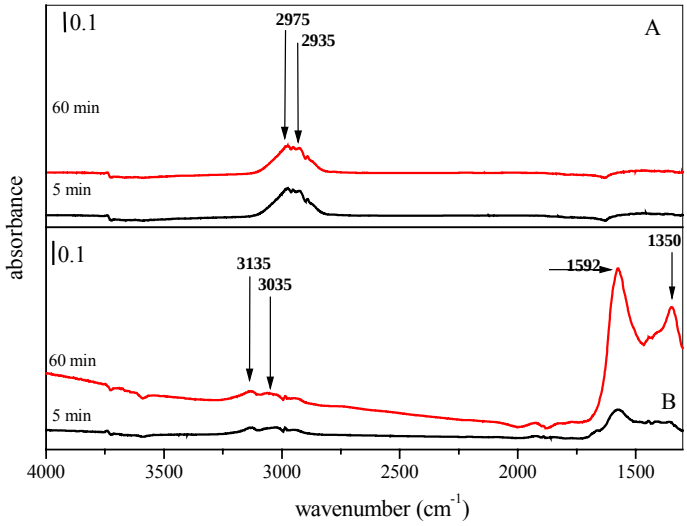

Figure IV.29 FTIR spectra of (A) ethane and (B) ethene over Co-*BEA-12.4-0.25-1.8 at 450°C, 5 % hydrocarbon in a helium stream.

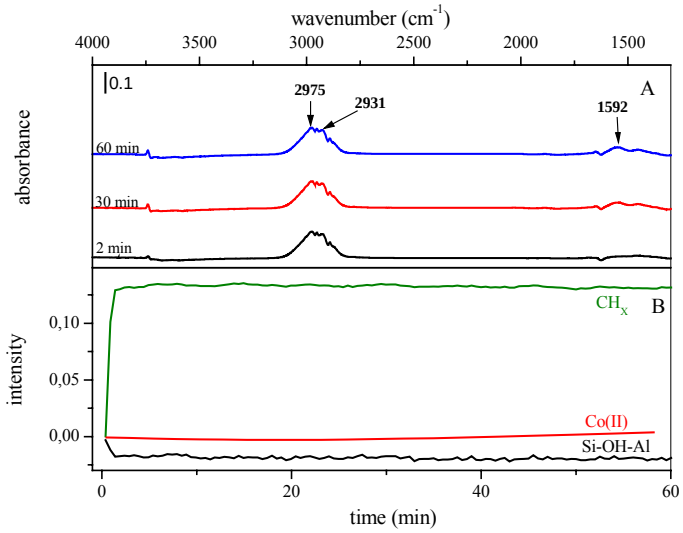

FigureIV.30 (A) Time-resolved FTIR spectra of ethane/oxygen reaction over Co-*BEA-12.4-0.25-1.8 at 450°C, 5 vol. % ethane, 6.5 vol. % oxygen, — 2 min, — 30 min, — 60 min **(B)** dependence of the intensity of vibrations at — 3587 cm^{-1}, — 2975 cm^{-1}, — 908 cm^{-1}.

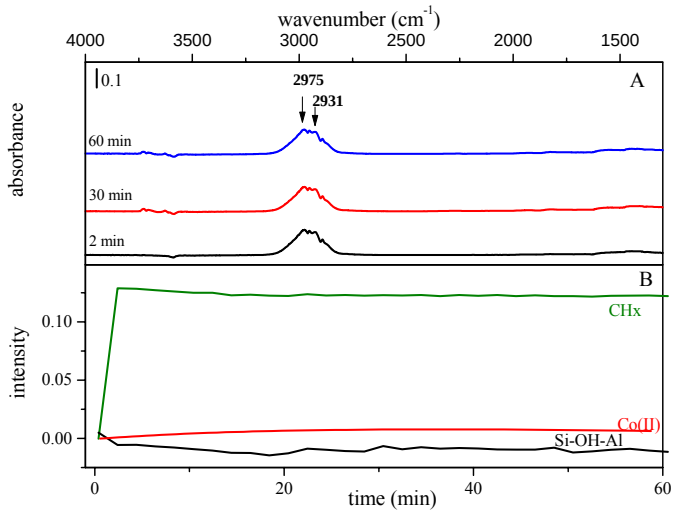

Figure IV.31 (A) Time-resolved FTIR spectra of ethane/oxygen reaction over Co-FER-8.6-0.23-1.0 at 450°C, 5 vol. % ethane, 6.5 vol. % oxygen, — 2 min, — 30 min, — 60 min **(B)** dependence of the intensity of FTIR vibrations at — 3587 cm^{-1}, — 2975 cm^{-1}, — 908 cm^{-1}.

The presence of ammonia in the reactant stream brought about dramatic changes of the sorbed intermediates and at the structural groups of Co-zeolites. The time-resolved FTIR spectra recorded during the reaction of ammonia with oxygen are shown in Figures IV.32 and IV.33. Formation of the absorption bands at 3333, 3272 and 3189 cm^{-1}, which are ascribed to tertiary, secondary and primary NH vibrations, respectively, were found. Relatively broad absorption band at 1425 cm^{-1} belongs to vibration of M-NO_2. The band at 1622 cm^{-1} could be ascribed to NH_4^+ or $(M\text{-}O)_2$=NO species, which both could occur on the surface. Ammonia adsorption is fast and it is strongly adsorbed on both zeolite centres – the exchanged Co ions and hydroxyl groups, as evidenced by an immediately reached intensity at 3272 cm^{-1} (N-H vibration) as well as by a decrease in intensity at 3587 (Si-OH-Al), and at 908 + 918 cm^{-1} (T-O-T vibration due to bonding of bare Co(II)). It follows that the ligation of NH (3272 and 3333 cm^{-1}) and/or NO_x (1425 cm^{-1}) might occur, but as NH is a stronger ligand, it can be suggested that the Co ions coordinate predominantly NH groups.

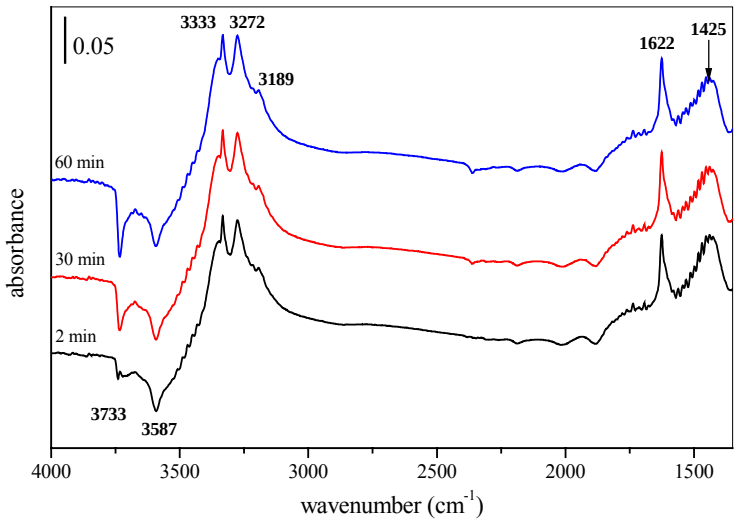

Figure IV.32 Time-resolved FTIR spectra of ammonia/oxygen mixture over Co-*BEA-12.4-0.25-1.8 at 450°C, 10 vol. % ammonia, 6.5 vol. % oxygen, — 2 min, — 30 min, — 60 min

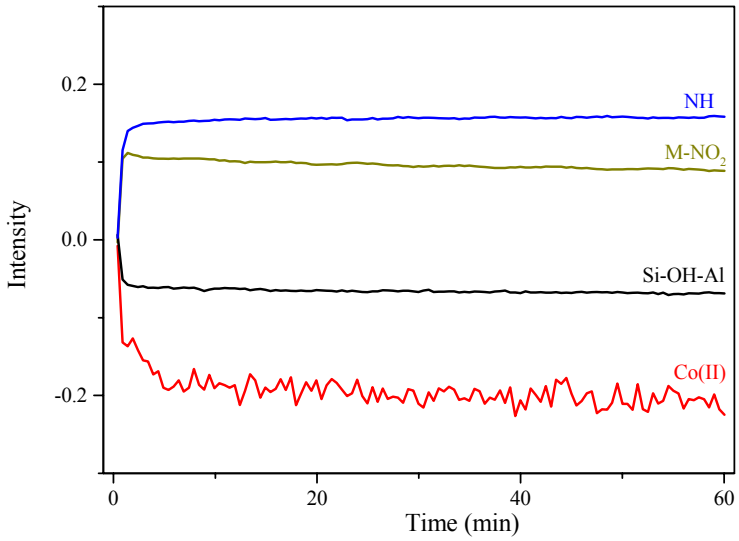

Figure IV.33 The intensity of vibrations of time-resolved FTIR spectra of ammonia/oxygen mixture over Co-*BEA-12.4-0.25-1.8 at 450°C, 10 vol. % ammonia, 6.5 vol. % oxygen, — 3587 cm^{-1}, — 3272 cm^{-1}, — 1425 cm^{-1} , — 908 cm^{-1}

The spectra of adsorbed intermediates during the reaction of ethane/O_2/ammonia over Co-*BEA-12.4-0.25-1.8 at 450°C are shown in Figure IV.34A. With a decrease in intensity of the bands of bridging hydroxyls, the NH (3333 and 3272 cm^{-1}) and CH_x (2975 cm^{-1}) vibration bands were formed. Moreover, three new bands were observed. The weak band at 2189 cm^{-1} was ascribed to adsorbed nitrile group, the band at 1667 cm^{-1} to vibration of an intermediate

formed from ethylamine (see Ref. 9) and the band at 1425 cm^{-1} to M-NO_2. The changes in intensity of the individual bands and formation of new bands indicate that both Si-OH-Al groups and Co ions are involved in the reaction and that the reaction propagates with formation of nitriles and nitrates.

On contrary, the spectra of adsorbed intermediates at similar conditions over Co-FER-8.6-0.23-1.0 exhibited different features (see Figure IV.35). While ammonia presence consumed OH groups, accompanied by formation of the bands at 3272 cm^{-1} (assigned to NH), and ethane adsorption was manifested in the band 2975 cm^{-1} (ascribed to CHx), no bands of nitrile and ethylamine were detected. Moreover, the relative intensity of the band at 1425 cm^{-1} of M-NO_2 exhibited much higher intensity with Co-FER compared to Co-*BEA. These findings on the adsorbed reaction intermediates over Co-*BEA and Co-FER correspond to the high activity of Co-*BEA zeolite and low activity of Co-FER. It implies that Co-FER provides high concentration of adsorbed NO_2 species, indicating oxidation of ammonia rather than its interaction with ethene.

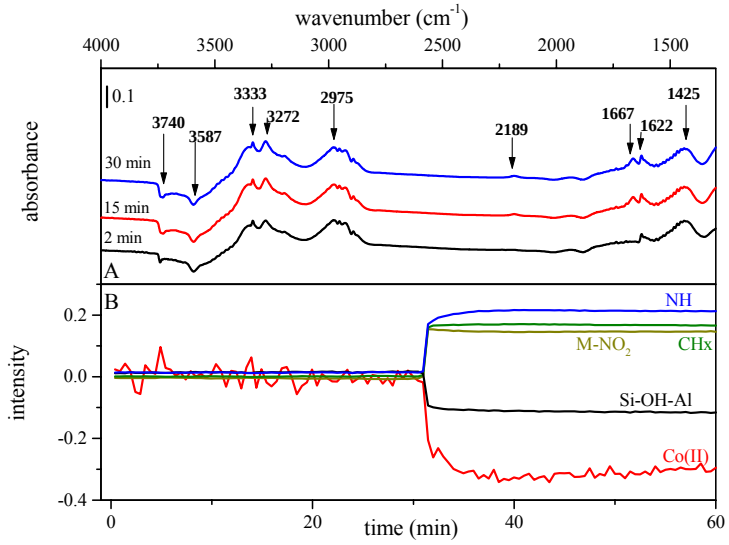

Figure IV. 34 (A) The time-resolved FTIR spectra of ethane/ammonia/oxygen mixture over Co-*BEA-12.4-0.25-1.8 at 450°C, 5 vol. % ethane, 10 vol. % ammonia, 6.5 % oxygen, — 2 min, — 30 min, — 30 min; (B) the intensity of vibrations at — 3587 cm^{-1}, — 3272 cm^{-1}, — 2975 cm^{-1}, — 1425 cm^{-1}, — 908 cm^{-1}.

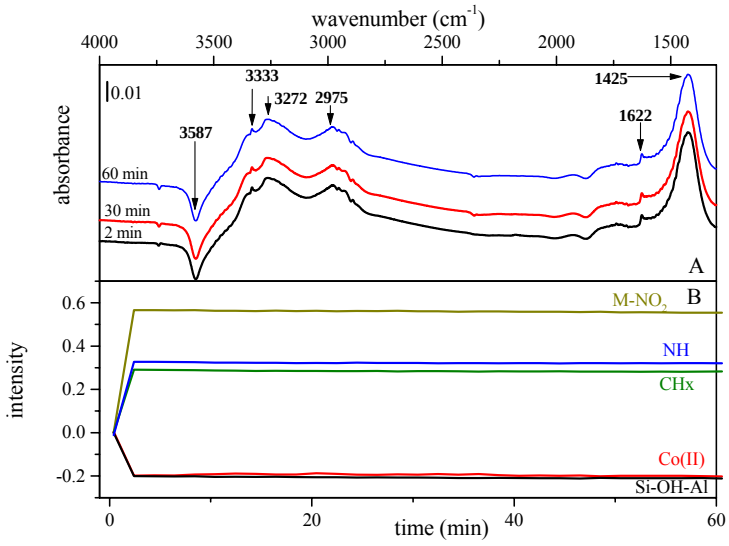

Figure IV.35 (A) The time-resolved FTIR spectra of ethane/ammonia/oxygemixture over Co-FER-8.6-0.23-1.0 at 450°C, 5 vol. % ethane, 10 vol. % ammonia, 6.5 vol. % oxygen, — 2 min, — 30 min, — 60 min **(B)** the intensity of vibrations at — 3587 cm^{-1}, — 3272 cm^{-1}, — 2975 cm^{-1}, — 1425 cm^{-1}, — 908 cm^{-1}

IV.4.2.2 Reactions at transition concentration regime over Co-*BEA zeolite

The IR experiments described above were carried out under the steady-state conditions of the catalytic reaction or during the time when the reaction was approaching the steady-state conditions. The transient measurements with short pulses of one of the reactants to the stream of the other reactants gave further information on the behaviour of the system.

In Figure IV.36, the FTIR spectra of pulses of ethane into ammonia/oxygen mixture are shown. It is clearly seen that ammonia in the ammonia/oxygen stream immediately interacted with both Co ions and strong acid hydroxyl groups (decrease in intensity of the bands at 908 + 918 and 3587 cm^{-1}, respectively) with formation of NH band (3272 cm^{-1}). When ethane was injected into this mixture a band at 2975 cm^{-1} of CH_x appeared. Bridging hydroxyls slightly increased in concentration as adsorbed ammonia and oxygen reacted with ethane, but Co ions were not affected. While concentration of NH-groups was not change, M-NO_2 vibrations increased in intensity. Appearance of ethene was also reflected in the band at 1425 $cm^{-1}$of the C=C bond (not shown). The pulses of ammonia into ethane/oxygen mixture at 450°C compared to pulses of ethane exhibited more dramatic changes in the intensities of the IR bands. Figure IV. 37 shows that ammonia during the pulses is adsorbed on Co(II) as well as protonic sites. Also the increase in intensity of the bands corresponding to M-NO_2 and

NH was observed. These intermediates were consumed very fast by adsorbed ethane, which was fed continuously in the helium stream.

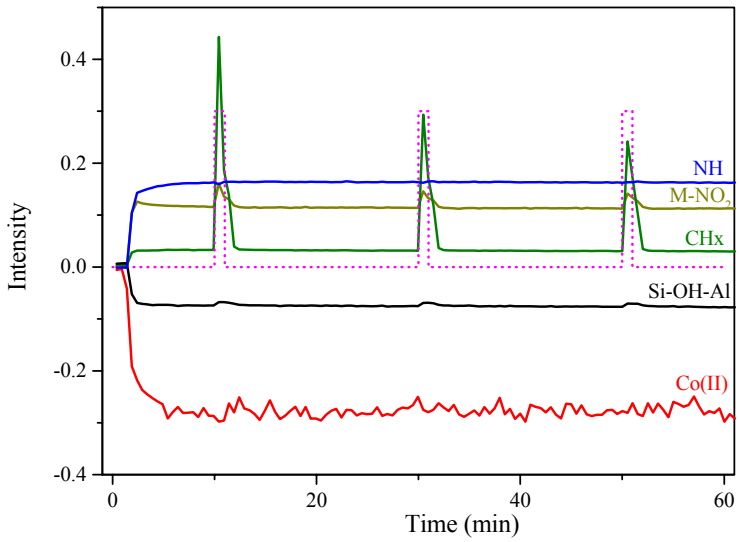

Figure IV.36 The intensity of vibrations of time-resolved FTIR spectra of ammonia/oxygen mixture with pulses of ethane over Co-*BEA-12.4-0.25-1.8 at 450°C, 10 vol. % ammonia, 6.5 vol. % oxygen, 0–5-0 vol. % ethane, — 3587 cm^{-1}, — 3272 cm^{-1}, — 2975 cm^{-1} corresponding to CH$_x$, — 1425 cm^{-1}, — 908 cm^{-1} , ... – concentration profile of ethane.

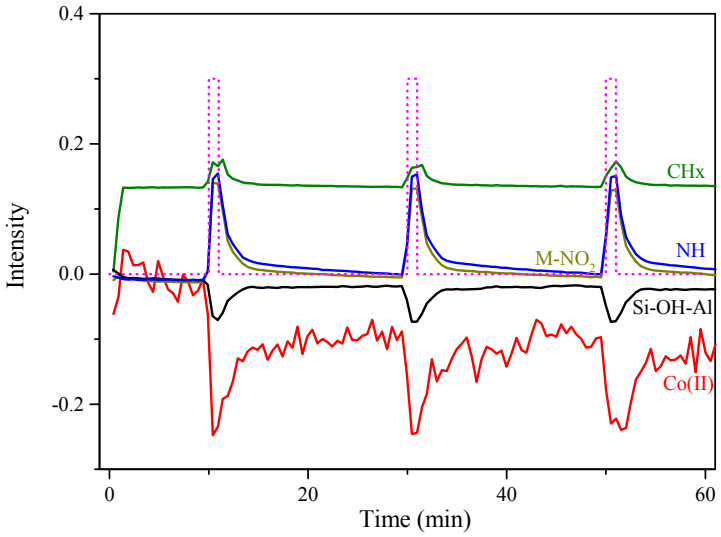

Figure IV.37 The intensity of vibrations of time-resolved FTIR spectra of hydrocarbon/oxygen mixture with pulses of ammonia over Co-*BEA-12.4-0.25-1.8 at 450°C, 0-10-0 vol. % ammonia, 6.5 vol. % oxygen, 5 vol. % ethane, — 3587 cm^{-1}, — 3272 cm^{-1}, — 2975 cm^{-1} corresponding to CH$_x$, — 1425 cm^{-1}, — 908 cm^{-1} , ... concentration profile of ammonia.

It is to be noted that ammonia pulses caused also an increase in intensity of CH_x vibrations, indicating higher level of adsorption of ethane in the presence of ammonia.

These transient experiments clearly indicate strong interaction of ammonia with both the bridging OH groups and Co(II) ions and, therefore,its dramatic effect on the reactivity of Co-zeolites in oxidation reactions.

IV.5 Temperature-programmed reduction of Co-zeolites

The nature of cobalt species and their redox behaviour were investigated by temperature programmed reduction by hydrogen. The reduction pattern (Figure IV.38) of Co-zeolites exhibited major reduction peak at 1000-1100 °C. Only at very high cobalt content Co/Al =1.17, H_2-TPR showed additional reduction peak around 350 °C. This low-temperature peak was compared with H_2-TPR of bulk Co_3O_4 oxide (see Figure IV.38) and attributed to the reduction of cobalt oxide deposited on the zeolite. Simultaneously with hydrogen consumption formation of water was detected at temperature when Co oxide is reduced as well as at the high-temperature reduction peak as reduction of single Co(II) ions. The amount of water evolved is constant to Co/Al 0.3-0.4, corresponding to 1.1 mols of water per mol Co, but increases substantially at higher Co content. It have to be noticed that there is some accordance between amount of evolved water and presence of different cobalt particles. The possible mechanism of reduction of individual cobalt particles in zeolite is shown in Scheme IV.1.

It can be assumed that for zeolites of low cobalt content up to Co/Al = 0.5, where isolated Co ions predominantly occur their reduction leads to formation of surface hydroxyls (see Scheme IV.1), which are dehydroxylated at high temperature of Co ion reduction. An increase in the amount of water evolved with increasing cobalt content (Figure IV. 39) is ascribed to an increase in concentration of cobalt species containing extraframework oxygen, either as some structural Co-O_x species or as supported Co oxides. It is clearly showed that Co(II) ions in the zeolite are very stable. Quantitative analysis of H_2-TPR results showed that cobalt ions in the zeolite exist as a divalent cation, which valency is very stable. Only the zeolite with the highest cobalt content exhibits apparent average valence 2.44 due to presence of substantial of dispersed Co oxides (see Table III.3).

reduction of single Co ions

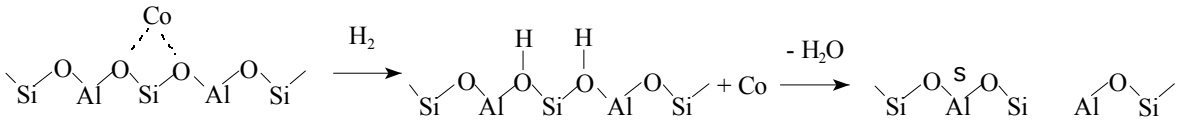

reduction of cobalt µ-oxo species

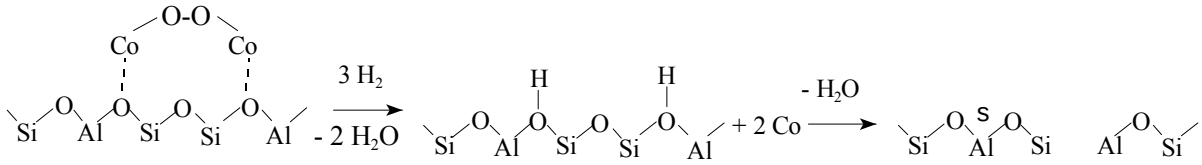

reduction of bulk cobalt oxide

$$Co_3O_4 + 4\ H_2 \longrightarrow 3\ Co + 4\ H_2O$$

Scheme IV.1 Proposed model of reduction and dehydroxylation of Co*-BEA zeolites during H_2-TPR

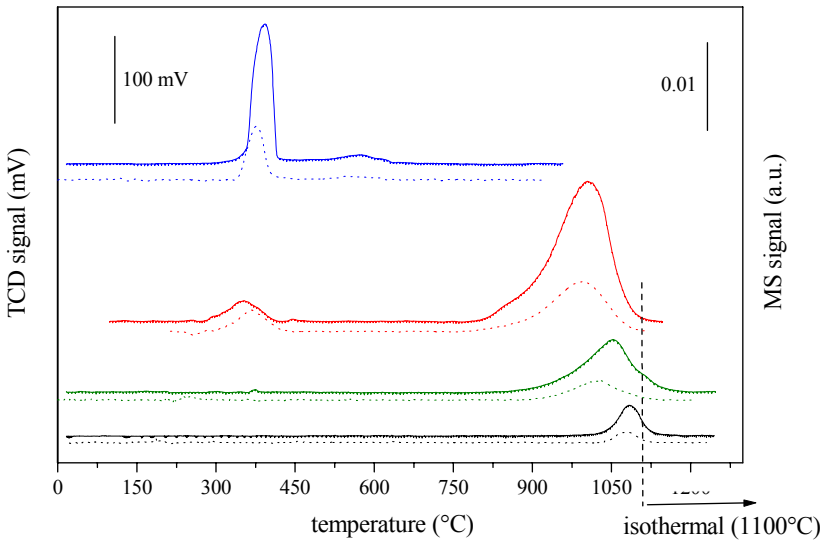

Figure IV.38 H_2-TPR patterns of Co-*BEA zeolites with various cobalt loading: hydrogen consumption (full line), water evolution (doted line): — bulk Co_3O_4 , — Co-BEA-13.0-1.17-7.8, — Co-BEA-11.9-0.6-3.2, — Co-BEA-13.1-0.15-1.0

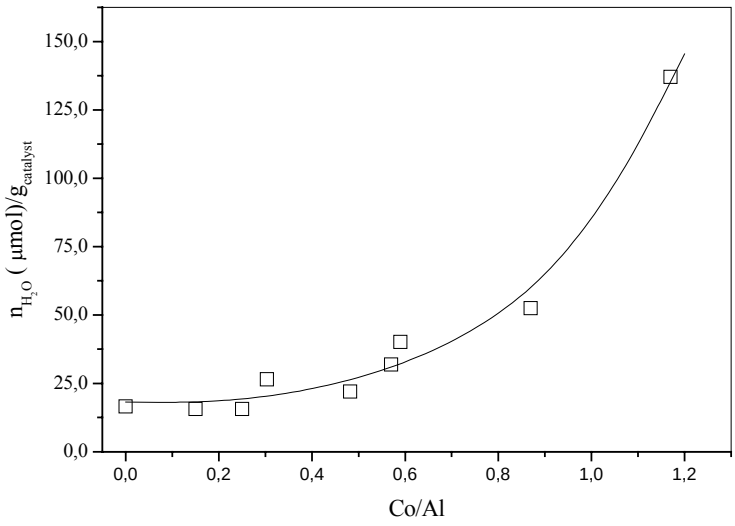

Figure IV. 39 Dependence of the amount of water evolution during the hydrogen temperature-programmed reduction on Co/Al ratio.

IV.6 References

[1] P. Kubánek, B. Wichterlová, Z. Sobalík; J. Catal. **211** (2002) 109.

[2] G.I. Panov, A.S. Kharitov, V.I. Sobolev; Appl: Catal. A: General **98** (1993) 1.

[3] J. Dědeček, B. Wichterlová; J. Phys. Chem. **103** (1999) 1462.

[4] D. Kaucký, J. Dědeček, B. Wichterlová; Micropor. Mesopor. Mater. **31** (1999) 75.

[5] J. Dědeček, D. Kaucký, B. Wichterlová; Micropor. Mesopor. Mater. **35-36** (2000) 483.

[6] J. Dědeček, L. Čapek, D. Kaucký, Z. Sobalík, B. Wichterlová; J. Catal. **211** (2002) 198.

[7] O.Bortnovsky, Z. Sobalík, B. Wichterlová; Micropor. Mesopor. Mat. **46** (2001) 265

[8] B. Wichterlová, Z. Sobalík, Y. Li, J.N. Armor; Stud. Surf. Sci. Catal. **130** (2000) 869.

[9] Z. Sobalík, Z. Tvarůžková, B. Wichterlová; J. Phys. Chem. B **102** (1998) 1077.

[10] K. Hadjiivanov; Catal. Rev. Sci. Eng. **42** (2000) 71.

[11] L. Čapek, K. Novoveská, Z. Sobalík, B. Wichterlová, L. Cider, E. Jobson; Appl. Catal. B: Environmental **60** (2005) 147.

V.1 Oxidation of ethane and propane with molecular oxygen

Among metal cations exchanged into high silica zeolites, highly interesting with respect to redox behaviour and catalytic function, have appeared namely Co, Cu and Fe ions[1,2,3]. We have centred the attention to the behaviour of the metal exchanged zeolites in dependence on the type of cation species and topology of the zeolite framework in the oxidation and ammoxidation of propane and ethane by using both molecular oxygen and nitrous oxide.

V.1.1 Comparison of Cu, Co, Fe zeolites

The oxidation activity of parent H-zeolites has been previously connected in the literature with the acidic Broensted and Lewis sites[4,5]. Later on it has been evidenced that the oxidation activity stems from very low concentration of Fe with SCR-NO_x, NO-NO_2 reactions, and benzene oxidation with N_2O[6,7,8]. We provided here additional evidence that the activity of H-zeolites originates from the trace concentration of iron (see Table III.1 and III.4). Iron is incorporated into zeolites in trace concentration during the synthesis via an aluminium source in the range ca 200 - 500 ppm. Preparation of H-MFI with only 30 ppm and with very low activity (Table IV.8) supports this conclusion.

From a comparison of conversion data for oxidation of propane over Fe- (Table IV.8), Cu- (Table IV.2) and Co- (Table IV.3) zeolites of various structures and compositions it follows that copper is the most active catalyst, but did not yield propene while iron is the least active. The most active and selective have appeared to be Co ions in Co-*BEA and Co-MFI, which yield olefinic products and nitriles (Tables IV.3 and IV.4, IV.11 and IV.12).

The presence of protonic sites inside zeolites besides metal ions leads to oligomerization of propene formed and subsequent cracking to lower hydrocarbons as low yield of ethane, ethene and methane (see Tables IV.2-IV.4) were found.

With respect to redox behaviour of the studied metallo-zeolites copper exhibits di- and mono-valent state depending on oxidizing or reducing atmosphere[9], while cobalt is highly stabilized in a divalent state. Co(II) ions are reduced only after their removal from cationic sites at high temperature (1100°C) by hydrogen (see Figure IV.38). The only species reducible are undefined cobalt-oxo species, which are reduced under the conditions close to those as for cobalt oxides.

V.I.2 Kinetics and mechanism of the reaction

The dependences of conversion of propane and ethane, and selectivity to olefins, CO and CO_2 on temperature and contact time (Figures. IV.3, IV.6 and IV.2) indicate that the oxidation of ethane and propane follows schematically the mechanism given in Scheme V.1. In general oxidation of ethane and propane proceed to corresponding olefins and further oxidation of the more reactive olefin compared to paraffin to CO and CO_2. However, the direct oxidation of paraffins can also occur, depending on the structure of the metal ion species. The conversion of propane increases with increasing W/F ratio, but the selectivity to propene decreases. The decrease of propene selectivity and increase in selectivity to CO and CO_2 show that propene is an intermediate product and the oxidative dehydrogenation of propane has a consecutive step mechanism. It implies that carbon oxides can be formed in the both parallel and consecutive reaction pathways.

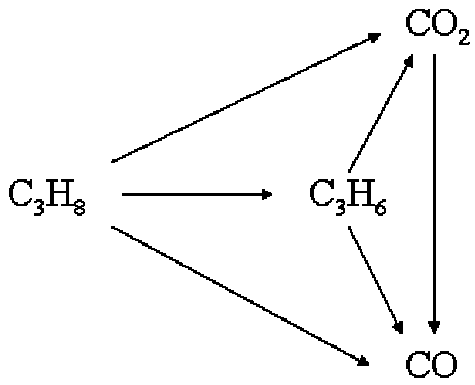

Scheme V.1 Formal reaction scheme of conversion of propane over Co-zeolites in the presence of oxygen

Formation of ethane and ethene in oxidation of propane (Table IV.3) can be connected with the presence of protonic sites, which balance the negative zeolite framework charge together with metal ions. It can be suggested that the acidic sites catalyze oligomerization of formed olefins and cracking of olefins and oligomeric olefinic compounds to lower chain paraffins and olefins, including methane; the extent of these reactions strongly depends on temperature. If the reactivity of ethane and propane in their oxidation is compared, it is seen that ethane reaction provides higher selectivity to and yields of olefin compared to propane (Tables IV.3 and IV.4). This can be accounted for much lower reactivity of ethene in comparison with propene in both their oxidation and oligomerization/cracking. It is supposed that if olefinic oligomers are formed, they are readily, due to their high reactivity, oxidized to

carbon oxides or cracked. This is the reason that no C_4 and olefins have been found among the products

In-situ FTIR spectra monitoring of the oxidative dehydrogenation of ethane revealed adsorption of ethane and ethene predominantly on acidic OH groups (Figure IV.29). Although some ethene (but not ethane) was adsorbed on Co ions (1592 cm^{-1}), as found by in-situ UV-Vis spectra (Figure IV.23), the bonding of Co ions to the framework T-O bonds was not affected, and thus ethene behaved like weak ligand. While ethane was at the beginning of the reaction immediately adsorbed, the bands of ethene were slowly with TOS developed, being accompanied by a consumption of acidic OH groups.

V.1.3 Effect of Co concentration, Co structure and Co siting

It has already been reported that Co ions in zeolites could form bear cations, cations with bound hydroxyls or oxo- or peroxo-like species and oxide-like particles [10,11,12].

According to Figure IV.22 with increasing cobalt concentration in Co-*BEA zeolites Co(II) ions are exchanged at the α and β cationic sites as bare cations, exhibiting characteristic d-d transitions in the Vis range 14 000 – 22 000 cm^{-1}. The Co-α sites are characterized by a band at 14 600 cm^{-1}, the Co-β sites are reflected in a quartet with the bands at 15 500, 16 300, 17 570 and 21 700 cm^{-1}. As also shown by Bortnovsky *et al.*[13], Co ions in *BEA zeolites are predominantly exchanged for perturbed OH groups bound to two close framework Al atoms placed in one ring, while only a small fraction of unperturbed bridging OH groups is replaced. Similar feature we have found in the Co-*BEA studied here (see Figure IV.26). Introduction of the Co ions into cationic sites is also reflected in the perturbation of framework T-O bonds giving rise to bands in the skeletal window around 900 cm^{-1}. The bands at 918 and 908 cm^{-1} were ascribed to perturbation of framework T-O-T bond vibrations, due to bonding of single Co ions[9,12,14] at the α- and β-sites (Figures IV.26 and IV.27). Intensity of changes of the individual bands reflects changes in the population of Co ions in these cationic sites. With the increasing cobalt concentration the intensity at 908 cm^{-1} became dominant, indicating prevailing population of β- sites. The integrated intensity of T-O-T vibrations increased nearly proportionally with increasing content of cobalt in the zeolite, but at high Co content levelled-off to a constant value. This indicates that at low Co loadings (Co/Al < 0.4) single bare cations are incorporated, while at higher Co concentrations some Co

other species (Figure IV.27), which exhibit very weak interaction with framework oxygens, are present in the zeolite.

Such Co species weakly interacting with the framework might be present in the form of cobalt-oxo or cobalt peroxo entities (Co-O_2-Co). The presence of such species was detected by Dědeček *et al.*[15] in some Co-*BEA zeolites by absorption band at 31 500 cm^{-1} indicating a charge transfer type of electronic transitions. Wu *et al.*[16] found out in Raman spectra of Co-APO-11 the bands ascribed to Co-O bond and O-O bonds, which were attributed to superoxo-cobalt species. Ohtsuka *et al.*[17] detected in Raman spectra of dehydrated Co-*BEA zeolites with Co/Al around 0.5 a band at 600 cm^{-1}, which they ascribed to peroxo-cobalt species. However, in all these cases the concentration of the peroxo-cobalt species was estimated to be very low, less than 10 % of cobalt content. At higher cobalt concentration, at Co/Al > 0.5 agglomeration of Co ions to cobalt oxides is expected, as also follows from the H_2-TPR results. Increasing of water amount simultaneously evolved during reduction (H_2-TPR) of Co ions with increasing cobalt content is ascribed to an increase in the amount of cobalt species containing extra-framework oxygen (i.e. oxo-like species or various cobalt oxides), cf. Figures IV.38 and IV.39.

Different cobalt species exhibited different catalytic activity. Bare cobalt ions prevailing in *BEA zeolite with Co/Al up to 0.3 exhibited the activity predominantly connected with formation of ethene. On the other hand, at higher Co loading (Co/Al > 0.4), when cobalt-oxo, cobalt peroxo and cobalt oxides can be expected to be also present oxidation of ethane toward carbon oxides prevails (see Figures IV.5, IV.6c and IV.7). Therefore, it can be suggested that a dramatic increase in the activity of Co-*BEA expressed in TOF per Co ion with increasing cobalt loading in the range Co/Al 0.3-0.5 can be caused by some extra-framework oxygen bound to Co species. Higher cobalt content (Co/Al > 0.5) increases amount of cobalt oxides resulting in both a decrease in the yield of ethene and the overall activity per Co atom in Co-*BEA catalysts. Therefore, it can be suggested that the single Co ions are active predominantly in selective oxidative dehydrogenation and the oxide-like species contribute to ethane (and ethene) oxidation to carbon oxides. These findings are in agreement with the results of Ohtsuka *et al.*[17], who observed a dramatic decrease in the activity of Co-*BEA in SCR-NO_x by propane in the presence of cobalt oxides in beta zeolite, where these oxides are active in combustion of propane and compete with propane oxidation by NO_x yielding N_2.

The presence of bridging oxygen in dinuclear metal complexes in zeolites has been discussed in various metallo-zeolites with respect to their activity. Cu-O-Cu dimers in the

over-exchanged Cu-MFI zeolites were suggested as the active sites in direct decomposition of NO[18]. Panov *et al.*[7] suggested the Fe-O-Fe bridged oxo-complexes as active sites in decomposition of N_2O and hydroxylation of benzene to phenol with N_2O. But so far there is not a straightforward correlation of the occurrence of these di-nuclear complexes and activity of zeolites in redox reactions.

V.1.4 Effect of the framework topology

The turn over frequency (TOF) values per Co ion (calculated from the total conversions of ethane or propane in the individual reactions) depending on the zeolite structural type are summarized in Tables IV.3 and IV.4. Dramatic differences in the activity were observed between the zeolite structural types. The sequence in activity of Co-zeolites *BEA > MFI >> MOR > FER can be accounted for the location of Co ions in different channel systems of zeolites of different topologies. Recently coordinations-positions of Co ions in pentasil ring zeolites of MFI, *BEA, MOR and FER topologies were suggested in ref. 19 and denoted as α, β and γ sites. The structures for the α-, β- and γ-sites were similar for the MFI, *BEA, MOR and FER zeolite structures[19]. The Co ion siting was estimated by employing Vis spectra of Co(II) ions in these zeolites. The Co-α cations are located in the straight well-accessible channels of MOR, FER, MFI and *BEA structures. The Co-α ions represent ca 10-25 % of all the Co ions in completely Co-exchanged zeolites. The Co ions of the γ-type are very low populated (ca 10 % of the Co ions), and thus their contribution to the zeolite activity can be expected to be low. In all structures of zeolites, the most populated site by the Co ions is the β-type cationic site (60-90 % of the Co loading[19]). In a wide pore of *BEA zeolite the Co-β ions are located in very open wide channels, and in MFI they are at the exposed site at the intersection of the straight and sinusoidal channels. On contrary, the Co-β sites in mordenite and ferrierite structures are located in the narrow inter-connected channels and in the 8-member ring channels, respectively. Thus, the Co-β type ions in MOR and FER topologies might not be easily accessible for reactants.

Thus strong shape selective effect also in redox reactions is revealed for oxidation of ethane and propane. The conversion values for both ethane and propane in oxidative dehydrogenation and oxidation to carbon oxides evidenced that Co-mordenite and Co-ferrierite are much less active compared to Co-*BEA and Co-MFI (Table IV.3 and IV.4).

However, this effect could hardly be explained by inaccessibility of the most populated Co-β ions to the individual reactants. Oxygen and ethane are molecules of smaller diameter (molecules < 3Å) compared to the channel diameter in FER (4.2 x 5.4 Å), and MOR (6.5 x 7.0 Å), where the most populated Co-β sites are located. Moreover, interaction of Co ions in FER with, e.g., ethane is evidenced by the CH_x vibration at 2962 cm^{-1} (Figure IV.31). Thus, it can be suggested that some steric hindrances occur with respect to formation of reaction intermediates during oxidative dehydrogenation of paraffins. Formation of surface intermediates during the in-situ measurements of FTIR spectra at ethane oxidation on Co-FER and Co-*BEA (Figures IV.30 and IV.31) show that olefinic intermediates (1592 cm^{-1}) are formed only with Co-*BEA zeolite.

V.2 Oxidation of propane with nitrous oxide and a mixture of nitrous oxide and oxygen

As it will be shown below the presence of Fe in zeolites (and Co zeolites), even in trace concentrations, is highly important for oxidation of paraffins with N_2O and N_2O/O_2 mixtures. Therefore, the attention has been paid to contribution of such low concentrations of Fe to oxidation of paraffins by N_2O.

V.2.1 Propane oxidation with N_2O over Fe zeolites

The intention of the study has been the analysis of the effect of presence of Fe at low concentrations on oxidation of paraffins with N_2O. This represents one of the first studies describing exceptional activity of Fe zeolites in propane oxidation, and providing a new route for obtaining propene from propane. The activity of Fe zeolites of various concentrations and variously prepared was investigated to obtain a qualitative picture on the paraffin oxidation with N_2O. The prepared Fe zeolites contained presumably Fe in cationic sites as well as in oligomeric Fe-O-Fe species and like Fe oxide. We had in mind that the structure of Fe sites in zeolites should play a decisive role in their activity. Nevertheless such analysis is not a subject of this study, but further investigations with this respect are carried out in our laboratory.

Replacement of oxygen with nitrous oxide in propane oxidation over FeH-MFI zeolites led to a dramatic increase in propane conversion, selectivity to propene and in

formation of various hydrocarbons and oxygenates (Table IV.8). A higher propane conversion with N_2O in comparison with molecular oxygen was accompanied by a substantial increase in the selectivity to propene (e.g. 44.0 vs. 55.9 % for FeH-MFI-1200-HT) and to the sum of aromatics and oxygenates (e.g. 0 vs. 29.0 %) for all Fe zeolites. Among the products appeared methanol, ethanol, *iso*-propanol, propanal, phenol and acetone. Also the products of propane cracking, i.e. methane, ethane and ethene were found. It implies that using of N_2O compared to molecular oxygen resulted in considerable propane cracking, propene dimerization/aromatization and formation of their oxygenates. As the activity and selectivity increased with increasing Fe content in the zeolite it evidences that the active sites are related to Fe species, but of very low concentrations. The effect of zeolite steaming on the propane oxidation as well as the changes in the structure of Fe and Al-related sites are not analysed here, but it is clear that they have a substantial effect on the zeolite activity. The high activity and selectivity was found particularly with the zeolite (1200 ppm Fe) steamed at 600 °C, (yield of propene 24 %) and that catalyst where protonic sites were mostly eliminated by Na^+ exchange. This indicates that the activity of Fe species is in some manner connected with the aluminium, which under steaming changes its location and related acidic properties.

With the reference to dehydrogenation of light alkanes to alkenes by O^- stabilized at the surface of MgO, prepared by the reaction of N_2O with electrons trapped on the surface, Aika and Lunsford[20,21] suggested that the net reaction involves hydrogen abstraction from alkane with formation of surface OH^- group and alkyl radical (like for gas phase reactions). The radical is then transformed to alkoxides via reaction with O^{2-}. However, the mechanism of formation of propene over Fe zeolites is most likely different[22,23]. It is clear that N_2O decomposes to the elemental nitrogen and highly reactive oxygen atom as shown Scheme V.2.

$$N_2O \rightarrow N_2 + \tfrac{1}{2}\, O_2$$

$$C_3H_8 + O \rightarrow C_3H_7OH \rightarrow C_3H_6 + H_2O$$

$$C_3H_6 + O \rightarrow CH_3CH_2CHO$$

Scheme V.2 Formal reaction scheme of propane reaction over Fe-zeolites in the presence of N_2O

The product composition indicates that the main initial product is propyl alcohol. Besides it a spectrum of C_1-C_6 alcohols is formed (sum of their selectivity is 15-25 %) by oxidation of the products of propane cracking and oligomerization to C_1-C_6 hydrocarbons.

This finding indicates that propene is likely formed via oxidation (insertion of an oxygen atom) of propane to propanol, through the atomic oxygen formed by N_2O decomposition. The so-called atomic α-oxygen was described by Panov group in a series of studies on N_2O decomposition and benzene oxidation to phenol with N_2O[7]. It has been suggested that α-oxygen is entrapped into dinuclear Fe species present in zeolites after N_2O decomposition and it is further transferred into benzene molecule. In the case of propane oxidation studied here, such α-oxygen species could also play such role. Thus propene, and olefins generally, can be formed by insertion of the α-oxygen into the paraffin molecule with subsequent dehydration of alcohol leading to propene and other olefins.

The results of propane oxidation in oxygen, nitrous oxide and in their mixture over FeH-MFI with various Fe content, regardless of the state of iron, evidence that the active sites are exclusively Fe centers, and that the protonic sites are not responsible for the zeolite redox activity, although they can participate in acid-like transformations within the reactant-product mixture. The results represent further support for the conclusion that the redox activity of H-zeolites is only apparent, caused in fact by the highly active Fe sites always present in trace concentrations in zeolites, as already reported for the reactions of NO-NO_2 equilibration[6], and benzene oxidation with N_2O[7,22]. Hundreds of ppm of Fe is usually present in the commercial or laboratory synthesized samples prepared by standard synthesis procedure.

However, with all the Fe-catalysts studied, their performance depended on the reaction time-on-stream, Figures IV.12 and IV.13. The most stable conversion was found with FeNa-MFI-1200-HT catalyst containing very low concentration of protonic acid sites. With decreasing propane conversion with TOS, the selectivity to propene increased as well as the yield of propene, which reached stable value of ca 24 % within 200 min of TOS. On the other hand, the selectivity to the sum of oxygenates as well as to the sum of products of propane cracking (7.1 %) remained nearly constant with TOS. The selectivity to products of propane oligomerization substantially decreased, aromatics nearly disappeared, and accordingly decreased the selectivity to phenol with TOS. It is supposed that the deactivation of catalyst is caused by formation of carbonaceous deposits blocking the active sites. Formation of coke can be mostly connected with the presence of strong acidic protons in the zeolite surface as well as by the presence of Fe and Al electron acceptor sites. Blocking of these acid sites is accompanied by the observed lower selectivity to aromatics and phenol, and thus the higher selectivity to propene and propanols. Such changes in the product composition with TOS indicate that if the acid sites are removed by replacement with Na^+ ions and by coke formation, then the Fe catalysts can provide stable performance (Figure IV. 12). Employing of

streams containing both N_2O and O_2 suppresses substantially deactivation of the catalyst, likely by oxidation of coke precursors, as also follows from the product composition at such mixtures (Figure IV.13)

V.2.2 Synergy effect of N_2O and O_2 over Co- and Fe-zeolites

Nitrous oxide is decomposed over Co-zeolites to molecular nitrogen and surface oxygen atoms, which are released from the surface as molecular oxygen (Figure IV.8). This process is not affected by the presence of molecular oxygen in the gas phase. This implies that there is no competitive adsorption on the identical active sites of molecular oxygen and atomic oxygen formed by N_2O decomposition. On the other hand, the presence of propane with N_2O significantly decreased N_2O conversion. Therefore, it can be suggested that propane molecules interact with the same sites, where oxygen atoms from N_2O are bound. An increase in N_2O conversion if oxygen is added to this fed mixture of N_2O and propane, suggests that the mentioned sites for N_2O decomposition also take part in selective reduction of N_2O by propane (see Figure IV. 8).

The increase in conversion of propane in its oxidation with molecular oxygen over Co-*BEA zeolites after N_2O addition indicates that atomic oxygen formed by N_2O decomposition takes part in paraffin oxidation (Figure IV.10). The conversion increase is also accompanied by an increase in the yield of propene and CO_2. After addition of 14 vol. % of N_2O to the reaction mixture of propane and oxygen at 450°C, there was observed a threefold higher propane conversion and increase in the yield of propene from 2 to 6 %. Such increase in selectivity to propene at comparable propane conversions was also observed after addition of N_2O into oxygen over VO_x/Al_2O_3 catalyst[24].

The increase in propane conversion did not, however, correspond to the sum of conversions of propane by molecular oxygen and nitrous oxide. Therefore, some synergetic effect of oxygen and N_2O operates. However, the nature of this effect is still not understood. Such synergy effect of O_2 and N_2O was not observed with Fe-zeolites. Using a mixture of O_2 and N_2O result in high propane conversion, but the yield of propene and alcohols was slightly lower.

V.2.3 Contribution of Co and Fe species to the zeolite oxidation activity

A comparison of oxidation of propane with molecular oxygen and nitrous oxide over Co-*BEA shows a substantially higher yields in propene with N_2O. These results opened the question on the contribution of Co and Fe to propane oxidation over Co-*BEA zeolites. Figure IV.8 clearly shows that Co zeolites decompose N_2O. Also Armor and Li[25,26] reported that zeolites with transition metals (e.g. Co, Ni) exhibit activity in decomposition of nitrous oxide[27] with formation of molecular oxygen and nitrogen in the gas phase. This finding is not in contradiction with Panov *et al.*[7] who reported that nitrous oxide decomposition takes place over transition metal ions in zeolites, but only iron in zeolites is able to decompose nitrous oxide and simultaneously to stabilize active oxygen atoms on the surface Fe sites[28]. It is well documented in this study (see Table IV.8) that zeolites containing only iron exhibit similar behaviour in oxidation of propane with oxygen, nitrous oxide and their mixture like Co zeolites. This supports the conclusion that only Fe sites are active in propane oxidation with N_2O by their ability to stabilize atomic oxygen.

Although the chemical analysis of the Co zeolites with respect to Fe was not done, all parent zeolites exhibited trace concentration of Fe. The presence of iron in Co zeolites was confirmed by the ESR signals at g = 4.3 and the broad signal at 2.3 (not included into the results) indicating presence of tetrahedrally coordinated Fe(III) ions and some iron oxide species.

If it is accepted that Fe plays a decisive role in the oxidation of propane with N_2O to alcohols transformed to olefins, then Co species can be connected predominantly with the oxidative dehydrogenation of propane to propene and with complete oxidation of propene, and alcohols and other oxygenates are formed by oxidation of propane with N_2O.

V.3 Ammoxidation of ethane and propane with molecular oxygen and nitrous oxide

The results indicate that completely different behaviour in oxidation of ethane and propane exhibited Co ion species if ammonia was present, i.e. at the ammoxidation reaction compared to oxidative dehydrogenation. Thus strong interaction of ammonia with Co species and acid protonic sites and its direct participation in paraffin activation can be expected. The

discussion of the results in this part concerns a comparison of the ammoxidation activity of Co ions at various concentrations and in zeolites of various topologies, composition of the surface reaction intermediates and final products in the gas phase at reaction conditions, including presence of NO_x and N_2O, as the products of ammonia oxidation. All these parameters are viewed in comparison between paraffin oxidation and ammoxidation.

V.3.1 Effect of Co concentration and zeolite topology

Catalytic activity expressed in TOF values with respect to ethane oxidation and ammoxidation in dependence on Co/Al molar ratio exhibited quite different features (see Figure V.1). The TOF values for ethane conversion in the ammoxidation exhibited very high value (TOF ca 35 h^{-1}) at low loading of cobalt, which remained constant up to ca Co/Al 0.4, compared to that at oxidation reaction, where TOF were rather low. This is approx. Co concentration up to which cobalt is loaded predominantly as single cations in cationic sites, and only small part of Co species is represented by Co-oxo species. For the oxidation of ethane some Co-oxide like species were necessary, but this at the same time increased dramatically selectivity to carbon oxides. Thus during the oxidation high selectivity to ethene could not be achieved (see Figure IV.5) in contrast to the ammoxidation reaction. This is manifested by the high TOF values with respect to the sum of ethane and acetonitrile TOFs. These both high TOF values at low Co loading and their both steadily decrease with increasing Co concentration suggests that the active sites are single Co ions bearing ammonia as ligands. The decrease in activity with the increasing concentration of Co shows that Co oxide like species besides single Co ions are also formed in a significant and increasing amount. Such behaviour of the reaction system also shows that adsorption of ammonia on strongly acidic OH groups (see the Discussion below) have not a decisive effect on the activity and selectivity of the ammoxidation reaction.

Similarly like with paraffin oxidation, the ammoxidation reaction also strongly depended on the zeolite topology. Most active were Co species planted in zeolites of *BEA and MFI structures, and those in MOR and FER where nearly inactive. While the activity of Co-*BEA and Co-MFI zeolites was increased at low Co loadings, when olefins were formed, with ammonia addition, the activity of Co-MOR and Co-FER was further decreased at ammonia presence (see Tables IV.3, IV4 and Figures IV.3, IV.4 and IV.14, IV.15). Therefore, there is evident some steric shape selective effect hindering likely formation of reaction

intermediates during both oxidation of paraffins to olefins and much more at ammoxidation of paraffins.

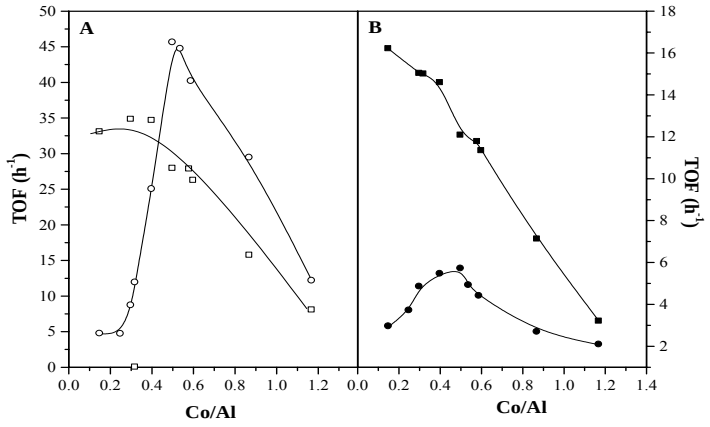

Figure V.1 Dependence of TOF (turn-over-frequency) values on Co/Al molar ratio in Co-*BEA catalysts at 450°C and F = 100 ml/min, 5 vol. % ethane, 6.5 vol. % oxygen, TOF related to (A) O - ethane conversion in oxidation, □ - ethane conversion in ammoxidation, (B) ● - ethene yield, ■ - sum of ethene and acetonitrile yield,

Thus it is concluded that the single Co ions exhibit the highest activity in ammoxidation reaction. At the same time it is important to stress that ammonia presence suppressed the activity of Co oxide like species with respect to complete oxidation of ethane. This is an important fact, which results in high selectivity of the ammoxidation reaction of paraffins to nitriles and olefins.

V.3.2 Mechanism of paraffin ammoxidation

Results of UV-Vis spectra showed strong ammonia adsorption of Co ions even at such high temperature as 450°C. Understandably the intensity of the cobalt ammonia complex is higher at lower temperature (Figure IV.24). If only ethane ad ammonia was fed at in-situ UV-Vis monitoring, when ethylamine cannot be formed, the same spectrum was obtained as during the ammoxidation reaction. This indicates that the spectrum reflects strong adsorption of ammonia on Co ions at the conditions of the ammoxidation reaction. Also in-situ IR spectra recorded at the ammoxidation of ethane over Co-*BEA showed strong adsorption of ammonia. Detailed IR study of ammonia adsorption on Co-*BEA zeolite indicated existence of stable Co-NH_3 1:1 complex[6] at high temperatures. It can be supposed that the presence of

ammonia will dramatically affect the behaviour of Co species present in zeolites during reaction.

Therefore, we suggest that during the reaction Co-NH_3 complex predominates on the surface. The most intensive band at 15 200 cm^{-1} could be ascribed to Co-NH_3 1:1 complex at Co-α sites; the second (at 17 000 cm^{-1}) could be attributed to the same complex at Co-β sites. However, we did not found the differences between the shape of the spectra for Co-FER (not shown in the Results) and Co-*BEA after adsorption of ammonia (Figure IV.24) and at in-situ reaction conditions, although Co-FER was much less active than Co-BEA. The intensities of the spectra were similar, but Co-FER contained higher concentration of Co ions. This might show lower adsorption capacity of Co ions in FER. Nevertheless, these results did not provide us with the answer for the difference between highly active Co-*BEA and low active Co-FER.

During oxidation of hydrocarbons over Co-*BEA-12.4-0.25-1.8 (Figure IV.30A) no new bands appeared in the spectra of adsorbed hydrocarbons recorded at 450°C compared to those observed with only adsorbed hydrocarbons (Figure IV.29). Addition of oxygen with Co-*BEA resulted in a formation of ethene adsorbed on cobalt species, while with Co-FER no C=C bonds appeared (Figure IV.31). On contrary to Co-*BEA zeolite, much lower intensity of the bands of C=C vibration in the region 1700-1300 cm^{-1} were observed over Co-FER.

The presence of ammonia in the stream brought about dramatic changes in the sorbed intermediates and at the structural groups of the Co-zeolites. The ammonia adsorption resulted in formation of absorption bands at 3333, 3272 and 3189 cm^{-1}, which are ascribed to tertiary, secondary and primary NH vibrations, respectively, of amines. Relatively broad absorption band at 1425 cm^{-1} belongs to vibration of M-NO_2. The band at 1622 cm^{-1} could be ascribed to NH_4^+ or $(M\text{-}O)_2$=NO species, which both could occur on the surface. It follows that ammonia adsorption is fast and it is strongly adsorbed on both zeolite centres – the exchanged Co ions and hydroxyl groups, as evidenced by an immediately reached intensity at 3272 cm^{-1} (N-H vibration) as well as by a decrease in intensity at 3587 (Si-OH-Al), and at 908 + 918 cm^{-1} (T-O-T vibration due to bonding bear Co (II)) (Figure IV. 34). It follows that the ligation of NH (3272 cm^{-1}) and/or NO (1425 cm^{-1}) might occur, but as NH is a stronger ligand, it can be suggested that Co ions coordinate predominantly NH groups.

On contrary, the spectra of adsorbed intermediates at similar conditions over Co-FER-8.6-0.23-1.0 exhibited different features (see Figure IV.35). While ammonia presence consumed OH groups, accompanied by formation of the bands at 3272 cm^{-1} (assigned to NH), and ethane adsorption was manifested in the band 2975 cm^{-1} (ascribed to CH_x), no bands of

nitrile and ethylamine were detected. Moreover, the relative intensity of the band at 1425 cm^{-1} of M-NO_2 exhibited much higher intensity with Co-FER compared to Co-*BEA. These findings concerning the adsorbed reaction intermediates correspond to the high activity of Co-*BEA zeolite and low activity of Co-FER. It is to be pointed out that Co-FER provides high concentration of adsorbed NO_2 species, indicating rather oxidation of ammonia than its interaction with ethene.

Thus it implies that the first step of the ammoxidation reaction is formation of olefins, supported by oxidation of ammonia to NO_x. Olefins further interact with ammonia, and amines are in a further step oxidized to nitriles (see Scheme V.3). The positive effect of ammonia on the ammoxidation reaction can be explained by the strong adsorption of ammonia at the reaction conditions on Co ions, as monitored by UV-Vis spectra of d-d transitions and IR spectra of N-H vibrations and changes in intensity of T-O vibrations induced by Co ion bonding to the framework (see in-situ FTIR spectra on Figure IV.32).

There was described the reaction mechanism of ammoxidation of propane over Sb-Ga-O oxide systems, which includes activation of a hydrocarbon via carbenium ion formed by its adsorption on basic centre. The activation of hydrocarbon on acidic catalyst is supposed to proceed on basic sites formed by adsorption of ammonia on acidic centres where $NH_2^{\delta-}$ or $NH^{\delta-}$ are formed which operate as basic centres[29]. The increase of conversion of hydrocarbons was observed with rising concentration of ammonia in the stream. Behaviour of Co-zeolites at the ammoxidation reaction might correspond to analogous mechanism.

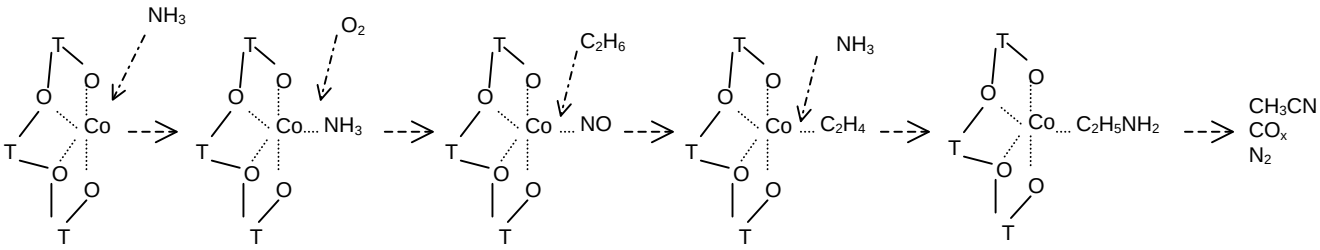

Scheme V.3 Suggested mechanism of ethane ammoxidation

From the intermediates observed by FTIR we suggest the following mechanism of ethane ammoxidation. We speculate that the substantial positive effect of ammonia is a result of an electron density transfer from ammonia to Co ions followed by ammonia oxidation to

NO_x involved then in paraffin oxidation to olefin, representing initial steps for acetonitrile formation (see Scheme V.3). This mechanism can explain enhanced oxidation activity of Co-zeolites in the ammoxidation reaction in comparison to the paraffin oxidation.

Also the in-situ FTIR experiments with the pulses of ammonia into paraffin/oxygen mixtures at reaction conditions show immediate response of both Co ions and strong acid hydroxyl to formation of NH band (3272 cm^{-1}). When, on the other hand, ethane was injected into the ammonia/oxygen mixture a band at 2975 cm^{-1} of CH_x appeared. Bridging hydroxyls slightly increased in concentration as adsorbed ammonia was released from bonding to OH groups. However, ammonia remained bonded to Co ions, as reflected in the unchanged intensity of TOT vibration (see Figure IV.37). Appearance of ethene was reflected in the band at 1425 $cm^{-1}$of the C=C double bond (not shown). Also the increase in intensity of the bands corresponding to M-NO_2 and NH was observed at ammonia pulses. These intermediates were consumed very fast by adsorbed ethane, which was fed continuously in the helium stream. It is to be noted that ammonia pulses caused also an increase in intensity of CH_x vibrations, indicating higher level of adsorption of ethane in the presence of ammonia. These transient experiments clearly indicate strong interaction of ammonia with both the bridging OH groups and Co(II) ions and, therefore, a dramatic effect on reactivity of Co-zeolites in oxidation reactions.

In ammoxidation of propane among the selective products surprisingly no acrolein was formed, but only propene, low concentration of ethene and acetonitrile. Clearly low concentration of ethylene formed during the oxidation reaction cannot be a source for such high concentration of acetonitrile formed. Mechanism of acetonitrile formation was suggested by Armor and Li[25,26]. According to these authors adsorption of propene on Co-amine complex occurs at β-position by Markovnikov rule leading to ammonolysis of the C-C bond and formation of acetonitrile. Also Sokolovskii[29] reported that in ammoxidation of propane over oxidic catalyst (V-Sb-O, Ga-Sb-O) acetonitrile is also formed, besides acrylonitrile.

Interaction of acetonitrile with ammonia over Co-MFI-12.5-0.42-2.9 zeolite at 450 °C was analyzed. Addition of ammonia to the reaction mixture (0.4 vol. % of acetonitrile, 6.5 vol. % of oxygen) up to ca 2 vol. % led to an increase in conversion of acetonitrile from 8 to 60 % and then at high ammonia concentration the conversion levelled-off. The selectivity to carbon dioxide increased to 97 % and the selectivity to CO decreased to 2 %. All nitrogen of acetonitrile was converted to molecular nitrogen. With acrylonitrile the presence of ammonia led to a rapid increase in conversion of acrylonitrile from 7 to 100 % and and new product – acetonitrile was formed with 80 % selectivity. At high ammonia concentrations increased

substantially selectivity to carbon dioxide. It follows that acetonitrile is less reactive compared to acrylonitrile. Acrylonitrile is readily converted already at low ammonia concentration to acetronitrile and its complete oxidation is also enhanced. It follows that even in the case that Markovnikov rule is not obeyed and acrylonitrile is formed then it would be readily transformed into acetonitrile under concentrations of ammonia present during the ammoxidation reaction. From these experiments, it also follows that too high concentrations of ammonia enhance substantially complete oxidation of the intermediate products – nitriles.

In contrast to the oxidation of paraffins addition of nitrous oxide at the ammoxidation reaction has no significant either positive or negative effect (see Table IV.15). Only a small decrease in hydrocarbon conversion and corresponding increase in the selectivity to nitriles and olefins was observed. It follows that the sites (suggested to be represented by Fe species) active in N_2O decomposition are completely blocked by adsorption of ammonia. Thus even though if N_2O would be formed during the ammoxidation reactions it would not have any effect on the procedure of this reaction.

V.4 References

[1] T. Sun, M.L. Trudeau, J.Y. Ying; J. Phys. Chem. **100** (1996) 13662.

[2] M. Iwamoto, H. Furukawa, Y. Mine, F. Uemura, S. Mikuriya, S. Kagawa; J. Chem. Soc., Chem. Commun. (1986) 1272.

[3] M. Iwamoto, H. Yahiro, S. Shundo, Y. Yu-u, N. Mizuno; Shokubai (Catalyst) **32** (1990) 430.

[4] P.Notté; Topics Catal. **13** (2000) 387.

[5] V.L. Zholobenko, I.N. Senchenya, L.M. Kustov, V.B. Kazanski; Kinet. Catal. **32** (1991) 151.

[6] Z. Sobalík, A. Vondrová, Z. Tvarůžková, B. Wichterlová; Catal. Today **75** (2002) 347.

[7] G.I. Panov, V.I. Sobolev, A.S. Gharitonov; J. Mol. Catal. **61** (1990) 85.

[8] P. Kubánek, B. Wichterlová, Z. Sobalík; J. Catal **211** (2002)109.

[9] R. Bulánek, B. Wichterlová, Z. sobalík, J. Tichý; Appl. Catal. B: Environmental **31** (2001) 13.

[10] T. Tabata, M. Kokitsu, H. Othsuka, T. Okada, L.M.F. Sabatino, G. Bellussi; Catal Today **27** (1996) 91.

[11] H. Othsuka, T. Tabata, T. Okada L.M.F. Sabatino, G. Bellussi;Catal Letters **44** (1997) 265.

[12] W. Aylor, L. J. Lobree, J:A. Reimer, A.T: Bell; Proc. 11 Intr. Congr. Catal. Baltimore, Elsevier, 1996, p.661.

[13] O. Bortnovsky, Z. Sobalík and B. Wichterlová; Micropor. Mesopor. Mater. **46**, 265 (2001).

[14] E.M. El-Malki, D.Werst, P.E. Doan, W.M.H. Sachtler; J. Phys. Chem. *B* **104**, 5924 (2000).

[15] J. Dědeček, L. Čapek, D. Kaucký, Z. Sobalík, B. Wichterlová; J. Catal. **211**, 198 (2002).

[16] C. Wu, K.J. Chao, H. Chang, L.J. Lee, C. Naccache; J. Chem. Soc., Faraday Trans., **93**, 3551 (1997).

[17] H. Ohtsuka, T. Tabata, O. Okada, L.M.F. Sabatino, G. Bellussi; Catal. Today **42**, 45 (1998).

[18] M. Iwamoto, H. Yahiro, N. Mizuno, W.X. Zhang, Y. Mine, H. Furukawa, S.J. Kagawa; J. Phys. Chem**. 96**, 9360 (1992).

[19] B. Wichterlová, J. Dědeček, Z. Sobalík; Proc. 12th Int. Zeol. Conf., Baltimore, Maryland, U.S.A., (1999), 941; J. Dědeček, B. Wichterlová; J. Phys. Chem. B, **103** (1999) 1462; D. Kaucký, J. Dědeček, B. Wichterlová; Microp. Mesop. Mater. **31** (1999) 75; J. Dědeček, D. Kaucký, B. Wichterlová; Microp. Mesop. Mater. **35-36** (2000) 483.

[20] K.I. Aika, J.H. Lunsford; J. Phys. Chem. **81** (1977) 1393.

[21] K.I. Aika, J.H. Lunsford; J. Phys. Chem. **82** (1978) 1794.

[22] J. Peréz-Ramirez, E.V. Kondratenko; Chem. Commun. (2003) 2152.

[23] J. Peréz-Ramirez, A. Gallardo-Llamas; Appl. Catal. A: General 279 (2005)117.

[24] G.Centi; Catal. Lett. **22** (1993)53.

[25] J.N. Armor, Y. Li; Appl. Catal. A: General, **188** (1999) 211.

[26] J.N. Armor, Y. Li; Appl. Catal. A: General, **183** (1999) 107.

[27] Y. Li and J.N. Armor; Appl. Catal. B: Environmental, **1** (1992) L21.

[28] G.I. Panov, G.A. Sheveleva, A.S. Kharitonov, V.N. Romannikov, L.A. Vostrikova; Appl. Catal. A: General, **82** (1992) 31.

[29] V.D. Sokolovskii, A.A. Davydov, O.Y. Ovsitser; Catal. Rev.-Sci. Eng**. 37**, 425 (1995).

Metallo-zeolites, with the well established redox activity in NO_x reactions, belong also to promising candidates as catalysts for selective transformation of ethane and propane to corresponding olefins, nitriles or other oxygenates. Understanding of their structure and performance at various reactant composition brings about a challenge for finding new reaction routes leading to the demanded products.

The present study represents contribution to understanding and thus shows capability and shortcomings of metallo-zeolites with respect to the structure of metal ion species, inner free volume architecture of crystalline structure and application of various reactants (O_2, N_2O and NH_3). The main results are as follows.

(i) It has been found that single Co ions in zeolites, in contrast to Co-oxo and Co oxide-like species leading to complete oxidation, are responsible for selective oxidation of ethane and propane to olefins. Substantially higher activity of Co ions in *BEA and MFI zeolites compared with those in MOR and FER structures is attributed to a high level of accessibility of the most populated β-type Co ions coordinated to the framework in open channels of *BEA zeolite and at intersection of the straight and sinusoidal channels of MFI structure to reaction intermediates. This conclusion is based on the analysis of UV-Vis spectra of Co(II) ions.

(ii) Presence of ammonia at the ammoxidation of paraffins results in a strong adsorption of ammonia on Co ion species. Ammonia bound to Co(II) ions increases substantially the rate of paraffin oxidation, and the selectivity and yields of olefins and nitriles. We speculate that the surprising increase of paraffin conversion and high conversion of ammonia to nitrogen might be due to coordination of ammonia and oxygen to the Co ions, oxidation of ammonia to NO_x increasing the rate of paraffin oxidation and leading to molecular nitrogen, and at the same time ammination of olefin formed to alkylamine, which is further oxidized to nitrile.

(iii) Formation of acetonitrile in the ammoxidation of propane is according to the literature caused by Markovnikov rule during the interaction of propene on the secondary carbon. Moreover, it has been found that surplus of ammonia enhances ammonolysis of acrylonitrile and its further oxidation. Thus optimization of the ammonia concentration is necessary.

(iv) As Fe is present in trace concentrations in zeolites, the observed activity with respect to nitrous oxide decomposition and transfer of an oxygen atom to a paraffin molecule can be explored for selective oxidations. Only minor part of Fe ion species in Fe-zeolites is extremely active in this oxygen transfer. However, there is no definite conclusion on the structure of this highly active site.

(v) The product composition for series of Fe-zeolites revealed that oxidation of propane over Fe-zeolites follows the reaction pathway from

$$propane + O \rightarrow propanol - H_2O \rightarrow propene + O \rightarrow propanal \rightarrow CO_x$$

(vi) In the ammonia presence at the ammoxidation reaction, ammonia should also be adsorbed on the Fe active sites necessary for N_2O decomposition and O atom transfer, as no effect of nitrous oxide (either positive or negative) was observed on the paraffin ammoxidation.

(vi) CoFe-zeolites have been revealed as bifunctional catalysts with respect to their function in oxidation of paraffins with molecular oxygen and nitrous oxide. Co ions are active in oxidation of paraffins by molecular oxygen to olefins, their Co-oxo species in complete oxidation to carbon oxides. Selected Fe ions (a minor part) bear ability to decompose nitrous oxide and transfer an oxygen atom to a hydrocarbon molecule. Moreover, there is some synergetic effect of oxygen and nitrous oxide. It implies application of CoFe-zeolites in paraffin oxidation for industrial streams containing both oxygen and harmful nitrous oxide.

Curriculum vitae

Born:	10 June 1978, Jihlava (former Czechoslovakia)
Primary School:	1984 - 1992 with extended English language
Secondary Grammar School:	1992 – 1996
	1995 - Basic Language State Examination in English
University of Pardubice:	1996 - 2001
	1999 – 2001 Analytical and Physical Chemistry
	2001 (Dipl. Ing.) State Examination, Diploma Thesis
Diploma Thesis:	"Oxidative dehydrogenation and ammoxidation of C_2 and C_3 hydrocarbons over Co-zeolites"
Ph.D.	2001 - University of Pardubice and J. Heyrovský Institute of Physical Chemistry, Academy of Sciences, Prague
	"Selective oxidation of paraffins over metallo-zeolites"
Supervisor:	B. Wichterlová, DrSc., J. Heyrovský Institute of Physical Chemistry
	Doc. Ing. Roman Bulánek, Ph.D., University of Pardubice
Position at doctoral study:	laboratory seminars for students in physical chemistry
Awards:	2002, 2003, 2004 the First Prize in each category at the Ph.D. Student Seminars of the Heyrovský Institute;
	2002 - Prize on Catalysis for Ph.D. students (Czech Chemical Society-Catalysis Group) "Influence of the presence and concentration of Co_xO_y on catalytic activity of Co-BEA zeolites", awarded at the Symposium on Catalysis, Prague;
	2004 - the best oral presentation at the International Pannonian Symposium on Catalysis, Srní, CZ
	2005 – Rhodia price for chemistry, (French embassy and Rhodia a.s.) – the first price
Stays:	2002 – three months, Department of Chemical Engineering, Faculty of Sciences, University of Malaga, Spain;
	2004 - eleven months, European project AMMONORE "NOx reduction by hydrocarbons to nitrogen for application at diesel engine exhausts over metal-zeolites" at Heyrovský Institute - experience – introduction of *in-situ* spectral methods at catalytic reactions

List of indexed publications

1) R. Bulánek, K.Novoveská, B. Wichterlová: Applied Catalysis A: General 235 (2002) 181. *Oxidative dehydrogenation and ammoxidation of ethane and propane over pentasil ring Co-zeolites*
2) R. Bulánek, K. Novoveská: Reaction Kinetics and Catalysis Letters 80 (2003) 337. *Oxidative dehydrogenation of propane by nitrous oxide and/or oxygen over Co BETA zeolite*
3) R. Bulánek, K. Novoveská: Polish Journal of Chemistry78 (2004) 149. *Oxidative dehydrogenation of propane over pentasil ring Co-zeolites*
4) R. Bulánek, B. Wichterlová, K. Novoveská, V. Kreibich: Applied Catalysis A: General 264 (2004) 13. *Oxidation of propane with oxygen and/or nitrous oxide over Fe-ZSM-5 with low iron concentrations*
5) K. Novoveská, R. Bulánek, B. Wichterlová: Catalysis Today 100 (2005) 315. *Oxidation of propane with nitrous oxide and oxygen over Co- and Fe-zeolites*
6) L. Čapek, K. Novoveská, Z. Sobalík, B. Wichterlová, L. Cider, E. Jobson: Appl. Catal. B: Environmental 60 (2005) 147. *Cu-ZSM-5 zeolite highly active in reduction of NO with decane under water vapor presence. Comparison of decane, propane and propene by in-situ FTIR*
7) L. Čapek, K. Novoveská, Z. Sobalík and B. Wichterlová: Stud. Surf. Sci. Catal. 158 (2005) 1993. *Metallo-zeolites active in the reduction of NO with decane at diesel exhaust conditions*
8) R. Bulánek, J. Adam, K. Novoveská, Z. Sobalík, B. Wichterlová: Stud. Surf. Sci. Catal. 158 (2005) 1977. *Occurrence of Fe species in Fe-zeolites active in propane oxidation with N_2O to propene and propanal*

List of non-indexed publications

1) K.Novoveská, R. Bulánek, B. Wichterlová: Sci.Pap. Univ. Pardubice ser.A 7 (2001) 175. *Oxidative dehydrogenative activity of high-silica Co-zeolites. Influence of presence of ammonia*

2) J.Fuchsová, R. Bulánek, K. Novoveská, D. Čermák, V. Lochař: Sci.Pap. Univ. Pardubice ser.A 8 (2002) 137. *On the incorporation of gallium ions into a cationic sites of pentasil ring zeolites and theis acid-base, redox and catalytic properties*.
3) K.Novoveská, R. Bulánek, B. Wichterlová: Sci.Pap. Univ. Pardubice ser.A 9 (2003) 111. *On the effect of cobalt loading on catalytic activity of Co-BEA zeolites in ethane oxidative dehydrogenation and ammoxidation*
4) P. Knotek, M. Pouzar, R. Bulánek, K. Novoveská: Sci.Pap. Univ. Pardubice ser.A 9 (2003) 97. *Determination of Extraframework Metal Content in Zeolitic Catalysts by Means of WD XRF Spectrometry*

International conferences – posters

1) R.Bulánek, B. Wichterlová, Z. Sobalík, K. Novoveská: 1st EFCATS School on Catalysis - New Trends in Catalysis, Research and Application, Prague, CZ (2001*). Oxidation and Ammoxidation of Ethane and Propane over Co-zeolites.*
2) R. Bulánek, B. Wichterlová, Z. Sobalík, K. Novoveská: 5th European Congress on Catalysis, EuropaCat V., Limmerick, Ireland, (2001). *Oxidation and ammoxidation of ethane and propane over metallo-zeolites.*
3) K. Novoveská, R. Bulánek, B. Wichterlová: 2nd EFCATS School on Catalysis – New Approaches in Catalysis Research and Application, Tihany, Hungary (2002). *Influence of preparation and composition on the catalytic activity of Co-BEA zeolites*
4) K. Novoveská, R. Bulánek, B. Wichterlová: 3rd Younger European Chemists Conference, Grenoble, France (2003). *Ethane oxidative dehydrogenation and ammoxidation over Co-zeolites. "In-situ" UV-Vis study.*
5) K. Novoveská, R. Bulánek, B. Wichterlová, J. Dědeček: 6th European Congress on Catalysis, EuropaCat VI., Innsbruck, Austria, (2003). *Oxidative dehydrogenation and ammoxidation of propane in the presence of N_2O over CoH-BEA catalyst*
6) R. Bulánek, K. Novoveská, B. Wichterlová: 11th Nordic Symposium on Catalysis, Oulu, Finland (2004). *Oxidation of propane with nitrous oxide and oxygen over Co- and Fe-zeolites*
7) K. Novoveská, R. Bulánek, B. Wichterlová: 13th International Congress on Catalysis, Paris, France (2004). *A comparison of oxidation of propane with nitrous oxide and oxygen over Co- and Fe-zeolites*

8) Roman Bulánek, Jan Adam, Kateřina Novoveská, Blanka Wichterlová; 3rd International Zeolite Symposium (3rd FEZA), Prague, Czech Republic (2005). *Utilization of Propane by N_2O over Fe-MFI zeolite*
9) L. Čapek, K. Novoveská, Z. Sobalík, B. Wichterlová; 3rd International Zeolite Symposium (3rd FEZA), Prague, Czech Republic (2005). *Metallo-zeolites active in the reduction of NO with decane at diesel exhaust conditions*

International conferences – oral presentations

1) K. Novoveská, R. Bulánek, B. Wichterlová: 6th Pannonian Symposium on Catalysis, Obergurgl, Austria (2002). *Influence of preparation on the catalytic activity of Co-BEA zeolites*
2) K. Novoveská, R. Bulánek, B. Wichterlová: 34th Symposium on Catalysis, Prague, CZ (2002). *The influence of presence and concentration Co_xO_y on catalytic activity of Co-BEA zeolites*
3) K. Novoveská, R. Bulánek, B. Wichterlová: 35th Symposium on Catalysis, Prague, CZ (2003). *Oxidation of propane by nitrous oxide over Fe-zeolites with low iron content*
4) K. Novoveská, R. Bulánek, B. Wichterlová: 7th Pannonian Symposium on Catalysis, Srní, CZ (2004). *Oxidation of propane with N_2O and O_2 over Co-zeolites containing traces of Fe*
5) K. Novoveská, B. Wichterlová, Z. Sobalík, R. Bulánek: 3rd EFCATS School on Catalysis, Ustroň, Poland (2004). *Selective Oxidation of Light Paraffins over Co-zeolites. Spectroscopic Study*
6) K. Novoveská, B. Wichterlová, Z. Sobalík, R. Bulánek: 36th Symposium on Catalysis, Prague, CZ (2004). *Selective oxidation of ethane over Co-zeolites. Spectroscopic study.*
7) L. Čapek, K.Novoveská, B. Wichterlová, J. Dědeček, Z. Sobalík: 7th Pannonian Symposium on Catalysis, Srní, CZ (2004).*Metallo zeolites active in the reuction of NO with decane, in-situ FTIR study*
8) L. Čapek, K.Novoveská, B. Wichterlová, J. Dědeček, Z. Sobalík: 36th Symposium on Catalysis, Prague, CZ (2004). *Metallo zeolites active in the reuction of NO with decane, in-situ FTIR study*

National Conferences – oral presentations

1) K. Novoveská, R. Bulánek, B. Wichterlová: Seminary of students, Prague (2002); *Oxidative dehydrogenation and ammoxidation over Co-zeolites*

2) K. Novoveská, R. Bulánek, B. Wichterlová: Seminary of students, Třešť (2003); *Selective oxidation of light paraffins over Co-zeolites*

3) K. Novoveská, L. Čapek, Z. Sobalík, B. Wichterlová: Seminary of students, Třešť (2004); *In-situ FTIR study of selective catalytic reduction of NO_x by hydrocarbons to nitrogen over Cu-ZSM-5*

Souhrn

V posledním desetiletí byly objeveny neobvyklé katalytické vlastnosti kation-zeolitů v redox reakcích, jako jsou amoxidace etanu na acetonitril, selektivní redukce oxidů dusíku na molekulární dusík a oxidace benzenu na fenol oxidem dusným.

Cílem této studie byla analýza struktury a reaktivity Co- a Fe-zeolitů a využití těchto znalostí pro porozumění oxidačních procesů, jakož i pro vývoj katalyzátorů pro selektivní oxidaci a amoxidaci nízkých parafínů molekulárním kyslíkem a oxidem dusným na olefíny, aldehydy a nitrily. Hlavní otázky se týkaly efektu typu (Cu, Co, Fe) a lokalizace kovových (Co) iontů a zeolitické struktury (FER, MOR, MFI a *BEA topologie) na katalytickou aktivitu zeolitických katalyzátorů ve výše uvedených reakcích.

Kromě kinetických měření transformací uhlovodíků molekulárním kyslíkem, oxidem dusným, a v přítomnosti amoniaku, byly použity ex-situ a in-situ (za podmínek katalytické reakce) UV-Vis a FTIR spektroskopie pro získání informací o stavu a chování potenciálních aktivních center a reakčních intermediátů. Katalyzátory byly dále charakterizovány teplotně-programovanou redukcí vodíkem, jejich krystalinita byla ověřena XRD a elektronová spinová resonance byla použita pro identifikaci přítomnosti Fe(III) iontů a jejich koordinaci v Co-zeolitech.

Bylo zjištěno, že atomárně dispergované Co ionty koordinované ke skeletu Co-zeolitů jsou zodpovědné za selektivní oxidaci etanu a propanu kyslíkem na olefiny, zatímco Co-oxo komplexy a Co-oxidické částice vedou k totální oxidaci. Jak vyplynulo z analýzy UV-Vis spekter Co(II) iontů významně vyšší aktivita Co iontů v zeolitech *BEA a MFI struktury ve srovnání s kationty lokalizovanými v MOR a FER strukturách je připisována vysoké přístupnosti nejvíce populovaných tzv. β typů Co iontů koordinovaných k mřížce v otevřených kanálech v *BEA zeolitu a v průsečících kanálů MFI struktury. V amoxidaci parafinů se uplatňuje silná adsorpce amoniaku na Co iontech i za reakčních teplot, která významně zvyšuje rychlost oxidace parafinu, a to zejména na selektivní produkty, t.j. olefiny a nitrily. Překvapivé zvýšení konverze parafinu a vysoké konverze amoniaku na dusík vysvětlujeme koordinací amoniaku a kyslíku k Co iontům, následnou oxidací amoniaku na NOx zvyšující oxidační aktivitu systému a vedoucí poté k tvorbě molekulárního dusíku, za současné aminace vzniklého olefinu na alkylamin a jeho oxidaci na nitril.

V oxidaci parafinů oxidem dusným na Fe-zeolitech, Fe centra (oproti Co iontům) v prvním kroku rozkládají oxid dusný na molekulární dusík a atomární kyslík a umožňují jeho stabilizaci a následnou inzerci do uhlovodíkové molekuly. Avšak jenom velmi malá část Fe iontů

v Fe-zeolitech je vysoce aktivní v rozkladu N_2O a přenosu atomárního kyslíku. Byl navržen mechanismus oxidace propanu oxidem dusným vedoucí zejména k propenu, propanolu a propanalu v následujících krocích:

$$propan + O \rightarrow propanol - H_2O \rightarrow propen + O \rightarrow propanal \rightarrow CO_x$$

Bylo ukázáno, že na CoFe-zeolitech při oxidaci propanu kyslíkem a oxidem dusným jsou konverze propanu, selektivita i výtěžek mnohem vyšší ve srovnání s oxidací propanu molekulárním kyslíkem. Tyto výsledky naznačují, že oxid dusný (škodlivý vedlejší produkt ve výrobě kyseliny adipové) by mohl být s výhodou využit jako aditivum ke kyslíku pro významné zvýšení konverse parafinů na alkeny.

klíčová slova: selektivní oxidace, oxidativní dehydrogenace, amoxidace, propan, etan, zeolity, Co-zeolity, Fe-zeolity, amoniak, oxid dusný

Summary

In recent years metallo-zeolites have been shown to exhibit unusual catalytic behaviour in redox reactions as ammoxidation of ethane to acetonitrile, selective catalytic reduction of NO_x to nitrogen and benzene oxidation to phenol by nitrous oxide.

The study has been aimed at analysis of the structure and reactivity of Co- and Fe-zeolites and exploitation of this knowledge for understanding of the oxidation processes and catalyst design for selective oxidation and ammoxidation of low chain paraffins by molecular oxygen and nitrous oxide to olefins, aldehydes and nitriles. The main questions have concerned the effect of the type of metal ion species (Cu, Co and Fe) and topology of the zeolite matrix (FER, MOR, MFI and *BEA) on the catalyst activity with respect to the above mentioned reactions.

Besides reaction kinetic measurements of hydrocarbon transformations with molecular oxygen, nitrous oxide and ammonia, the ex-situ and in-situ (at true reaction conditions) UV-Vis and FTIR spectroscopy have been employed to obtain information on the state and behaviour of potential active sites and reaction intermediates. Catalysts were characterized by means of temperature programmed reduction by hydrogen, the crystallinity of zeolites was checked by X-ray diffraction and electron spin resonance was used to identify presence and coordination of Fe ions in zeolite.

It has been found that single Co ions coordinated to the framework in zeolites, in contrast to Co-oxo and Co oxide-like species supporting complete paraffin oxidation, are responsible for selective oxidation of ethane and propane to olefins. Substantially higher activity of Co ions in *BEA and MFI zeolites compared with those in MOR and FER structures is attributed to a high level of accessibility of the most populated β-type Co ions coordinated to the framework in open channels of *BEA zeolite and at intersection of the straight and sinusoidal channels of MFI structure. At the ammoxidation reaction strong adsorption of ammonia on Co ion species increases substantially the rate of paraffin oxidation as well as selectivity and yields of olefins and nitriles. We speculate that the surprising increase of paraffin conversion and high conversion of ammonia to nitrogen might be due to coordination of ammonia and oxygen to the Co ions, oxidation of ammonia to NOx increasing the rate of paraffin oxidation and leading to molecular nitrogen, with simultaneous ammination of the formed olefin to alkylamine and its oxidation to nitrile.

In oxidation of paraffins by nitrous oxide over Fe zeolites, the Fe sites (in contrast to Co ions) decompose nitrous oxide to molecular nitrogen and atomic oxygen, and enable its insertion to a hydrocarbon molecule. Only minor part of Fe ion species in Fe-zeolites is extremely active in

N_2O decomposition. It has been revealed that the oxidation of propane over Fe-zeolites follows the reaction pathway leading mainly to propene, propanol and propanal in the following steps:

$$propane + O \rightarrow propanol - H_2O \rightarrow propene + O \rightarrow propanal \rightarrow CO_x$$

It has been shown that propane oxidation over bifunctional CoFe-zeolites, using a mixture of molecular oxygen and nitrous oxide compared to molecular oxygen, exhibit much higher propane conversion and yield of propene. The Co ions catalyse oxidative dehydrogenation of paraffins to olefins by molecular oxygen and over Fe ions atomic oxygen from nitrous oxide decomposition is transferred to propane molecule. These results indicate that nitrous oxide (a harmful by-product, e.g., in adipic acid plants) added to streams of molecular oxygen could be exploited in enhancement of transformation of paraffins to olefins.

keywords: selective oxidation, oxidative dehydrogenation, ammoxidation, propane, ethane, zeolites, Co-zeolites, Fe-zeolites, ammonia, nitrous oxide

FER	ferrierite, zeolite topology according to IUPAC
MOR	mordenite, zeolite topology according to IUPAC
MFI	ZSM-5, zeolite topology according to IUPAC
*BEA	beta, zeolite topology according to IUPAC
FAU	faujasite, zeolite topology according to IUPAC
USY	ultrastable zeolite Y, zeolite topology according to IUPAC
X	zeolite topology according to IUPAC
Y	zeolite topology according to IUPAC
LTA	Linde Type A, zeolite topology according to IUPAC
CHA	chabazite, zeolite topology according to IUPAC
APO	aluminum phosphate, topology according to IUPAC
UV-Vis	ultraviolet-visible absorption spectroscopy
UV-Vis-NIR	ultraviolet-visible-near-infrared absorption spectroscopy
FTIR	fourier transformed infrared spectroscopy
EXAFS	extended X-ray absorption spectroscopy
XPS	X-ray photoelectron spectroscopy
XRD	X-ray diffraction
WD XRF	wavelength-dispersive X-ray fluorescence analysis
GC	gas chromatography
H_2-TPR	temperature-programmed reduction by hydrogen
ESR	electron-spin resonance
ICP OES	inductively coupled plasma optical emission spectrometry
AAS	atomic absorption spectrometry
NO_x	oxides of nitrogen
IUPAC	International Union of Pure and Applied Chemistry
RT	room temperature
ppm	part per million (10^{-6})
X_i	conversion of reactant i
S	selectivity
Y	yield
TOF	turn over frequency
GHSV	gas hourly space velocity
TCD	thermal-conductivity detector
FID	flame ionization detector

TP	temperature-programmed
IR	infrared spectroscopy
W/F	contact time
W	weight of catalysts
F	flow of key reactant
HT	hydrotermally-treated
C	calcined
TOS	time on stream
vol.	volume
M-	metal
SCR-NOx	selective catalytic reduction of NO_x
Å	angstroem (10^{-10} m)